

**Sustaining Ecosystem Functions Under  
Environmental Change: The Combined Impacts of  
Temperature, Species Diversity and Limiting  
Resources on Phytoplankton Communities**

Submitted in partial fulfillment of the requirements of the Degree of  
Doctor of Philosophy

**Leah Lewington-Pearce**

August 2018

I, Leah Lewington-Pearce, confirm that the research included within this thesis is my own work or that where it has been carried out in collaboration with, or supported by others, that this is duly acknowledged below and my contribution indicated. Previously published material is also acknowledged below.

I attest that I have exercised reasonable care to ensure that the work is original, and does not to the best of my knowledge break any UK law, infringe any third party's copyright or other Intellectual Property Right, or contain any confidential material.

I accept that the College has the right to use plagiarism detection software to check the electronic version of the thesis.

I confirm that this thesis has not been previously submitted for the award of a degree by this or any other University.

The copyright of this thesis rests with the author and no quotation from it or information derived from it may be published without the prior written consent of the author.

Signature:

Date: 21<sup>st</sup> July 2018

## Details of collaborations and publications

Author contributions and additional collaborators are listed below for each chapter, as well as details of publications where applicable. This work was fully funded by Queen Mary University of London. I use the term ‘we’ throughout the thesis to acknowledge the contribution of authors.

- **Chapter 1:** Leah Lewington-Pearce wrote the chapter.
- **Chapter 2:** Leah Lewington-Pearce and Pavel Kratina designed the study. Leah Lewington-Pearce and Ben Parker collected the data. LLP, PK, BP and Anita Narwani were involved in analyzing the data and writing the paper.
- **Chapter 3:** Leah Lewington-Pearce, Pavel Kratina and Anita Narwani designed the study. LLP and Helena Vogler collected the data. LLP, PK, AN, Mridul Thomas and Colin Kremer analysed and wrote the paper. MT and CK in particular developed the models associated with the parameter estimations.
- **Chapter 4:** Leah Lewington-Pearce and Anita Narwani designed the study. LLP and Aaron Pereira collected the data from the *Chlamydomonas* strains evolved from the selection experiment performed previously by AN. LLP, AN, and Pavel Kratina analysed and wrote the paper.
- **Chapter 5:** Leah Lewington-Pearce wrote the chapter.

# **Sustaining Ecosystem Function Under Environmental Change: The Combined Impacts of Temperature, Species Diversity and Limiting Resources on Phytoplankton Communities**

Leah Lewington-Pearce

## **ABSTRACT**

Plankton play a key role in regulating nutrient and carbon cycles in freshwater ecosystems. The uptake and processing of nutrients in planktonic biomass are highly sensitive to changes in the environment, such as alterations in the availability of limiting nutrients, increasing temperature due to climate change, and changes to the composition of interacting species. The focus of this thesis is to use a variety of experimental and theoretical methods to assess and predict the impact of multiple perturbations on community structure, dynamics and ecosystem function, with a particular focus on interactions between phytoplankton and their consumers (zooplankton). Increases in both temperature and phytoplankton species diversity independently decreased CO<sub>2</sub> concentrations when the number of non-resource species (those inedible to the zooplankton) were high. Using structural equation modeling I show that the effect is indirect, resulting largely from the positive impacts on total biomass of phytoplankton. Phytoplankton are limited by a range of resources, and differences in the functional traits used to utilize light and nutrients can explain the distributions of species under different temperature regimes. I found that under light and nitrogen limitation, resource requirements are generally lowest at intermediate temperatures, and that changes in temperature may therefore alter the competitive hierarchy amongst species. Using the model freshwater phytoplankton *Chlamydomonas reinhardtii*, I also find that previous selection environments govern future competitive abilities in phytoplankton. Adaptation to a high salt and low nutrient stress increases competitive ability under light limited conditions, indicating a strong dependency of selection environment for overall competitiveness. This thesis provides a mechanistic insight into the role of diverse plankton communities for community dynamics and ecosystem functioning.

# CONTENTS

<b>CHAPTER 1</b>	<b>1</b>
<i>General Introduction</i>	1
Climate warming modifies ecological communities	1
Resources structure ecological communities	2
Planktonic communities as a model system	3
Microcosms as experimental ecosystems	4
Using functional traits to predict community structure	5
Research aims and thesis organization	6
<b>CHAPTER 2</b>	<b>9</b>
<i>Diversity and Temperature Indirectly Reduce CO<sub>2</sub> Concentrations in Experimental Freshwater Communities</i>	9
Abstract	9
Introduction	10
Methods	12
Results	18
Discussion	26
<b>CHAPTER 3</b>	<b>30</b>
<i>How Temperature Governs Resource Competition in Phytoplankton</i>	30
Abstract	30
Introduction	31
Methods	34
Results	37
Discussion	43
<b>CHAPTER 4</b>	<b>45</b>
<i>Selection Drives Evolution of Minimum Resource Requirements in <i>Chlamydomonas reinhardtii</i></i>	45
Abstract	45
Introduction	46
Methods	49
Results	56
Discussion	62
<b>CHAPTER 5</b>	<b>67</b>
<i>General Conclusions</i>	67

<b>SUPPLEMENTARY MATERIAL</b>	<b>69</b>
Supplementary Chapter 2	69
Supplementary Chapter 3	78
Supplementary Chapter 4	89
<b>REFERENCES</b>	<b>112</b>

## ACKNOWLEDGEMENTS

Firstly and foremost, I would like to show my gratitude to my supervisor Pavel Kratina for his expertise, guidance and support throughout my thesis. I would have not become the confident and capable Scientist I am today without the amount of time and effort he has sacrificed.

Thank you also to my honorary second supervisor Anita Narwani. Switzerland was one of the most exciting and most productive times in my life. She is an amazing female role model and I aspire to become just as successful as she.

A special acknowledgement must be made to the PhD gang from the beginning to the end; Flick, Vicky, Louise, Martin, Esther, Tor, Lowri, Sahmorie, Dom, Hanrong, Ade, Emma, Miles (You too Ian). Thank you for your encouragement and support through the lows and for sharing the many, many highs.

A final thank you to my boyfriend Jordan for cheering me on through the most challenging times of the PhD and for encouraging me to push on til' the end.

*I dedicate this thesis to my parents Sally and Adam and my sister Lew for their endless encouragement, love and support throughout all of my academic endeavors – I certainly could not have done the last 3 and a half years without you.*

## FIGURES

- 2.1. The effects of non-resource diversity on time-averaged CO<sub>2</sub> concentration (a), time-averaged total phytoplankton biomass (b), time-averaged consumer density (c) and time-averaged resource density (d). Each bar represents means across all time points and temperature treatments (n = 24 replicates); error bars represent ± 1 standard error. ....19
- 2.2. The effects of environmental temperature on time-averaged CO<sub>2</sub> concentration (a), time-averaged total phytoplankton biomass (b), time-averaged consumer density (c) and time-averaged resource density (d). Each bar represents means across all time points and diversity treatments (n = 32 replicates); error bars represent ± 1 standard error. ....20
- 2.3. The best-fit structural-equation model (SEM) showing how the covariance's among the variables predict the pathway of outcome of CO<sub>2</sub> concentration. (a) Before correction for the effect of temperature on CO<sub>2</sub> solubility in the water, the SEM retains a significant direct effect of temperature on CO<sub>2</sub> concentration. (b) After correction for the effect of temperature on CO<sub>2</sub> solubility, the SEM retains only an indirect effect of temperature on CO<sub>2</sub> concentration. ....22
- 2.4. The independent effects of non-resource diversity (a) and environmental temperature (b) on the temporal dynamics of CO<sub>2</sub> concentration. Points represent mean of 24 replicates ± 1 standard error for each diversity treatment level and 32 replicates ± 1 standard error for each temperature treatment level. Dashed lines represent CO<sub>2</sub> concentration at 19°C, 23°C and 27°C, atmospheric equilibration is 15.98 μmol L<sup>-1</sup>, 14.24 μmol L<sup>-1</sup> and 12.79 μmol L<sup>-1</sup> respectively. a) Higher non-resource diversity (LME,  $F_{1,89} = 9.719$ ,  $P < 0.001$ ) and b) elevated temperature (LME,  $F_{1,89} = 48.942$ ,  $P < 0.001$ ) both independently reduced mean CO<sub>2</sub> concentration in the water. ....24
- 2.5. The effect of non-resource diversity (a-c) and temperature (d-f) on the community dynamics of consumer density (d and d), total phytoplankton biomass/chlorophyll-a (b and e) and resource density (c and f). Points represent mean



of 24 replicates  $\pm 1$  standard error for each diversity treatment and 32 replicates  $\pm 1$  standard error for each temperature treatment. ....25

3.1. Temperature alters minimum light ( $I^*$ ) and nitrogen ( $N^*$ ) requirements of six phytoplankton species (different symbols). (a)  $I^*$  values are lowest and least variable at intermediate experimental temperatures, (b)  $N^*$  values increase at the highest experimental temperatures. (c, d) illustrate the same data that were corrected to remove differences among species in the mean trait value across a temperature gradient. The x-axis represents temperatures standardized so that all species have their trait minimum at the same value (0 °C). (c)  $I^*$  as a function of temperature relative to the minimum trait value, with a fitted GAMM, (d)  $N^*$  as a function of temperature relative to the minimum trait value, with a fitted GAMM. ....39

3.2. Temperature alters within species responses to light ( $I^*$ ) and nitrogen ( $N^*$ ) limitation.  $I^*$  and  $N^*$  show opposite relationship with temperature for some species (a, c, f), or similar trends for other species (d). Note different y-axis. ....40

3.3. The key traits for nitrogen and light competition depend on experimental temperature. The effect of temperature on (a) the growth rate measured under unlimited light ( $\mu_{max}$ ) (calculated as the sum of  $\mu_{max}$  and  $h$  to allow for a non-zero specific growth rate in pure darkness,  $I = 0$ ) (e) the initial slope of the growth-light curve ( $\alpha$ ), (i) the specific growth rate at  $I = 0$ , implying heterotrophic growth ( $h$ ), (m) the optimal irradiance for growth ( $I_{opt}$ ). (c) growth rate measured under unlimited nitrate, (g) the initial slope of the growth-nitrogen curve, and (k) the specific growth rate at  $N = 0$ . The GAMMs fitted to four growth-irradiance traits modified by experimental temperature: (b)  $\mu_{max}$ , (calculated as the sum of  $\mu_{max}$  and  $m$  to account for mortality in the absence of any nutrients). (f)  $\alpha$ , (j)  $h$  and (n)  $I_{opt}$ . The GAMMs fitted to three nitrogen competition traits modified by experimental temperature: (d)  $\mu_{max}$ , (h)  $\alpha$ , and (l)  $m$ . ....42

4.1. Conceptual diagram showing the process and timeline for (a) the isolation of ancestral populations, (b) derivation of evolved descendants by exposing ancestral populations to six different selection environments, (c) measurement of descendants'

population growth rates under a gradient of light, nitrogen and phosphate availability, and (d) estimation of the competition growth parameters under light, nitrogen and phosphate resource. ....51

4.2. Minimum resource requirements evolve in response to selection environment and depend on the type of limiting resource. (a-c) The ancestral and environmentally selected descendant minimum light ( $I^*$ ), nitrogen ( $N^*$ ) and phosphate requirements ( $P^*$ ). (d) Variation in the descendants'  $R^*$  for light, nitrogen and phosphate measured as the log response ratio of each descendant relative to its ancestor for each limiting resource. (e-g) The ancestral and environmentally selected descendants initial growth response ( $\alpha$ ) to increasing light, nitrogen and phosphate resource. (h) Variation in the descendants'  $\alpha$  for light, nitrogen and phosphate measured as the log response ratio of each descendant relative to its ancestor for each limiting resource. ....57

4.3. Ancestral genotypes only explain variation in descendant's response to nitrogen. The ancestral and environmentally selected descendant minimum (a) light ( $I^*$ ), (b) nitrogen ( $N^*$ ) and (c) phosphate requirements ( $P^*$ ), coloured by ancestral genotype for each selection treatment. ....59

4.4. (a) Principle components analysis (PCA) showing the separation of the descendants and ancestors minimum resource requirements for light ( $I^*$ ), nitrogen ( $N^*$ ) and phosphate ( $P^*$ ) depending on the selection treatment onto the first two PC axes of a PCA (b) PCA showing clear separation of the ancestor and descendants' initial response to increases in resource ( $\alpha$ ) (c) An RDA constrained by selection treatment indicates a possible trade-off between  $R^*$  and  $\alpha$  (Note  $R^*$  and  $\alpha$  loading onto opposite orthogonal axes for each resource). The scores for the genetically diverse ancestor *CC1690* under each selection treatment are plotted as open circles to distinguish from the isoclonal ancestors. ....61

## TABLES

2.1. Experimental phytoplankton community compositions with individual species for each non-resource diversity treatment. The 0 non-resource diversity treatment received only resource species *C. vulgaris*. All experimental assemblages received an

equal amount of resource species *C. vulgaris* ( $1.6 \times 10^6$  ESD) and had equivalent total biovolume of non-resource species ( $8 \times 10^5$  ESD) in the 2, 4 and 8 diversity treatments. ....14

## SUPPLEMENTARY MATERIAL

### SUPPLEMENTARY FIGURES

S2.1. Conceptual path diagram illustrating the alternative hypotheses based on the models presented in Table S5, of how warming ( $^{\circ}\text{C}$ ) and phytoplankton diversity (number of non-resource species), may affect consumer density, resource density, total phytoplankton biomass (total chlorophyll-a concentration) and  $\text{CO}_2$  concentration. Red and black colors indicate negative and positive effects respectively. .... 69

S2.2. Mean consumer density, chlorophyll-*a* concentration (total phytoplankton biomass) and resource density over the over the experimental duration for different diversity levels and community compositions (error bars are  $\pm 1$  standard error,  $N=4$ ). Horizontal lines are means of each diversity category (grey for all 0, 2 and 4 non-resource diversity treatments combined, orange for 8 non-resource composition A and green for 8 non- resource composition B). ....71

S3.1. The interactive effect of temperature and light on growth rate of six freshwater phytoplankton species. Fitted models are of equation (1). (a-d) *Synechococcus, sp.* (e-h) *Kirchneriella subcapitata*, (i-l) *Microcystis*, (m-p) *Pediastrum boryanum*, (q-t) *Cyclotella meneghiniana*, (u-x) *Scenedesmus acuminatus*. Growth rate estimates were weighted based on the uncertainty in each point. The grey lines represent represents the 95% confidence interval of the curve using 1000 bootstrapped values. .... 78

S3.2. The interactive effect of temperature and nitrate concentration ( $\mu\text{mol L}^{-1}$ ) on growth rate of six freshwater phytoplankton species. Fitted models are of equation (2). (a-d) *Synechococcus, sp.* (e-h) *Kirchneriella subcapitata*, (i-l) *Microcystis*, (m-p) *Pediastrum boryanum*, (q-t) *Cyclotella meneghiniana*, (u-x) *Scenedesmus*

*acuminatus*. Growth rate estimates were weighted based on the uncertainty in each point. The grey lines represent represents the 95% confidence interval of the curve using 1000 bootstrapped values. .... **79**

S3.3. Within species comparisons of the estimated minimum resource requirements for light ( $I^*$ ) and nitrogen ( $N^*$ ) across a gradient of temperature for (a-b) *Synechococcus sp.*, (c-d) *P. boryanum*, (e-f) *K. subcapitata*, (g-h) *C. meneghiniana*, (i-j) *M. aeruginosa* and (k-l) *S. acuminatus*. It was observed that *M. aeruginosa* did not grow at 15°C and therefore  $I^*$  could not be estimated (denoted by the \*). .... **80**

S4.1. Estimates of biomass reduction of all ancestral strains assigned to each selection treatment relative to the control (indicated by the dotted line). Estimates of biomass reduction for each treatment were calculated by taking the log response ratio of the mean biomass estimate (RFU) of the last 4 time points of the selection experiment relative to the last 4 time points of the control. .... **89**

S4.2. Growth curves of all ancestors under limiting light, nitrogen and phosphate resource. Rows demonstrate the response of each descendant’s ancestral history to each limiting resource. Growth rate estimates were weighted based on the uncertainty in each point. The grey lines represent represents the 95% confidence interval of the curve using 1000 bootstrapped values. .... **90**

S4.3. Growth curves of all descendants selected under the biotic treatment, for limiting light, nitrogen and phosphate resource. Rows demonstrate the response of each descendant’s ancestral history to each limiting resource. Growth rate estimates were weighted based on the uncertainty in each point. The grey lines represents the 95% confidence interval of the curve using 1000 bootstrapped values. .... **91**

S4.4. Growth curves of all descendants selected under the biotic treatment, for limiting light, nitrogen and phosphate resource. Rows demonstrate the response of each descendant’s ancestral history to each limiting resource. Growth rate estimates were weighted based on the uncertainty in each point. The grey lines represents the 95% confidence interval of the curve using 1000 bootstrapped values. .... **92**

S4.5. Growth curves of all descendants selected under the biotic x salt treatment, for limiting light, nitrogen and phosphate resource. Rows demonstrate the response of each descendant’s ancestral history to each limiting resource. Growth rate estimates were weighted based on the uncertainty in each point. The grey lines represent the 95% confidence interval of the curve using 1000 bootstrapped values. ....**93**

S4.6. Growth curves of all descendants selected under the low phosphate treatment, for limiting light, nitrogen and phosphate resource. Rows demonstrate the response of each descendant’s ancestral history to each limiting resource. Growth rate estimates were weighted based on the uncertainty in each point. The grey lines represent the 95% confidence interval of the curve using 1000 bootstrapped values. .... **94**

S4.7. Growth curves of all descendants selected under the high osmotic stress (salt) treatment, for limiting light, nitrogen and phosphate resource. Rows demonstrate the response of each descendant’s ancestral history to each limiting resource. Growth rate estimates were weighted based on the uncertainty in each point. The grey lines represent the 95% confidence interval of the curve using 1000 bootstrapped values. .... **95**

S4.8. Growth curves of all descendants selected under the biotic x salt treatment, for limiting light, nitrogen and phosphate resource. Rows demonstrate the response of each descendant’s ancestral history to each limiting resource. Growth rate estimates were weighted based on the uncertainty in each point. The grey lines represent the 95% confidence interval of the curve using 1000 bootstrapped values. ....**96**

S4.9. (a-f) Reaction norms of absolute fitness of each descendant and it’s ancestor; green = selected under low light, blue = selected under low nitrogen and red = ancestor). Lines connect the fitness of the descendants or ancestor in each assay environment. (g) Trade-offs in fitness resulting from divergent selection. Lines connect a pair of evolved descendants from their common ancestor selected in one of two environments (filled circles: selected in low light (wL); open circle: selected in low nitrogen (wN). Values are expressed as relative fitness calculated as the Log response ratio of each environmentally selected descendant to its relative ancestor.

The fitness of the ancestor is by definition given by the intersection of the two dashed lines in the figure. .... 97

S4.10. The weak, but significant negative correlation between  $R^*$  and  $\alpha$ , indicating a negative trade-off between the requirements of a resource and its initial growth response to increasing resource availability. Due to little variation in  $P^*$  observed in this experiment, we use only the  $R^*$  and  $\alpha$  estimates from the light and nitrogen experiments. .... 99

## SUPPLEMENTARY TABLES

S2.1. Inocula of phytoplankton species that originated from the Experimental Phycology and Culture Collection of Algae at the University of Göttingen (EPSAG) and the Culture Collection of Algae of Charles University in Prague (CAUP). The last column indicates the number of lakes each phytoplankton species occurs across North America as found in the US EPA's National Lakes Assessment survey (2007). .... 72

S2.2. Chemical composition of Volvic Mineral Water used as experimental media. .... 73

S2.3. Linear mixed effects (LMEs) model summary statistics illustrating the independent and combined effects of non-resource diversity and environmental temperature on the time averaged response variables: (i) consumer density (number of *D. pulex* per sample), (ii) resource density (number of *C. vulgaris* cells per sample), (iii) total phytoplankton biomass (aggregated biomass of all phytoplankton taxa in the community) and (iv) concentration of CO<sub>2</sub> (amount of CO<sub>2</sub> in the water uncorrected for the difference in solubility at each temperature). .... 74

S2.4. Linear mixed effects (LMEs) model summary statistics illustrating the independent and combined effects of non-resource diversity and environmental temperature on four response variables: (i) consumer density (number of *D. pulex* per sample), (ii) resource density (number of *C. vulgaris* cells per sample), (iii) total phytoplankton biomass (aggregated biomass of all phytoplankton taxa in the community) and (iv) concentration of CO<sub>2</sub> (amount of CO<sub>2</sub> in the water uncorrected

for the difference in solubility at each temperature). This model was fit to the whole time series data. ....	75
S2.5. A comparison of different structural equations models (SEMs) used to explain patterns of covariance among variables analyzed in this experiment (Lefcheck 2016). ....	76
S3.1. The list of phytoplankton taxa used for both, the light and nitrogen competition experiments. The culture collection names are abbreviations: SAG = Sammlung von Algenkulturen Göttingen (Göttingen, Germany), CCAP = the Culture Collection of Algae and Protozoa (Oban, Scotland). ....	81
S3.2. Light limitation experimental parameter estimates for six freshwater phytoplankton species. $\alpha$ is the species' initial response to elevated resource availability, $\mu_{max}$ is the maximum growth rate under non-limiting light conditions, $I_{opt}$ is the optimal irradiance for growth and $I^*$ is the species minimum light requirement. Parameter uncertainty (in parentheses) was measured as the 95% confidence width estimated from 1000 bootstrap values. ....	82
S3.3. Nitrate limitation experimental parameter estimates for six freshwater phytoplankton species. $\alpha$ is the species' initial response to elevated resource availability, $\mu_{max}$ is the maximum growth rate under non-limiting nitrate conditions, $m$ is the specific growth rate at $N = 0$ and $N^*$ is the species minimum nitrate requirement. Parameter uncertainty (in parentheses) was measured as the 95% confidence intervals estimated from 1000 bootstraps. ....	84
S3.4. $Q_{10}$ values calculated from the fitted slope of a linear model fit to the log-transformed response of each trait estimate to temperature. $Q_{10}$ values represent the temperature sensitivity of the change in the trait value due to an increase by $10^{\circ}\text{C}$ . ....	86
S4.1. Experimental treatments applied monthly during the evolution experiment. All treatments are resource depletion treatments, except for the control and the NaCl treatments. ....	100

S4.2. Light limitation experimental parameter estimates for descendants under each selection treatment.  $\alpha$  is the species' initial response to elevated resource availability,  $\mu_{max}$  is the maximum growth rate under non-limiting light conditions,  $I_{opt}$  is the optimal irradiance for growth and  $I^*$  is the species minimum light requirement. Parameter uncertainty (in parentheses) was measured as the 95% confidence width estimated from 1000 bootstrap values.

..... **101**

S4.3. Nitrogen limitation experimental parameter estimates for descendants under each selection treatment.  $\alpha$  is the species' initial response to elevated resource availability,  $\mu_{max}$  is the maximum growth rate under non-limiting nitrate conditions,  $m$  is the specific growth rate at  $N = 0$  and  $N^*$  is the species minimum nitrate requirement. Parameter uncertainty (in parentheses) was measured as the 95% confidence intervals estimated from 1000 bootstraps. .... **103**

S4.4. Phosphate limitation experimental parameter estimates for descendants under each selection treatment.  $\alpha$  is the species' initial response to elevated resource availability,  $\mu_{max}$  is the maximum growth rate under non-limiting phosphate conditions,  $m$  is the specific growth rate at  $P = 0$  and  $P^*$  is the species minimum phosphate requirement. Parameter uncertainty (in parentheses) was measured as the 95% confidence intervals estimated from 1000 bootstraps. .... **105**

S4.5. Linear model (LM) summary statistics illustrating the independent effects of selection treatment and ancestor on six response variables: (a) descendants minimum light requirements ( $I^*$ ), (b) descendants minimum nitrogen requirements ( $N^*$ ), (c) descendants minimum phosphate requirements ( $P^*$ ), (d) descendants initial response to elevated light availability ( $\alpha$ ), (e) descendants initial response to elevated nitrogen availability ( $\alpha$ ) and (f) descendants initial response to elevated phosphate availability ( $\alpha$ ). Either the selection treatment or the ancestral genotype was treated as fixed effects. .... **107**

S4.6. Results for the Principle Component Analysis evaluating the variation in  $R^*$  and  $\alpha$  under selection by limiting light, nitrogen and phosphate resource. .... **108**



S4.7. Assigned acclimation concentrations for experimental nitrogen and phosphorus concentrations. .... **110**

## **SUPPLEMENTARY METHODOLOGY**

S3.1. Acclimation to nitrogen and parameter estimation in Chapter 3. .... **87**

S4.1. Acclimation to nitrogen and phosphorus and parameter estimation in Chapter 4.  
..... **109**

# CHAPTER 1

## General Introduction

### Climate warming modifies ecological communities

Human activities result in global climate warming, with an estimated surface temperature rise of between 2.6 and 4.8°C by the end of the century (IPCC 2014). Unfortunately, scientists seldom know if, or how quickly populations can respond to changes in the climate (Urban *et al.* 2016) because populations differ greatly in their adaptive potential (Hoffmann and Sgrò 2011, Merilä and Hendry 2014), and ability to track suitable climates into new regions through dispersal and range shifts (Schloss *et al.* 2012). The warming of our climate has a strong impact on freshwater communities in particular because they are often spatially confined, strongly size-structured and dominated by ectotherms, whose contributions to ecosystem functioning largely depend on environmental temperature (Woodward *et al.* 2012). It is therefore pivotal to understand and predict how environmental warming might affect the future properties of freshwater species and communities.

Environmental temperature is one of the fundamental drivers of biological activity, influencing processes at multiple levels of organization, from sub-cellular to entire communities (Eppley 1972, Brown *et al.* 2004, Kingsolver 2009, Dell *et al.* 2011, Kratina *et al.* 2012, Sentis *et al.* 2017). The vital rates of individual populations involved in biotic interactions, may respond differentially to temperature changes (Dell *et al.* 2011), generating cascading effects throughout ecological communities (Harley 2011, Kratina *et al.* 2012). Increased temperatures accelerate the reaction rate of enzymes, where the respiratory rates of heterotrophic organisms are more sensitive to changes in temperature than the photosynthetic rates of autotrophic organisms (Allen *et al.* 2005). Thus greater sensitivity of consumers to temperature, compared to producers can generate a stronger top-down control of food webs, in comparison to resource (bottom-up) control and enhance the strength of consumer-resource interactions (O'Connor 2009, Yvon-Durocher *et al.* 2010, Kratina *et al.* 2012, Eklöf *et al.* 2015). Alternatively, temperature can shift elemental stoichiometry and the uptake rates of resources (Yvon-Durocher *et al.* 2015b),

potentially strengthening bottom-up control of food webs through increased competition of autotrophs for non-substitutable resources.

These changes in bottom-up and top-down control of ecological communities governed by climate warming, can alter the taxonomic composition, distribution and strength of biotic interactions and stability of entire ecosystems (Pawar *et al.* 2012). Therefore understanding how individual species or functional groups respond to temperature is an important step toward forecasting species persistence and community composition in future warmer environments.

### **Resources structure ecological communities**

Resource availability strongly governs the structure, dynamics and temporal stability of ecological communities (Rosenzweig 1971, Ives and Carpenter 2007, Li and Stevens 2017). Climatic or environmental events can cause resource supply to fluctuate (Yang *et al.* 2008, Hastings 2012), so that periods of resource abundance are followed by periods of resource scarcity. The consequences of fluctuating resource abundance are likely to be highly species and context dependent, such that opportunistic generalist species can cope with the environmental change (Li and Stevens 2017). Such variable resource availability can select for populations with high growth rates during resource abundance, a common example of which includes fast growing local phytoplankton blooms, commonly found in eutrophic water (Anderson *et al.* 2002). Over time, competition for a common resource that is in limited supply can result in a superior competitor eliminating inferior populations or species from a location, also known as the competitive exclusion principle (Gause 1934). Competitive exclusion principle states that the number of co-existing species cannot exceed the number of limiting resources (Hardin 1960).

The ability of multiple species to coexist on a few limiting resources, in spite of the tendency for competition that excludes other species is known as the “paradox of the plankton” (Hutchinson 1961). One of the main explanations of the “paradox of the plankton” is that fluctuations in resource availability can enable diverse communities because species differ in their growth strategies, where one species grows fast on abundant resources and another can survive on scarce resources (Hutchinson 1961, Grover 1997, Chesson 2000, Descamps-Julien and Gonzalez 2005). Further explanation of high diversity in phytoplankton communities is that

phytoplankton species differ in their requirements for distinct non-substitutable resources (Tilman 1982, Grover 1997). One such example of this resource partitioning is found in diatoms that are limited chiefly by the availability of silica, whereas other phytoplankton functional groups such as cyanobacteria are not (Reynolds *et al.* 2002). Therefore the variability in the availability of different resource types is important for determining community composition.

Competition for limiting resources may also lead to character displacements among species, where evolution of niche differentiation alleviates the negative influence of resource limitation and competition for limiting resources. Some of the most compelling and important examples of adaptive evolution include Darwin's finches, sticklebacks, and anolis lizards among others (Schluter and McPhail 1992, Losos *et al.* 1998, Grant and Grant 2006). However, because phytoplankton compete for non-substitutable resources that cannot be compensated by the consumption of another resource, competition for a single limiting resource may result in species converging on a single optimum phenotype (Abrams 1987, Vasseur and Fox 2011). Therefore characterising how phytoplankton evolve in response to limiting resource environments is also important for determining community composition.

### **Planktonic communities as a model system**

Plankton are an excellent model system to investigate ecological interactions and population dynamics for a variety of reasons. Planktonic populations show large changes in their population numbers over a short period of time due to their relatively short generation times and high population growth rates (Klausmeier *et al.* 2008, Edwards *et al.* 2013). Zooplankton in particular are key organisms in many lentic ecosystems, due to their strong links to both phytoplankton resources and fish predators (Carpenter *et al.* 2001). Plankton also play a crucial role in the top-down control of phytoplankton species due to their gape-limited feeding, allowing larger phytoplankton to escape predation (Gliwicz and Siedlar 1980). It is relatively easy to collect large amounts of data on the population dynamics of plankton in the field because populations cover large spatial areas, the data of which can then be used to parameterize predictive models (Litchman and Klausmeier 2008).

Phytoplankton have been used to develop and test fundamental ecological principles such as species coexistence (Hutchinson 1961), competition for resources (Tilman 1982) and ecological stoichiometry (Sterner and Elser 2002). At a global scale, phytoplankton are also ecologically important. As major primary producers in most aquatic ecosystems, they are responsible for nearly half of primary production for the planet, form the basis of aquatic food webs, and also influence global cycles of nitrogen and phosphorus among other elements (Falkowski *et al.* 1998, Field *et al.* 1998). Phytoplankton are also sensitive to environmental forcing such as climate change (Falkowski and Oliver 2007). The composition of phytoplankton communities can strengthen or mitigate climate change by fixing atmospheric carbon through photosynthesis (Field *et al.* 1998). The relative abundance of phytoplankton also has profound effects on the trophic dynamics in aquatic ecosystems by altering the relative species abundances at higher trophic levels (Falkowski *et al.* 1998). The supposed simplicity of phytoplankton life histories makes them an ideal system with which to study general ecological questions regarding the effects of biotic and abiotic forcing on community structure and ecosystem function. However, the perceived simplicity of plankton may hide a range of complex interactions that should not be underestimated.

### **Microcosms as experimental ecosystems**

Laboratory microcosms are a useful tool, in particular for the study of population and community dynamics. Experimental microcosms are miniature-constructed ecosystems, which offer a possibility to test ecological concepts involving different levels of organization from the individual populations to community-based extrapolations (Altermatt *et al.* 2015). They enable manipulation of physical and biological factors in a controlled laboratory set up (Drake and Kramer 2012). Many natural communities are too complex to permit the level of replication and control needed to empirically validate ecological theory. Moreover, the type of experimental design is so logistically complex that it is impossible to directly perform them in the field (Altermatt *et al.* 2015). Various groups of organisms, including phytoplankton, bacteria and arthropods are frequently used in model microcosms, to investigate the mechanistic underlying of patterns in predator-prey dynamics, the importance of biodiversity, significance of trade-offs, effects of environmental change on food web

structure and to determine the role of keystone species (Gause 1934, Petchey *et al.* 1999, Gonzalez and Chaneton 2002, Kratina *et al.* 2010, Narwani and Mazumder 2010, 2012). The relatively short generation times of these organisms allow investigations of long-term effects over a relatively short experimental duration. The results of the microcosm studies may be difficult to scale directly to natural conditions, but the findings can be used to identify underlying mechanisms and as well as generate new hypotheses to test in natural conditions (Drake and Kramer 2012).

There are, however, specific challenges associated with microcosm-based experimental work (Carpenter 1996, Schindler 1998, Carpenter 1999). First, it cannot be assumed that the full complexity of an organisms' interactions with its environment can be approximated due to the subset of species included in the microcosms (Drake and Kramer 2012). Reduced complexity of microcosms may eliminate the ability to reliably predict the ecosystem function in question and to directly extrapolate the results from microcosm to the whole natural ecosystem (Carpenter 1996, Schindler 1998). Second, even though microcosm experiments are designed specifically to tease apart one or only a few processes, multiple ecological and environmentally stochastic processes may be acting in concert. This makes it inherently difficult to develop a comprehensive understanding of the whole system, for example the process of species migration (Drake and Kramer 2012, Altermatt *et al.* 2015). Third, processes that act on different spatiotemporal scales may be difficult to tease apart, especially in long-term experiments on large spatial scales. Natural ecosystems have fluctuating environmental conditions (Bulling *et al.* 2006), which may not be fully represented in microcosm experiments that tend to last less than a year (Ricklefs 2004). Due to these shortcomings, a combination of modeling and microcosms is the most ideal approach (Altermatt *et al.* 2015).

### **Using functional traits to predict community structure**

A fundamental goal in community ecology is to understand and predict how environmental change impacts biodiversity and how these changes alter ecosystem functioning. One approach to understanding the mechanisms governing species coexistence and biodiversity in a phytoplankton community is to identify and characterize the key functional traits and trade-offs for multiple species in a

community (Litchman *et al.* 2010). Trait based approaches are being increasingly used to explain community organization along environmental gradients in both aquatic and terrestrial ecosystems (McGill *et al.* 2006, Litchman and Klausmeier 2008), and can be used to leverage sparse data to make more general inferences about unstudied species (Urban *et al.* 2016). Understanding phytoplankton trait diversity is essential because changes in phytoplankton communities inevitably affect higher trophic levels, from zooplankton to fish, biogeochemical cycling and may alter water quality and services that aquatic ecosystems provide to humans (Menden-Deuer and Kiørboe 2016). Species traits measured under the laboratory conditions are good predictors of phytoplankton performance in nature (Edwards *et al.* 2013). Resource utilization traits such as the maximum nutrient uptake rate, half-saturation constant and uptake affinity, in particular are among the key response traits that define the ecological niche of an organism (Chase and Leibold 2003, Litchman and Klausmeier 2008), and different values in these traits correspond to distinct ecological strategies (Sommer 1985, Litchman *et al.* 2007). Investigating how functional traits vary along environmental gradients is therefore an essential prerequisite to predicting how ecological communities may respond to climate change.

In phytoplankton, nutrient acquisition traits and nutrient requirements for population growth are among the major response traits affecting fitness. A variety of studies have linked nutrient physiology to population dynamics through simple mathematical models (Droop 1973, Tilman 1982, Grover 1991). The parameters derived from these models can be measured empirically in the laboratory, and then used to predict the outcome of competition for limiting resources. These parameters therefore represent informative response traits that relate directly to a populations growth. By comparing traits across species, we can identify the important trade-offs defining resource competition.

### **Research aims and thesis organization**

In the following chapters, I describe my efforts to understand how temperature, species diversity and resource limitation affect freshwater planktonic community structure and function by altering the ecological interactions. Whilst the individual effects of these environmental drivers are relatively well understood, little is known

about how these drivers combine to shape community assembly. The thesis chapters address these objectives from a ‘top-down’ perspective. I begin by describing how temperature and species diversity impact ecosystem function as a result of interactions across trophic levels, how temperature alters the competitive interactions among species within a trophic level, how competitive traits evolve within individual species and finally whether trade-offs in competitive traits within a population of the same species also occur between taxonomically different species.

In Chapter 2, I analysed the independent and combined effect of warming and non-resource diversity on a zooplankton-phytoplankton model system to investigate their impact on community structure and ecosystem function. I focused on the concentration of CO<sub>2</sub> in the water, because zooplankton and phytoplankton are important in controlling concentrations of atmospheric CO<sub>2</sub> through changes in the rates of photosynthesis and respiration (Allen *et al.* 2005). I applied structural equation modelling to identify whether the temperature and non-resource diversity directly affect the amount of CO<sub>2</sub> concentrations or whether the effects operated indirectly through changes in the zooplankton-phytoplankton community structure.

In Chapter 3, I examined how temperature alters the minimum requirements of six phytoplankton species for essential limiting resources. I showed that the key traits governing phytoplankton competition for light and nitrogen are strongly temperature-dependent with notable increases in minimum resource requirements at temperatures above the species optima. These temperature-dependent responses are also different across multiple species.

The variation in the traits that govern resource competition within a single species may be important and possibly as large as the variation among species. In chapter 4, I therefore used an established model species, *Chlamydomonas reinhardtii*, to investigate the evolutionary response of competitive traits of many environmentally selected populations to resource limitation. I showed that resource requirements of individual populations respond to selection under different resource availability. In particular, populations selected under nitrogen limitation resulted in the adaptation of low requirements of nitrogen. I discuss the importance of the intraspecific variability within ecological communities as a signature of the previous selection environment.



Chapter 5 provides a general summary and discussion of the main results from all data chapters and places these findings into the broader context of global environmental change and species diversity. Biological mechanisms such as the life history and evolutionary potential of a species are fundamentally important in mediating present and future responses to abiotic environmental variation (Urban *et al.* 2016). This thesis fills some of the gaps in empirical data and advances our current mechanistic understanding of the affect of environmental change on the diversity of freshwater planktonic communities.

## CHAPTER 2

### **Diversity and Temperature Indirectly Reduce CO<sub>2</sub> Concentrations in Experimental Freshwater Communities**

#### **Abstract**

Biodiversity loss and climate warming are occurring in concert, with potentially profound impacts on ecosystem functioning. We currently know very little about the combined effects of these changes on the links between the community structure, dynamics, and the resulting *in situ* CO<sub>2</sub> concentrations in freshwater ecosystems. We performed a simple food web experiment, where we analyzed the responses of freshwater phytoplankton, zooplankton, and dissolved CO<sub>2</sub> to factorially manipulated gradients of inedible/non-resource species diversity and environmental temperature. We aimed to determine the individual and combined effects of temperature and non-resource diversity on CO<sub>2</sub> concentration, either directly, or indirectly via influences on the phytoplankton and zooplankton biomass. There were no interactive effects of temperature and diversity on CO<sub>2</sub> concentration in the water. Increases in both temperature and non-resource diversity independently decreased CO<sub>2</sub> concentrations, with a substantial reduction in CO<sub>2</sub> concentrations at the highest non-resource diversity. A structural equations model showed that the effects of non-resource diversity and warming on CO<sub>2</sub> were indirect, resulting largely from the positive impacts on total biomass of primary producers. Our study is the first to experimentally partition the impacts of temperature and diversity, providing a mechanistic insight into the role of diverse plankton communities for ecosystem functioning and their importance in regulating CO<sub>2</sub> dynamics under ongoing climate warming.

## **Introduction**

Biodiversity loss and climate warming are both occurring simultaneously, and at unprecedented rates (Butchart *et al.* 2010, IPCC 2014). Yet, very little is known about their combined effects on community structure, dynamics, and on the flux of *in situ* CO<sub>2</sub> between aquatic systems and the atmosphere (Traill *et al.* 2010, Atwood *et al.* 2015). A detailed assessment of the relationship between community structure and ecosystem function across diversity and temperature gradients is pivotal to improving our understanding of the role that biodiversity can play in mitigating the impact of climate warming.

Human activities have increased the concentrations of heat-trapping gases in the atmosphere, inducing global climate warming. There is no evidence of a reduction in the rate of global surface warming, known as the ‘warming hiatus’, indicating that climate warming is still accelerating (Karl *et al.* 2015). Climate models forecast mean rises in global surface temperatures of 1.5°C to 4.5°C by the year 2100, with CO<sub>2</sub> being the main contributor (Meinshausen *et al.* 2011, IPCC 2014). Freshwater communities are particularly sensitive to warming because they are often spatially confined, strongly size-structured and dominated by ectotherms, whose contributions to ecosystem functioning largely depend on environmental temperature (Woodward *et al.* 2012). Ectotherms include diverse phytoplankton taxa that play a key role in carbon sequestration in freshwaters, through primary production (Kratina *et al.* 2012, Low-Décarie *et al.* 2014, Davidson *et al.* 2015, Low-Décarie *et al.* 2015).

Changes in plankton interaction networks, via climate warming or biodiversity loss, alter the ratio of heterotrophs to autotrophs and shift the rates of photosynthesis and community respiration - two biological processes that drive the global carbon cycle and concentrations of atmospheric CO<sub>2</sub> (Allen *et al.* 2005). Greater sensitivity of consumers to temperature, compared to producers, can amplify top-down control by increasing interaction strengths (O'Connor *et al.* 2009, Kratina *et al.* 2012, Eklöf *et al.* 2015). Increased herbivory can indirectly enhance emissions of CO<sub>2</sub> into the atmosphere by reducing the phytoplankton biomass, thus reducing the rate of carbon sequestration (Atwood *et al.* 2013). Alternatively, zooplankton grazing on phytoplankton could weaken at higher temperatures due to the stronger

temperature dependence of metabolism than feeding in consumers (Rall *et al.* 2010, Fussmann *et al.* 2014). Depending on the relative impacts of temperature on trophic interactions and community structure, warming may either reduce or increase CO<sub>2</sub> concentrations in aquatic ecosystems.

Species diversity may alter the effects of warming on community structure, dynamics and CO<sub>2</sub> concentration. For example, lakes with diverse phytoplankton communities contain many species that are inedible to herbivorous zooplankton (Hillebrand and Cardinale 2004). These ‘non-resources’ are species outside of the focal consumer-resource relationship that may interfere with zooplankton foraging, effectively reducing the strength of top-down control (Kratina *et al.* 2007, Narwani and Mazumder 2010, 2012), enhancing food web stability and persistence (Narwani and Mazumder 2012, Hammill *et al.* 2015). Consequently, the increased biomass of phytoplankton resource and non-resource species can enhance sequestration of CO<sub>2</sub>, thereby reducing its concentration in the water (Davidson *et al.* 2015). However, we currently know very little about the combined effects of diversity and temperature on ecological community structure and dynamics, and particularly on the resulting changes in *in situ* CO<sub>2</sub> concentrations. The carbon metabolism and carbon balance are inherently dynamic processes but it is unknown how closely CO<sub>2</sub> concentrations track the dynamics of plankton communities.

Previous research has only examined the independent effects of diversity (Naeem *et al.* 1994, Schleuss *et al.* 2014) and temperature (Davidson and Janssens 2006) on carbon storage in terrestrial ecosystems, despite the fact that freshwater ecosystems emit a similar amount of CO<sub>2</sub> due to changing land-use patterns (Cole *et al.* 2007). Only one previous study has investigated the combined effect of species richness and temperature on multiple ecosystem processes in aquatic environments (Perkins *et al.* 2015). The authors investigated the diversity of benthic macro invertebrates and found that at the low and high temperature, multifunctionality increased with species richness so that approximately two species were required to drive an additional ecosystem process (Perkins *et al.* 2015). However, this work did not monitor consumer, resource, non-resource or CO<sub>2</sub> dynamics and did not establish the temporal link between the CO<sub>2</sub> dynamics and community structure.

Here, we experimentally tested both the independent and interactive effects of temperature and gradients of non-resource diversity on several causal pathways (changes in plankton community structure) that affect CO<sub>2</sub> concentration.

Corresponding time-series of phytoplankton biomass, consumer and resource densities and CO<sub>2</sub> concentrations were established for 96 experimental plankton communities. We hypothesized that higher temperature causes an indirect increase of CO<sub>2</sub> concentration in the water by enhancing consumer respiration and intensifying consumer grazing on phytoplankton. By contrast, we expected that non-resource diversity indirectly reduce CO<sub>2</sub> concentration by weakening the consumer-resource interactions, increasing autotroph biomass and fixing CO<sub>2</sub> through photosynthesis. A greater freshwater carbon storage capacity can result from plant biomass being deposited in the sediment, thus escaping decomposition and re-mineralization in the water column. These hypothetically antagonistic impacts of temperature and diversity have the potential to further exacerbate or mitigate ongoing climate warming.

## **Methods**

### **(a) Model communities and experimental design**

We used the freshwater filter-feeding zooplankton *Daphnia pulex* (hereafter ‘*D. pulex*’ or ‘consumer’) feeding on the freshwater green algae *Chlorella vulgaris* (hereafter ‘*C. vulgaris*’ or ‘resource’) as our consumer-resource model system. *Daphnia* is a key zooplankton in many lentic ecosystems, with strong links to both phytoplankton resources and fish predators (Carpenter *et al.* 2001). The experimental design consisted of four-phytoplankton diversity treatments consisting of 0 (only *C. vulgaris*), 2, 4 and 8 non-resource species, assembled into two different community compositions (A and B; Table 2.1). The two community compositions allowed us to test the effect of diversity *per se*, as there may be variation in the composition of natural communities. The 14 species used in the non-resource phytoplankton species pool were selected for the following reasons (i) their cell (or colony) size was larger than ~45 µm and were therefore less easily consumed by *D. pulex* (Burns and Gilbert 1986, Narwani and Mazumder 2010); (ii) the species exist in combinations that represent communities that occur naturally (US EPA’s National Lakes Assessment survey, Table S2.1); (iii) species could be distinguished morphologically under a microscope. Due to the limited size of the species pool, the two 8 non-resource species treatments inevitably shared some species with the 4 and

2 non-resource species compositions (Table 2.1). The original sources of the phytoplankton taxa and their relative inoculation biovolumes can be found in Table S2.1.

All non-resource diversity treatments and species compositions were maintained at different temperatures in separate incubators (Stuart SI500, Orbital) set to 19°C, 23°C and 27°C. Preliminary studies were used to determine the range of temperatures that enabled positive growth rates of all consumer, resource and non-resource species in monoculture. Incubators were lit with cool white LED light panels (Mirrorstone™) set to a 12h light: 12h dark cycle. Each LED light panel emitted ca.  $100 \mu\text{mol m}^{-2} \text{s}^{-1}$  of Photosynthetically Active Radiation (PAR). We collected 60 mL samples twice a week for 8 weeks, resulting in 16 temporal samples. The experiment consisted of two blocks (due to space limitation in the incubators) and all treatment combinations were replicated twice in each block, yielding a total of 96 experimental units (4 diversity treatments x 2 community compositions x 3 temperatures x 2 replicates x 2 blocks = 96).

**Table 2.1.** Experimental phytoplankton community compositions with individual species for each non-resource diversity treatment. The 0 non-resource diversity treatment received only resource species *C. vulgaris*. All experimental assemblages received an equal amount of resource species *C. vulgaris* ( $1.6 \times 10^6$  ESD) and had equivalent total biovolume of non-resource species ( $8 \times 10^5$  ESD) in the 2, 4 and 8 diversity treatments.

No. of non-resource phytoplankton species	Phytoplankton species	
	Composition A	Composition B
2	<i>Closterium acerosum</i>	<i>Micrasterias crux-melitensis</i>
	<i>Cosmarium botrytis</i>	<i>Staurastrum pingue</i>
4	<i>Closterium acerosum</i>	<i>Closterium littorale</i>
	<i>Cosmarium botrytis</i>	<i>Eudorina elegans</i>
	<i>Micrasterias crux-melitensis</i>	<i>Micrasterias crux-melitensis</i>
	<i>Mougeotia sp.</i>	<i>Staurastrum pingue</i>
8	<i>Closterium acerosum</i>	<i>Ankistrodesmus falcatus</i>
	<i>Cosmarium botrytis</i>	<i>Closterium littorale</i>
	<i>Eremosphaera viridis</i>	<i>Cosmarium botrytis</i>
	<i>Eudorina elegans</i>	<i>Eremosphaera viridis</i>
	<i>Micrasterias crux-melitensis</i>	<i>Eudorina elegans</i>
	<i>Mougeotia sp.</i>	<i>Micrasterias crux-melitensis</i>
	<i>Pediastrum duplex</i>	<i>Staurastrum pingue</i>
	<i>Staurastrum pingue</i>	<i>Volvox aureus</i>

### (b) Inoculation densities and biovolumes

Phytoplankton species were grown in batch monocultures in Bold's Basal Medium (BBM) and the zooplankton were grown in batch culture with the green alga *Chlamydomonas reinhardtii* in Volvic Mineral Water (Volvic, France), which closely resembles the chemical composition of natural lake water (see Table S2.2). Prior to the start of the experiment, we measured the density and mean biovolume (estimated as the equivalent spherical diameter, 'ESD') of 30 natural units (cells, colonies or filaments) of each monoculture in the species pool, at stationary phase, with a stage micrometer. Species biovolumes were calculated using equations based on body shape and cell size of each phytoplankton species (Hillebrand *et al.* 1999). Experimental microcosms received a constant resource (*C. vulgaris*) biovolume of  $1.6 \times 10^6 \mu\text{m ESD}$  and a total biovolume of  $8 \times 10^5 \mu\text{m ESD}$  of all other appropriate species in the mixture, split equally between all non-resource species present (Table

1, Table S2.1). This approach ensured that higher diversity treatments received the same total biovolume as the lower diversity treatments, regardless of different phytoplankton cell size. Each microcosm also received seven *D. pulex*, which were first acclimated to their assigned temperature treatment for three days prior to the experiment.

Experimental communities were established in 1L glass media bottles filled with sterile Volvic Mineral Water, that were randomly distributed within the incubators. We used commercial spring water for the experimental medium as preliminary tests using BBM resulted in extremely high phytoplankton densities and the rapid extinction of the zooplankton consumers. Media bottle tops were modified with small holes on the sides, large enough to prevent lethal build-up/depletion of gases. However, the holes were small enough to prevent evaporative losses and minimize bacterial contamination. Side holes were only exposed when microcosms were inside the incubators, which had previously been sanitized with 70% ethanol.

### **(c) Sampling and sample processing**

To homogenize the experimental communities and to ensure a representative sample, the microcosms were inverted and gently shaken, prior to each sampling, with bottle tops securely fastened and without the air holes exposed. All sampling and media replacement was done using sterile technique in a vertical lamina flow cabinet (PCR6, Labcaire), to prevent contamination. Each sample was microscopically inspected to ensure that there was no contamination of cultures with bacteria, fungi or protozoa over the duration of the study.

Each 60mL sample was divided up into smaller sub-samples, to measure the CO<sub>2</sub> concentration in the water, the density of consumer and resource and the total phytoplankton biomass. We estimated the phytoplankton biomass as chlorophyll-*a* concentration, because counting densities of all individual non-resource species over time was not logistically feasible. To measure CO<sub>2</sub> concentration, the sample was transferred to 3 mL gastight vials (Labco), which were then sealed. Samples were taken during the light cycle to represent maximum CO<sub>2</sub> uptake. A 500 µL headspace was introduced by withdrawing the sample and simultaneously replacing with 500 µL of oxygen free nitrogen via a needle and 3-way valve. After equilibration (30 minutes shaking), 100 µL samples were withdrawn from the headspace and injected into a gas chromatograph (GC) fitted with a flame-ionisation detector (Agilent



Technologies; for details see Sanders *et al.* (2007). Headspace concentrations of CO<sub>2</sub> were calculated from peak areas calibrated against known standards (Scientific and Technical Gases), and the total amount in the vial (headspace plus sample) was calculated using solubility coefficients (Weiss 1974, Yamamoto *et al.* 1976). Final CO<sub>2</sub> concentrations were corrected for media addition days by subtracting the concentration of CO<sub>2</sub> measured in control microcosms (only media without living organisms), measured at each experimental temperature treatment.

To estimate consumer density over time, two observers checked each experimental community for the presence of *D. pulex*. If *D. pulex* were present at low density, i.e. fewer than 20 individuals, we counted all the individuals in the microcosms (1L). If there were a greater number of individuals, we counted the number of individuals in the 60 mL sub-sample. To measure resource density (number of *C. vulgaris* cells), 10 mL sub-samples were fixed with Lugol's iodine solution. *C. vulgaris* density was estimated by counting cells using a haemocytometer under a compound light microscope at 40x magnification. To estimate total phytoplankton biomass, we filtered 30 mL sub-sample onto glass fiber filters (Whatman, Grade 1, 25mm) and stored them at -20°C. We extracted the chlorophyll-a in acetone (90% v/v with ultra high purity water) for 24 h in a dark refrigerator. We used a spectrophotometer and measured absorption of light at 665 nm (Dalsgaard 2000). We replaced the volume sampled with 120 mL of sterile Volvic water starting from day 10, and continuing weekly. After each sampling event, bottles were placed back into incubators (with lids exposing air holes to allow gas exchange) in a haphazard fashion to eliminate edge effects.

#### **(d) Statistical analyses**

We analyzed the independent and interactive effects of non-resource diversity and environmental temperature on four continuous response variables: (i) time-averaged consumer density (number of individuals per L), (ii) time-averaged resource density (number of *C. vulgaris* cells per mL), (iii) time-averaged total phytoplankton biomass (aggregated biomass of all phytoplankton taxa in the community), and (iv) time-averaged concentration of CO<sub>2</sub> (amount of CO<sub>2</sub> in the water).

To illustrate the effects of the treatments and their interactions, we used linear mixed effects (LME) models with non-resource diversity and environmental temperature as fixed effects. We accounted for the temporal blocks, non-resource

community composition and position of the microcosms in the incubators as random effects. We used the *varIdent* function to improve homogeneity of variance in the model fit (Zuur *et al.* 2009). This model represented a good fit to the data for all response variables, as denoted by the  $R^2$  values (Nakagawa and Schielzeth 2013) (Table S2.3). Moreover, we fit this LME model to the time-series across the entire experiment and included time into the random factor term (Table S2.4). We also fit this same LME model to the time-series that accounted for temporal autocorrelation instead of time in the random factor term. Statistical outcomes of LME's including all time-series data with and without temporal autocorrelation, and time-averaged data were qualitatively identical; therefore we present the time-averaged model outputs only (Table S2.3). All analyses were performed in R 3.2.3 (R Development Core Team, 2016), using the function *lme* in the package *nlme*; and *r.squaredGLMM* in the package *MuMIn*.

We then tested whether temperature had a direct effect on CO<sub>2</sub> concentration due to the lower solubility of CO<sub>2</sub> at higher temperatures (Wiebe and Gaddy 1940), or indirect effect due to the shift in community structure. To separate the physico-chemical effects from the biological effects of community structure, we adjusted the entire data set to the lowest temperature treatment (19°C), therefore CO<sub>2</sub> concentrations measured at 23°C were increased by 10.2% and CO<sub>2</sub> concentrations measured at 27°C were increased by 20.5%. This adjustment was based on the CO<sub>2</sub> measurements in control microcosms with no organisms and incubated at the three experimental temperatures. We then applied a piecewise structural equation modeling (SEM) approach (Lefcheck 2016) to both corrected and uncorrected data to test whether the changes in CO<sub>2</sub> concentrations resulted directly from the experimental diversity and temperature manipulations, indirectly through the changes in community structure or from the effect of temperature on CO<sub>2</sub> solubility (Atwood *et al.* 2015). The path diagrams (Fig. S2.1. Supplementary material) were expressed as a set of biologically relevant, linear structured equations, which reflected our hypotheses and were then evaluated individually. SEMs incorporated random effects of block, position in the incubator, non-resource composition and an additional temporal autocorrelation term for each day of the experiment. To test the directed separation of linear models, a Fisher's C test was performed following the piecewise SEM function proposed by Lefcheck (2016). The Fisher's C statistic was then used to obtain AIC values. We compared seven different models and selected

the model with the lowest AIC score, representing the best fit to our data (model 1, Table S2.5). The piecewise SEM returned parameter estimates and partial correlations, allowing our hypotheses to be tested at a significance level  $\alpha = 0.05$  (Fig. S2.1).

## **Results**

### **(a) Ecosystem function**

Higher non-resource diversity (LME,  $F_{1, 89} = 9.719$ ,  $P < 0.001$ ; Fig. 2.1a, Table S2.3) and elevated temperature (LME,  $F_{1, 89} = 48.942$ ,  $P < 0.001$ ; Fig. 2.2a, Table S2.3) both independently reduced time-averaged CO<sub>2</sub> concentration in the water. There was no interactive effect of temperature and diversity on time-averaged CO<sub>2</sub> concentration (LME,  $F_{1, 89} = 0.838$ ,  $P = 0.407$ ; Table S2.3). There were significant differences in CO<sub>2</sub> concentrations only between the highest (8 non-resource) diversity treatment and all other diversity treatments (Fig. 2.1a). The 8 non-resource diversity treatment reduced CO<sub>2</sub> concentration by 15.4% compared to treatment with 0 non-resource. CO<sub>2</sub> concentration declined by 14.9% when temperature was raised from 19°C and 23°C, by 27.1% when temperature was raised from 19°C to 27°C, but did not change when temperature was raised from 23 to 27°C (Fig. 2.2a).

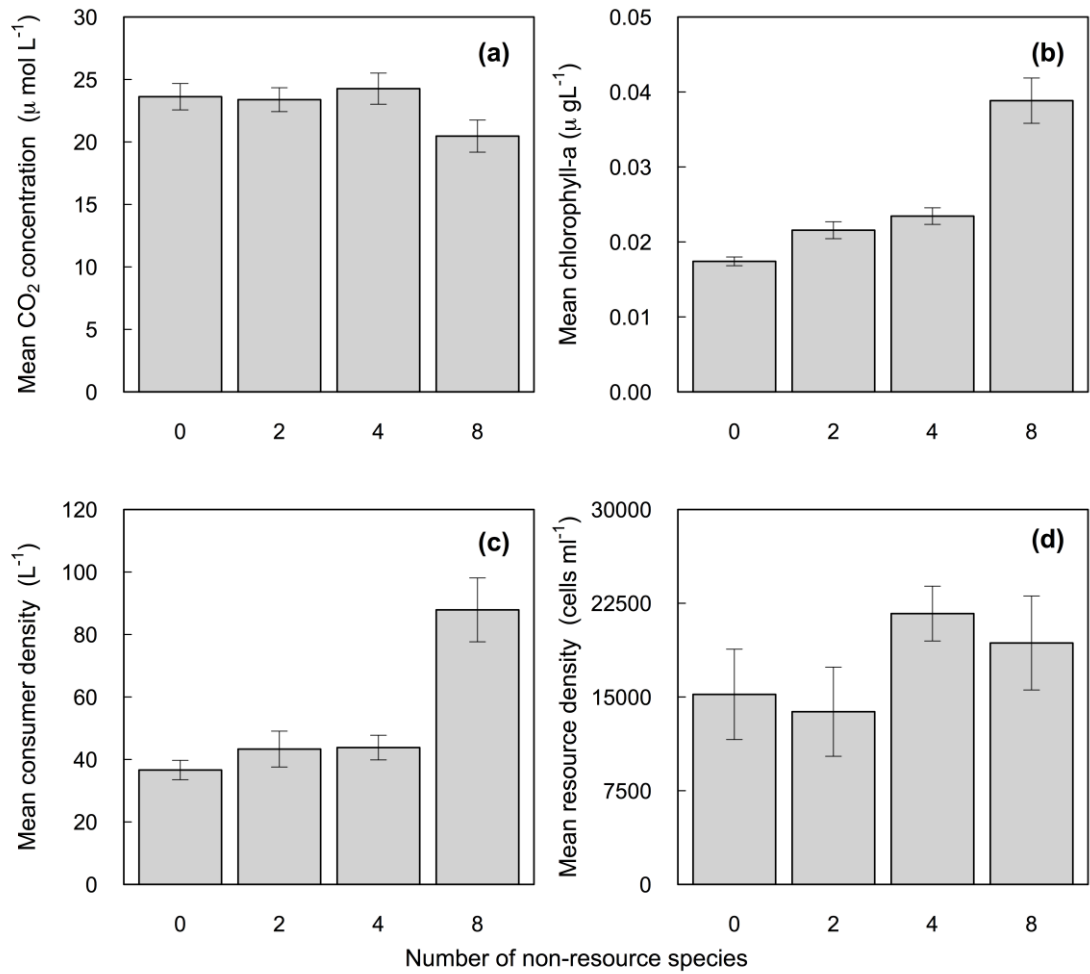


**Figure 2.1.** The effects of non-resource diversity on time-averaged CO<sub>2</sub> concentration (a), time-averaged total phytoplankton biomass (b), time-averaged consumer density (c) and time-averaged resource density (d). Each bar represents means across all time points and temperature treatments (n = 24 replicates); error bars represent  $\pm 1$  standard error.

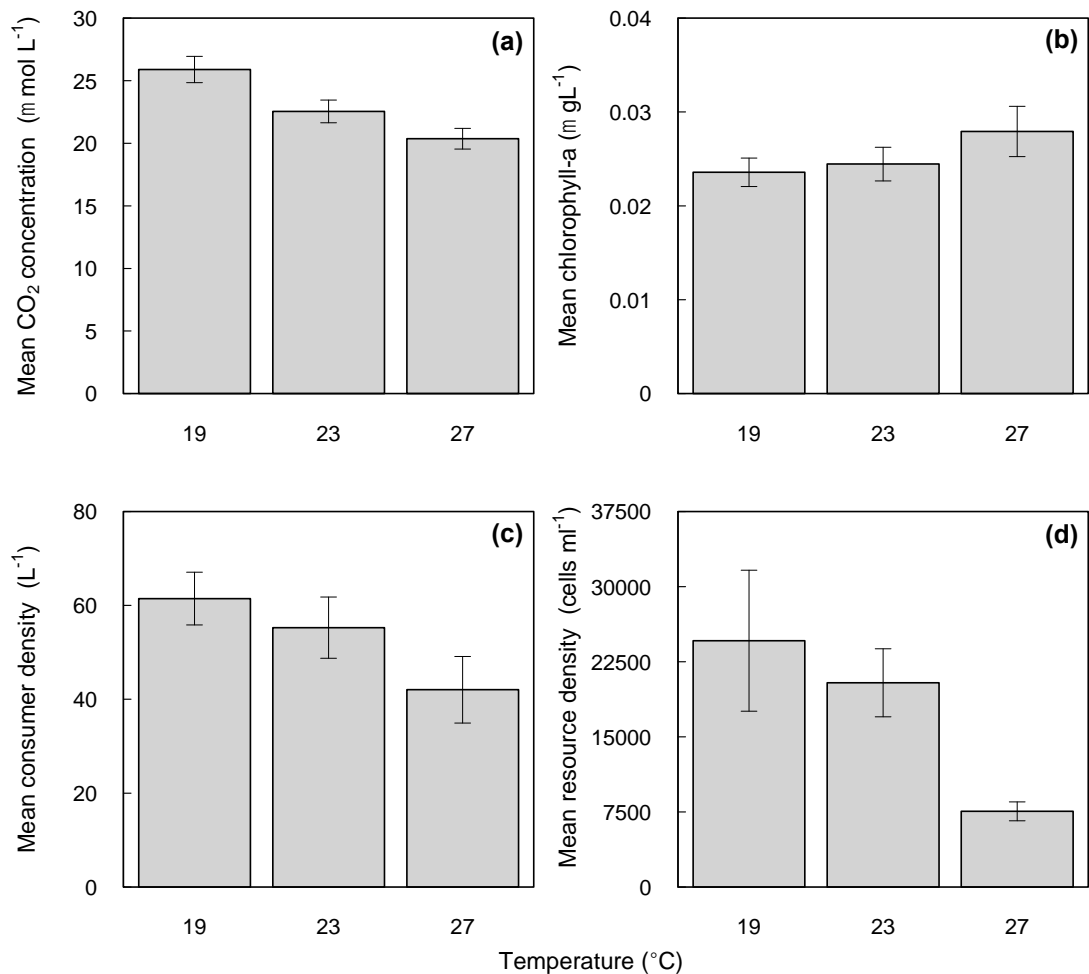


**Figure 2.2.** The effects of environmental temperature on time-averaged CO<sub>2</sub> concentration (a), time-averaged total phytoplankton biomass (b), time-averaged consumer density (c) and time-averaged resource density (d). Each bar represents means across all time points and diversity treatments (n = 32 replicates); error bars represent  $\pm 1$  standard error.

### (b) Community structure

Alongside a reduction in time-averaged CO<sub>2</sub> concentration, total phytoplankton biomass (LME,  $F_{1, 89} = 60.931$ ,  $P < 0.001$ ; Fig. 2.1b, Table S2.3) and consumer density (LME,  $F_{1, 89} = 13.333$ ,  $P < 0.001$ ; Fig. 2.1c, Table S2.3) increased significantly in the 8 non-resource species diversity treatment. However, resource density was not affected by non-resource diversity (LME,  $F_{1, 89} = 1.309$ ,  $P = 0.256$ ; Fig. 2.1d, Table S2.3). Temperature had a positive effect on time-averaged total phytoplankton biomass (LME,  $F_{1, 89} = 3.788$ ,  $P = 0.050$ ; Fig. 2.2b, Table S2.3) and consumer density (LME,  $F_{1, 89} = 20.358$ ,  $P < 0.001$ ; Fig. 2.2c, Table S2.3), but had a

negative effect on resource density (LME,  $F_{1, 89} = 10.023$ ,  $P = 0.002$ ; Fig. 2.2d, Table S2.3).

### **(c) Direct and indirect effects of diversity and temperature**

Before accounting for reduced CO<sub>2</sub> solubility at higher temperatures, SEM showed a direct negative effect of temperature on CO<sub>2</sub> concentration (-0.21, Fig. 2.3a), i.e. an increase of 1 x standard deviation (SD) in temperature resulted in a decrease of 0.21 SD in the concentration of CO<sub>2</sub> in the water. However, after accounting for CO<sub>2</sub> solubility, the direct effect of temperature disappeared and SEM analyses instead supported the indirect negative effects of temperature (standardized  $\beta = -0.04$ ,  $P = 0.314$ ) and diversity (standardized  $\beta = -0.08$ ,  $P = 0.063$ ) on CO<sub>2</sub> concentration via shifts in the community structure (Fig. 2.3b). In agreement with our predictions, diversity enhanced the total phytoplankton biomass (standardized  $\beta = 0.36$ ,  $P < 0.001$ ) and resource density (standardized  $\beta = 0.08$ ,  $P = 0.045$ ), indirectly reducing the CO<sub>2</sub> concentration (standardized  $\beta = -0.11$ ,  $P < 0.001$  and standardized  $\beta = -0.10$ ,  $P < 0.001$ , respectively). Furthermore, the indirect negative effect of diversity on CO<sub>2</sub> via total phytoplankton biomass (-0.040, Fig. 2.3b) was more important than the indirect negative effect of temperature (-0.012, Fig. 2.3b).

Density of consumers was also increased by non-resource diversity (standardized  $\beta = 0.26$ ,  $P < 0.001$ ), increasing the CO<sub>2</sub> concentration (standardized  $\beta = 0.06$ ,  $P = 0.021$ ). The positive indirect effect of diversity on CO<sub>2</sub> mediated through increased consumer density (0.016, Fig. 2.3b) was smaller than the negative effect on CO<sub>2</sub> mediated through increased total phytoplankton biomass (-0.040, Fig. 2.3b). Temperature enhanced total phytoplankton biomass (standardized  $\beta = 0.11$ ,  $P = 0.009$ ), and reduced resource (standardized  $\beta = -0.10$ ,  $P = 0.012$ ) and consumer densities (standardized  $\beta = -0.13$ ,  $P < 0.001$ ), causing a net reduction in CO<sub>2</sub> concentration. The negative effect of temperature on consumer was weaker than the positive effect of diversity, leading to a net positive effect of consumers on CO<sub>2</sub> concentrations in the high diversity and high temperature treatments. There was no direct effect of consumer on resource density (standardized  $\beta = -0.03$ ,  $P = 0.290$ ).

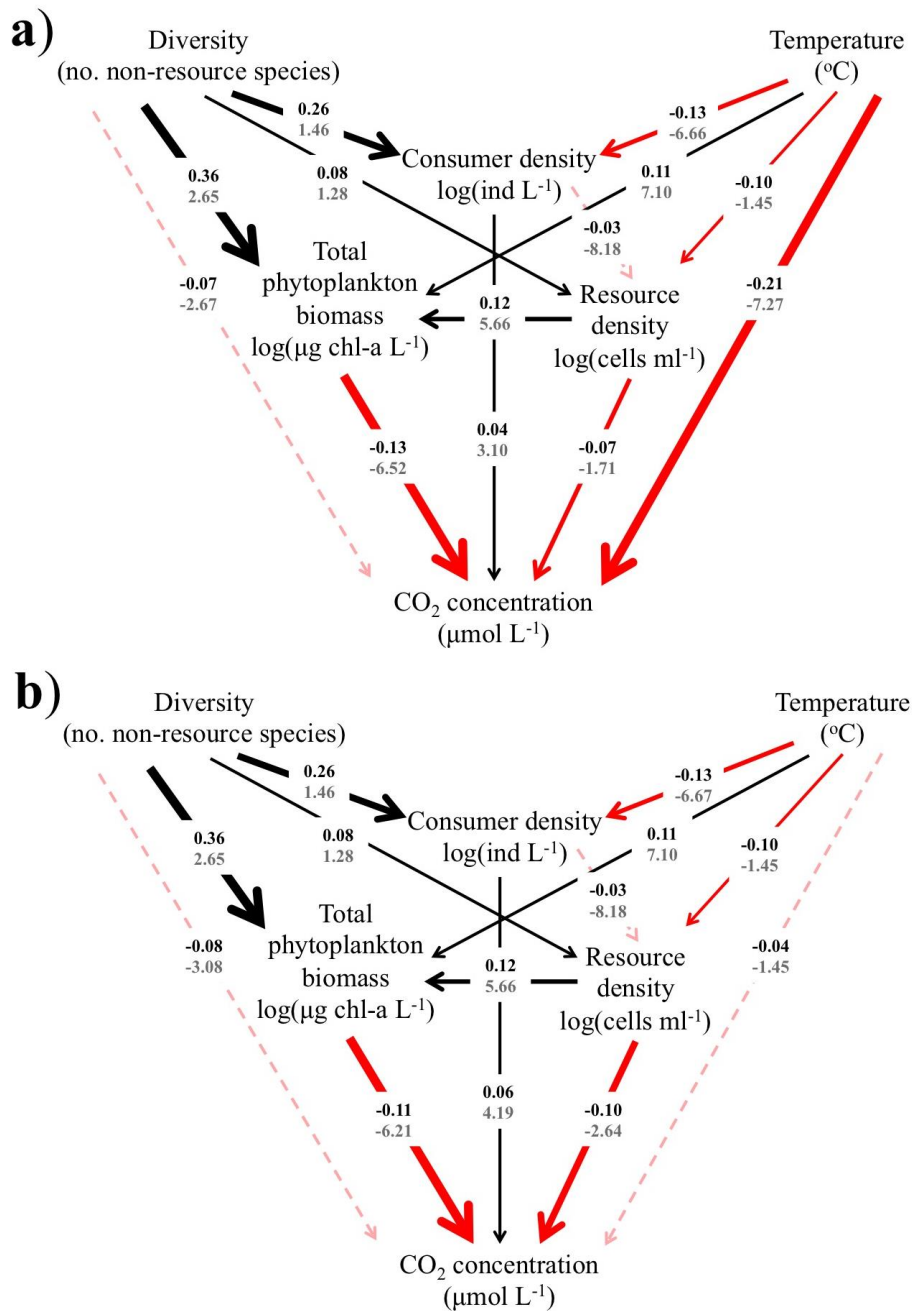


**Figure 2.3.** The best-fit structural-equation model (SEM) showing how the covariance's among the variables predict the pathway of outcome of CO<sub>2</sub> concentration. (a) Before correction for the effect of temperature on CO<sub>2</sub> solubility in the water, the SEM retains a significant direct effect of temperature on CO<sub>2</sub> concentration. (b) After correction for the effect of temperature on CO<sub>2</sub> solubility, the SEM retains only an indirect effect of temperature on CO<sub>2</sub> concentration. Significant direct pathways are displayed as solid lines ( $P < 0.05$ ), while non-significant direct pathways are displayed as dashed lines. Red lines denote the

negative effects; black lines denote the positive effects. The strength of the effect is proportional to the thickness of the lines and represented as the magnitude of the regression coefficients. Two types of path coefficients are placed next to corresponding pathways. Standardized regression coefficients (bold, black font) represent the standard deviation change in variable  $Y$  per unit change in variable  $X$ . Unstandardized regression coefficients (grey font) represent the standard deviation change in  $Y$ , given a standard deviation change in  $X$ . The amount of variation explained by the models was (a)  $R^2 = 0.30$  for consumer density,  $R^2 = 0.16$  for total phytoplankton biomass,  $R^2 = 0.23$  for  $\text{CO}_2$  concentration and  $R^2 = 0.02$  for available resources; (b)  $R^2 = 0.30$  for consumer density,  $R^2 = 0.16$  for total phytoplankton biomass,  $R^2 = 0.26$  for  $\text{CO}_2$  concentration and  $R^2 = 0.02$  for available resources.

#### **(d) Community dynamics**

The temporal changes in  $\text{CO}_2$  concentration were associated with concurrent changes in the plankton community structure (compare Figs. 2.4 and 2.5). The  $\text{CO}_2$  peak around day 20 coincided with an increase in consumer density, and a decline in available resource (Fig. 2.5). After this peak observed in all treatments combinations, the highest non-resource diversity treatment diverged from the other treatments, with its  $\text{CO}_2$  concentration declining closer to the atmospheric equilibrium compared to lower non-resource diversity treatments (Fig. 2.4a).



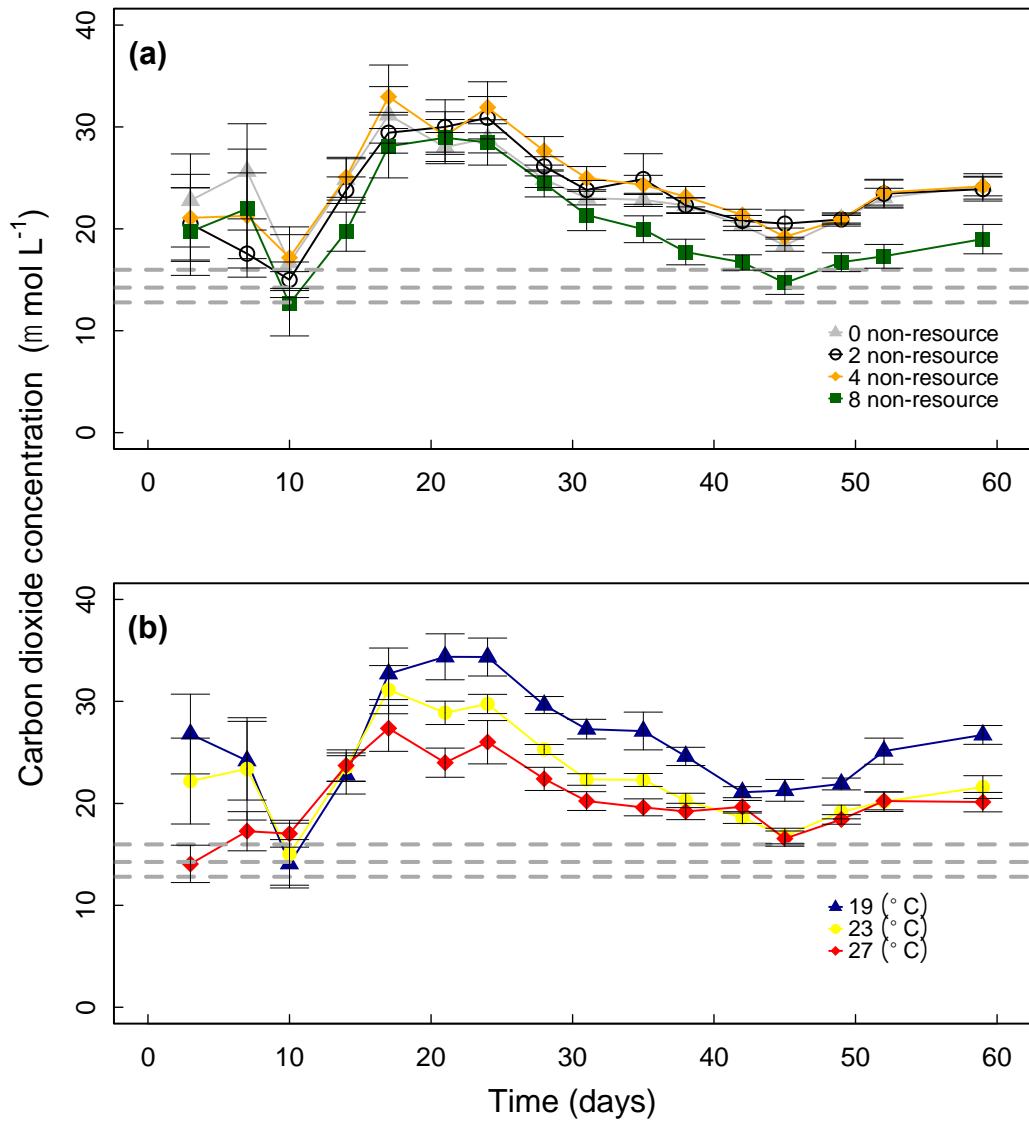


**Figure 2.4.** The independent effects of non-resource diversity (a) and environmental temperature (b) on the temporal dynamics of CO<sub>2</sub> concentration. Points represent mean of 24 replicates  $\pm$  1 standard error for each diversity treatment level and 32 replicates  $\pm$  1 standard error for each temperature treatment level. Dashed lines represent CO<sub>2</sub> concentration at 19°C, 23°C and 27°C, atmospheric equilibration is 15.98  $\mu\text{mol L}^{-1}$ , 14.24  $\mu\text{mol L}^{-1}$  and 12.79  $\mu\text{mol L}^{-1}$  respectively. a) Higher non-resource diversity (LME,  $F_{1, 89} = 9.719$ ,  $P < 0.001$ ) and b) elevated temperature (LME,  $F_{1, 89} = 48.942$ ,  $P < 0.001$ ) both independently reduced mean CO<sub>2</sub> concentration in the water.

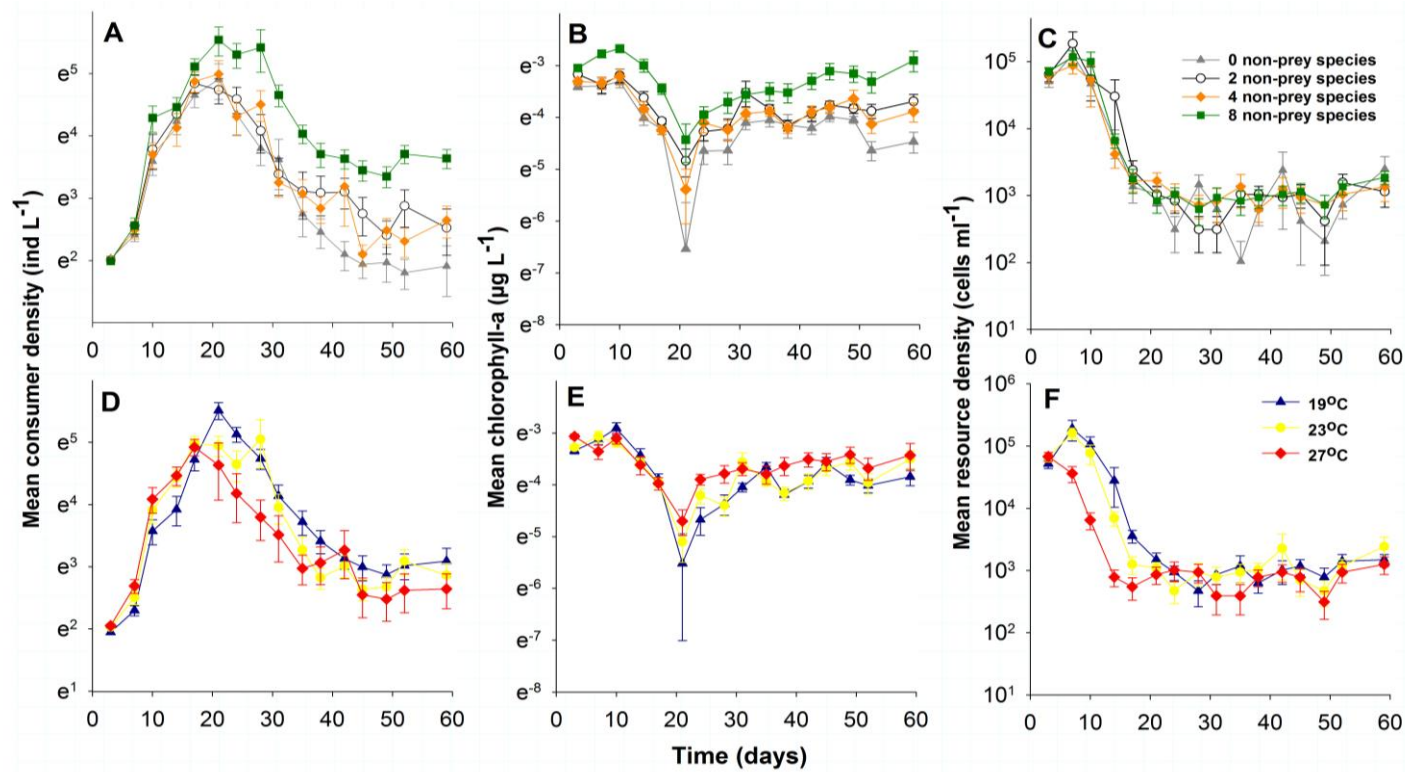


**Figure 2.5.** The effect of non-resource diversity (a-c) and temperature (d-f) on the community dynamics of consumer density (d and d), total phytoplankton biomass/chlorophyll-a (b and e) and resource density (c and f). Points represent mean of 24 replicates  $\pm$  1 standard error for each diversity treatment and 32 replicates  $\pm$  1 standard error for each temperature treatment.

## Discussion

We show that the responses of plankton community structure to temperature and diversity gradients can govern the dynamics of CO<sub>2</sub> concentrations in experimental freshwater communities. The effects of consumers and producers (phytoplankton biomass) were both driven by phytoplankton non-resource species diversity. Although consumers did not significantly modify the standing stock of resource (Fig. 2.3), increased resources in the high diversity treatment were likely incorporated into the consumers, allowing an increase in consumer population density (Fig. S2.4).

Mean CO<sub>2</sub> concentration, consumer density, and total phytoplankton biomass differed only when 8 non-resource species were included in the experimental community. This suggests that diversity effects on some communities and ecosystem processes may only become evident after reaching a specific threshold. The existence of a diversity threshold has been documented in consumer assemblages, with effects becoming apparent only at the highest diversities containing six species (Duffy *et al.* 2003). Although our highest diversity treatment reduced CO<sub>2</sub> concentration to values closer to atmospheric equilibration (Fig. S2.2), the experimental systems were still a net source of CO<sub>2</sub>. This corresponds to the majority of freshwater lakes that are supersaturated with CO<sub>2</sub> relative to the atmosphere, allowing a net flux of CO<sub>2</sub> from the water column to the air by a concentration gradient (Cole and Caraco 1998, Cole *et al.* 2007). However it is important to note that the supersaturating effect of CO<sub>2</sub> relative to the atmosphere may also be due to the sampling methodology carried out. Measurements of CO<sub>2</sub> were taken in the morning after a period of darkness, such that in the period preceding measurements, heterotrophic processes would have dominated, allowing the microcosms to be supersaturated with CO<sub>2</sub> in the morning. The random selection of non-resource species in the diversity compositions also contributed to the variation in each response variable (Fig. S2.5). Community composition B with 8 non-resource species had higher consumer density and phytoplankton biomass than composition A with 8 non-resource species (Fig. S2.5).

In addition to the diversity effect *per se*, phytoplankton community compositions with the highest diversity, also likely altered the CO<sub>2</sub> concentration in the water, as indicated by the higher consumer density and total phytoplankton biomass in community composition B than in composition A (Fig. S2.5). Species

identity can affect the long-term dynamics of edible (Behl and Stibor 2015) and inedible (Narwani and Mazumder 2010) phytoplankton, and plays a major role in the net biodiversity effects on ecosystem functioning, contributing roughly 50% of the biodiversity effects across different ecosystems (Cardinale *et al.* 2011). Identifying species that have key effects on ecosystem stability and functioning, through reducing CO<sub>2</sub> concentration, is a fruitful avenue for future research. The photosynthetic responses of individual phytoplankton species differ in their sensitivity to temperature and to species interactions. Some species benefit from increases in temperature and diversity if conditions favour their individual temperature optima (Huertas *et al.* 2011, Schabhüttl *et al.* 2013). Other taxa pushed away from their temperature optima can go locally extinct or experience competitive displacement from dominant species (Schabhüttl *et al.* 2013). This also stands true for the carbon capture abilities of individual phytoplankton species. In particular cyanobacteria have very efficient carbon capture mechanisms, raising their internal concentration relative to their environment by 1000-fold (Low-Décarie *et al.* 2014). This suggests that some species are more important than others in determining the community level response to biodiversity losses and climate warming.

Although we analyzed two different community compositions for each diversity level, a larger range of species and compositions can unequivocally tease apart the relative effects of diversity and species identity (Bell *et al.* 2009). Five of the non-resource species in our study were shared between the two high diversity compositions, precluding us from directly identifying non-resource species with the largest effect on the CO<sub>2</sub> concentration or consumer dynamics. While not logistically feasible in our study, control monocultures and regular counts of all non-resource species would partition the expected additive effect of individual species from the observed effect of total phytoplankton biomass. As an example, larger phytoplankton species settle out of suspension faster than smaller species, which may have acted as a defense against grazing and contribute to losses of CO<sub>2</sub> by organic carbon sedimentation (Tranvik *et al.* 2009). Our study was also limited by considering only a single zooplankton consumer. Although *Daphnia* spp. are keystone grazers in freshwater ecosystems (Carpenter *et al.* 2001), more diverse communities can consume a wider range of resources (Narwani and Mazumder 2010).

CO<sub>2</sub> concentrations were higher at 19°C compared to 23°C or 27°C, supporting the negative relationship between CO<sub>2</sub> concentration and temperature.

This contrasts with other work indicating increased CO<sub>2</sub> emissions at higher temperatures (Allen *et al.* 2005, Lopez-Urrutia *et al.* 2006). The effect in our study is driven by lower CO<sub>2</sub> solubility at higher temperatures (Wiebe and Gaddy 1940), but the direct effect of temperature on CO<sub>2</sub> concentration was not retained in the best model after the data were corrected for solubility (Fig. 2.3b). Instead, the SEM analysis of corrected data revealed an indirect effect of temperature via an increase in phytoplankton biomass and a reduction in zooplankton density. This is in agreement with other studies indicating indirect effects of temperature on CO<sub>2</sub> (Davidson *et al.* 2015, Finlay *et al.* 2015).

Surprisingly, there were no interactive effects of temperature and non-recourse diversity on CO<sub>2</sub> concentration. The independent negative effects of both non-recourse diversity and warming on CO<sub>2</sub> concentrations resulted from increasing the total phytoplankton community biomass. The SEM showed no significant relationship between phytoplankton biomass and consumers (*D. pulex*). This suggests that in our study, primary producers are the main drivers of the observed changes in CO<sub>2</sub>, by sequestration of carbon from the water into phytoplankton via photosynthesis (Watson *et al.* 1992, Trolle *et al.* 2012). Consumers presumably altered CO<sub>2</sub> concentration directly by respiratory losses and indirectly by reducing phytoplankton biomass. This highlights the importance of photosynthetic organisms in mitigating CO<sub>2</sub> emissions into the atmosphere (Low-Decarie *et al.* 2011).

Logistical constraints have limited previous studies investigating the causal links between the community structure and CO<sub>2</sub> emissions in freshwaters to one or two temporal sampling points (Butman and Raymond 2011, Raymond *et al.* 2013, Atwood *et al.* 2015, Rasilo 2015). Furthermore, it remains unknown how CO<sub>2</sub> concentrations in aquatic ecosystems respond to plankton diversity. To our knowledge, this is the first study to investigate the combined influences of biodiversity and temperature on aquatic CO<sub>2</sub> dynamics. Our experimental design allowed us to partition the effects of temperature and diversity, thus providing more mechanistic insight into the processes operating in plankton communities. In natural systems, the impact of climate warming will be either weakened or exacerbated, depending on whether the temperature effect on phytoplankton richness is negative (Petchey *et al.* 1999, Hillebrand *et al.* 2012), positive (Yvon-Durocher *et al.* 2015a) or neutral (Hillebrand *et al.* 2010, Kratina *et al.* 2012).

Controlled microcosm experiments have been identified as an important tool

to advance gaps in our understanding of CO<sub>2</sub> dynamics in a multiple stressor environment (Hasler *et al.* 2016). Our results indicate that systems with more diverse non-resource phytoplankton communities can help to mitigate the pace of climate warming by increasing primary production and carbon capture, and reducing the return of CO<sub>2</sub> to the atmosphere by primary consumers. With this information in hand, we may begin to develop models that more realistically predict the impacts of changing biodiversity and climate warming on ecosystems.

## **CHAPTER 3**

### **How Temperature Governs Resource Competition in Phytoplankton**

#### **Abstract**

Resource competition theory is a framework for predicting the outcome of competition among species with different resource requirements. However, there is little empirical evidence about whether and how species' requirements depend on other environmental factors, including temperature. If so, climate warming may alter the outcomes of resource competition and community dynamics. We experimentally demonstrate how environmental temperature alters the minimum light and nitrogen requirements and other growth parameters of six widespread phytoplankton species from distinct taxonomic groups. We found that species require the least light at intermediate temperatures, whereas nitrogen requirements tend to increase with rising temperature. Changes in temperature alter the competitive hierarchy amongst species for both resources, which can reorganize community composition under future climate warming.

## **Introduction**

Resource availability and environmental temperature exert strong control on biological processes across all scales, from individual metabolism and population growth to community assembly and dynamics (Eppley 1972, Tilman 1982, Sterner and Elser 2002, Brown *et al.* 2004). Species' resource-dependent growth rates can be used to predict competitive outcomes according to resource competition theory (Tilman 1982, Chase and Leibold 2003), whereas the temperature-dependence of species' metabolic rates can explain population, community and bulk ecosystem metabolism (Brown *et al.* 2004, Yvon-Durocher *et al.* 2010). While the independent influences of these two environmental drivers on populations and communities are relatively well understood, each alone leaves substantial variation in community dynamics unexplained. This highlights the fact that very little is known about how these drivers combine to shape community assembly, despite some indication of their interactive effects on population growth rates (Thomas *et al.* 2017), competitive dominance (Tilman 1981), and community composition (Hillebrand 2011, Kratina *et al.* 2012). The lack of experimental data from multiple species are critically limiting our current understanding of how temperature alters species' resource requirements, shifts competitive hierarchies and modifies dynamics in different ecological communities.

The resource-dependence of population growth rate drives competition for resources, one of the principal forces governing community composition and dynamics (Keddy 2002). Competition for resources has been modelled in numerous phenomenological ways, for example by using interaction coefficients (Chesson 2000) or the degree of resource-use overlap (MacArthur and Levins 1967), but adopting resource competition theory (RCT) has an advantage of explicitly modelling competition as a function of species' resource-dependent growth rates (Tilman 1982, Chase and Leibold 2003). One of the key predictions of RCT is that the species that can survive at the lowest level of the limiting resource outcompetes other species in an environment with constant resource supply (Tilman 1977, Tilman 1980, 1982, Miller *et al.* 2005). This minimum level of resource required to maintain a break-even population growth rate is therefore an important trait, known as  $R^*$ .  $R^*$  and related parameters of resource competition models have been used to accurately



predict the outcomes of competition under constant environment in the lab, and more recently, also in natural ecosystems (Miller *et al.* 2005, Dybzinski and Tilman 2007, Edwards *et al.* 2013).

Environmental temperature places fundamental constraints on organismal metabolism, with effects scaling from individual physiology to the ecology of entire communities (Eppley 1972, Brown *et al.* 2004, Kingsolver 2009, Dell *et al.* 2011, Kratina *et al.* 2012, Sentis *et al.* 2017). The metabolic theory of ecology (MTE) posits that the temperature-dependence of an organism's metabolic rate is determined by the most rate-limiting underlying biochemical reaction. Scaling up, the temperature-dependence of a population or community's metabolic rate is the aggregate of the contributions of individuals or species, respectively (Savage *et al.* 2004, Cross *et al.* 2015). Previous work has used different temperature-dependencies of photosynthesis and respiration (Allen *et al.* 2005, Schaum *et al.* 2017) to predict how biomass distribution within food webs is affected by warming (O'Connor 2009, Yvon-Durocher *et al.* 2010). Empirical work indicates that warming can enhance the strength of consumer-resource interactions (O'Connor 2009, Yvon-Durocher *et al.* 2010), food web-wide respiration rates (Yvon-Durocher *et al.* 2010) and relative heterotrophic biomass (Kratina *et al.* 2012, Shurin *et al.* 2012). It has also been proposed that temperature has differential impacts on various resource uptake and assimilation pathways (Toseland *et al.* 2013, Daines *et al.* 2014), which would have knock-on effects on competitive interactions. For example, reaction rates of phosphorus-rich ribosomes are more temperature-sensitive than nitrogen-rich photosynthetic proteins, suggesting that warming can shift elemental stoichiometry and resource requirements (Martiny *et al.* 2013, Yuan and Chen 2015, Yvon-Durocher *et al.* 2015b). Nevertheless, how temperature influences species minimum resource requirements, competitive interactions and multispecies community assembly remains to be tested.

In this study, we investigate the temperature-dependence of phytoplankton resource requirements for two essential limiting resources, nitrogen and light. We focus on phytoplankton because they are globally important primary producers, accounting for nearly half of all primary production and support consumers across many aquatic ecosystems (Field *et al.* 1998). Phytoplankton rely on a limited number of essential resources for survival and reproduction, including light and macronutrients like nitrogen and phosphorus. Furthermore, phytoplankton

competitive and thermal traits have been extensively studied, and are amenable to measurements of resource requirements and temperature-dependent population growth rates (Wilson *et al.* 2007, Kremer *et al.* 2017a, Thomas *et al.* 2017).

For any given species, it is assumed that  $R^*$  is minimized at a particular temperature, and increases steeply as temperature rises or declines, following a U-shaped response curve (Lehman *et al.* 2000, Tilman 2004). However, there are very few empirical examples of the temperature-dependence of  $R^*$ 's, and those focus only on the silica and phosphorus requirements of individual diatom species (Tilman 1981, van Donk and Kilham 1990, Shatwell *et al.* 2014). This restricts our understanding of the temperature-dependence of  $R^*$ s across different resources and species. Determining the general shape of  $R^*$ 's response to temperature for multiple limiting resources and across multiple species would improve our ability to forecast shifts in community composition and ecosystem processes under future climate warming.

We experimentally test how temperature influences the traits that govern species' competition for resources, with special emphasis on  $R^*$ . We quantify the temperature-dependence of competitive traits for six common and widely distributed phytoplankton taxa. By characterizing the shape of the temperature responses of  $R^*$  and other key population growth traits, we aim to address the following questions: i) Do  $R^*$  and other growth parameters increase symmetrically or asymmetrically as temperature departs from the optimum? ii) How do the sensitivities of  $R^*$  and other growth parameters to warming differ for limiting nitrogen and light resources?

## **Methods**

### **Quantifying resource- and temperature-dependent growth rates**

To investigate the temperature-dependence of resource competition for light and nitrogen, we measured population growth rates of six species spanning three groups of freshwater phytoplankton: cyanobacteria, chlorophytes and diatoms (Table S3.1). We refer to species by their genus name for simplicity. We estimated their growth rates in two separate experiments that crossed gradients of temperature with: (i) light, and (ii) nitrogen. Prior to each experiment, species were maintained in batch culture in a modified sterile COMBO freshwater medium which did not contain animal trace elements or vitamins (Kilham *et al.* 1998).

We estimated the growth rates of each species at each of ten levels of nitrogen and light by measuring changes in chlorophyll-*a* fluorescence over time. We also estimated phycocyanin fluorescence for the cyanobacteria species during the nitrogen experiment. We took daily measurements of these proxies for phytoplankton biomass using a Biotek Cytation 5 multi-mode plate reader. We measured chlorophyll-*a* fluorescence at excitation and emission wavelengths of 435nm and 685nm. We measured the phycocyanin using excitation and emission wavelength of 620nm and 665nm. Experimental units were tissue-culture plates that were sealed with Breathe-Easy™ membranes to prevent evaporative losses and cross-contamination between adjacent wells. To reduce the risk of contamination, all acclimation and experimental inoculation steps were performed in a laminar flow hood using sterile technique. Well-plates were randomly assigned a location within a grid in the temperature-controlled incubators (Multitron, Infors HT, Switzerland), which were set to rotate at 100 rpm. Cultures were illuminated at  $140.6 \mu\text{mol photons m}^{-2}\cdot\text{s}^{-1}$  of photosynthetically active radiation (PAR), except for the light-limited treatments (see below), for a 18L:6D photoperiod and maintained at 15°C, 20°C, 25°C or 30°C. These temperatures encompassed the approximate range of each species' previously-estimated optimal temperature for growth ( $T_{opt}$ ) (Thomas *et al.* 2016).

### *Experiment 1: Temperature-dependence of light limitation*

In the light limitation experiment, we factorially manipulated temperature (four levels) and light (ten levels). Sub-cultures of each phytoplankton species were acclimated to the four experimental temperatures and the ten light levels (0.15, 0.95, 3.6, 6.8, 18.7, 29.3, 49.2, 77.3, 105.5, 140.6  $\mu\text{mol photons m}^{-2}\cdot\text{s}^{-1}$ ) for six days prior to the start of the experiment. Before inoculating each species into the final growth rate experiment, we estimated population level biomass using chlorophyll-*a* fluorescence as a proxy, and aimed to equalize the starting values across all treatment combinations using dilutions. We measured raw fluorescence units (RFU) of chlorophyll-*a* by pipetting 1 mL samples of each acclimated culture into 48-well tissue-culture plates. Dilutions were conducted to achieve a starting RFU  $\leq 1,500$ .

The light requirements were estimated by inoculating 100  $\mu\text{L}$  of diluted, acclimated phytoplankton culture into 900  $\mu\text{L}$  of sterile COMBO medium in a 48-well Falcon tissue-culture plate to achieve an initial biomass of  $\leq 150$  RFU. We used neutral density filters (Solar Graphics™, Clearwater, Florida) to manipulate the total amount of light supplied without changing light spectrum. The light filters on the opaque frames prevented unmeasured light from entering the wells from the sides of the plates. Experimental light intensities under the filters were measured using a Skye PAR Quantum sensor.

Measurements of population-level RFU were made in two replicate wells for all temperature and light combinations daily for 10 days. Temperature treatments were applied in two temporal blocks. The 20 °C treatment was repeated in both blocks as a control for the effect of block, i.e. the 20 °C treatment was replicated four times (twice in each block). The growth rate estimates at controlled 20°C did not differ between blocks. In total we estimated 600 growth rates from 6,000 biomass measurements.

### *Experiment 2: Temperature-dependence of nitrogen limitation*

In the nitrogen limitation experiment, we factorially manipulated temperature (four levels) and the concentration of elemental nitrogen in the form of nitrate,  $\text{NaNO}_3$  (1, 4, 6, 10, 40, 60, 100, 400, 600, 1000  $\mu\text{mol N}\cdot\text{L}^{-1}$ ). These nitrate concentrations were derived from the experimental estimates of resource limitation of freshwater phytoplankton (Narwani *et al.* 2015) and additional pilot experiments where we estimated minimum resource requirements for the six focal species. For

comparison, standard COMBO media (Kilham *et al.* 1998) contains 1,000  $\mu\text{mol}\cdot\text{L}^{-1}$  of  $\text{NaNO}_3$ .

Sub-cultures of each phytoplankton species were acclimated to all temperature and nitrate combinations for 13 days prior to the start of the experiment (see supplementary methodology S3.1). We first diluted the acclimated cultures to 500 RFU or less, and then inoculated 1 mL of the cultures with 9 mL of sterile COMBO containing the assigned nitrogen level into 6-well tissue culture plates, achieving an initial biomass of less than 50 RFU. We measured population biomass of all species in three replicated wells and calculated their means at all temperature and nitrogen combinations daily over 9 days. This resulted in 720 growth rate estimates from 6,480 biomass measurements.

### *Models of population growth*

We described variation in light-dependent growth using the Eilers-Peeters model (Eilers and Peeters 1988):

$$\mu(I) = \frac{\mu_{\max} I}{\frac{\mu_{\max}}{\alpha I_{\text{opt}}^2} I^2 + \left(1 - 2\frac{\mu_{\max}}{\alpha I_{\text{opt}}}\right) I + \frac{\mu_{\max}}{\alpha}} \quad (1)$$

where  $\mu$  is the specific growth rate (per day) as a function of irradiance  $I$  (in  $\mu\text{mol photons m}^{-2} \text{s}^{-1}$ ),  $I_{\text{opt}}$  is the optimal irradiance for growth,  $\mu_{\max}$  is the maximum specific growth rate and  $\alpha$  is the initial slope of the curve.

We described variation in nitrogen-dependent growth using the Monod equation (Monod 1949):

$$\mu(N) = \frac{\mu_{\max} N}{N + \frac{\mu_{\max}}{\alpha}} - m, \quad (2)$$

where  $\mu$  is the specific growth rate (per day) as a function of nitrogen concentration  $N$  (in  $\mu\text{mol}\cdot\text{L}^{-1}$ ),  $\alpha$  is the initial slope of the curve,  $m$  is the background mortality rate (i.e. the specific growth rate at  $N = 0$ ), and  $\mu_{\max}$  is the maximum growth rate only when  $m = 0$ . We modified the Monod equation by including the  $m$  parameter, which accounts for mortality in the absence of any nutrients. The estimated maximum growth rate ( $\mu_{\max}$ ) is therefore the sum of  $\mu_{\max}$  and  $m$ .

We fit equations (1) and (2) to our experimental data and used the resulting parameters to numerically estimate  $R^*$  values (the irradiance and nitrate levels where each species' net growth rate equaled zero,  $I^*$  and  $N^*$  respectively).

### **Temperature-dependence of competition parameters**

We applied two approaches to characterize the shape of the temperature-dependence of competitive traits around their maxima (or minima for  $R^*$ ). First, to characterize the shape of the temperature-trait response curve, we fit a generalized additive mixed model (GAMM) where the trait value (fixed effect) was a smooth non-parametric function of temperature, while a random effect accounted for differences in species' mean trait value (across all temperatures). A significant random effect term indicates differences in the temperature response among individual phytoplankton. Because species have different temperature optima, we standardized the temperature so that all species had their trait minimum (for  $R^*$ ) and maximum (for all other traits) at the same position on the temperature axis (set to 0).

Second, to measure the temperature sensitivity of each trait, we quantified how steeply the trait values rise or fall with increasing temperature, by breaking each curve into portions below and above the trait maximum (or minimum for  $R^*$ ) if the trait showed a non-linear response to temperature. To characterize the rising and falling parts of the curve above or below the trait maximum or minimum for  $R^*$  (set to 0 on the temperature axis) we fit a linear model with log-transformed trait estimate as the response, which is equivalent to assuming that the trait increases or decreases exponentially with temperature. For the traits that showed a linear response, we fit a linear model to the entire standardized temperature range. We used the estimated slope to calculate a  $Q_{10}$  coefficient, representing the temperature sensitivity of the change in the trait value due to an increase in temperature of 10°C. For the analyses, we only used  $I_{opt}$  estimates when the estimated  $I_{opt}$  was less than the maximum irradiance used in the experiment.

## **Results**

### *Temperature-dependence of minimum light and nitrogen requirements*

Minimum light ( $I^*$ ) and nitrogen ( $N^*$ ) requirements of all phytoplankton species were influenced by experimental temperature (Fig. 3.1).  $I^*$  were consistently lowest at intermediate temperatures and highest and most variable at both maximum (30 °C) and minimum (15 °C) experimental temperatures (Figs. 3.1a, c). There was

an overall positive relationship between  $N^*$  and temperature across species. However, this relationship differed among individual phytoplankton species, as the model that included the random effect of species term described the data better than the model without this random effect (GAMM,  $R^2 = 0.10$ ,  $F_{2,00} = 3.93$ ,  $p = 0.036$ ; Figs. 3.1b, d).

In order to estimate the temperature sensitivity of  $I^*$  and  $N^*$ , we divided the temperature-dependent curve for all species combined into the increasing and falling portions, and defined the “optimal temperature” as that at which  $I^*$  and  $N^*$  were minimized (Figs. 3.1c, d). The estimated temperature sensitivities ( $Q_{10}$ ) across all species for the increasing portions of the curves for  $I^*$  and  $N^*$  were 0.70 and 0.45 respectively (95% CI were [0.61, 0.79] and [0.39, 0.51] respectively; Table S3.4). The estimated temperature sensitivity ( $Q_{10}$ ) for the falling portions of the curves for  $I^*$  and  $N^*$  were 2.25 and 1.01 respectively (95% CI were [2.03, 2.50] and [0.86, 1.16] respectively, Table S3.4). This shows that species'  $I^*$  and  $N^*$ s are more sensitive to lower than-optimal temperatures, than higher-than optimal temperatures (Table S3.4), indicating an asymmetric response of  $I^*$  and  $N^*$  around the optimum. Species  $I^*$  are also more than twice as sensitive to higher than optimal temperatures compare to  $N^*$ , indicating differences in the sensitivity of species  $R^*$  to different resource types (Table S3.4).

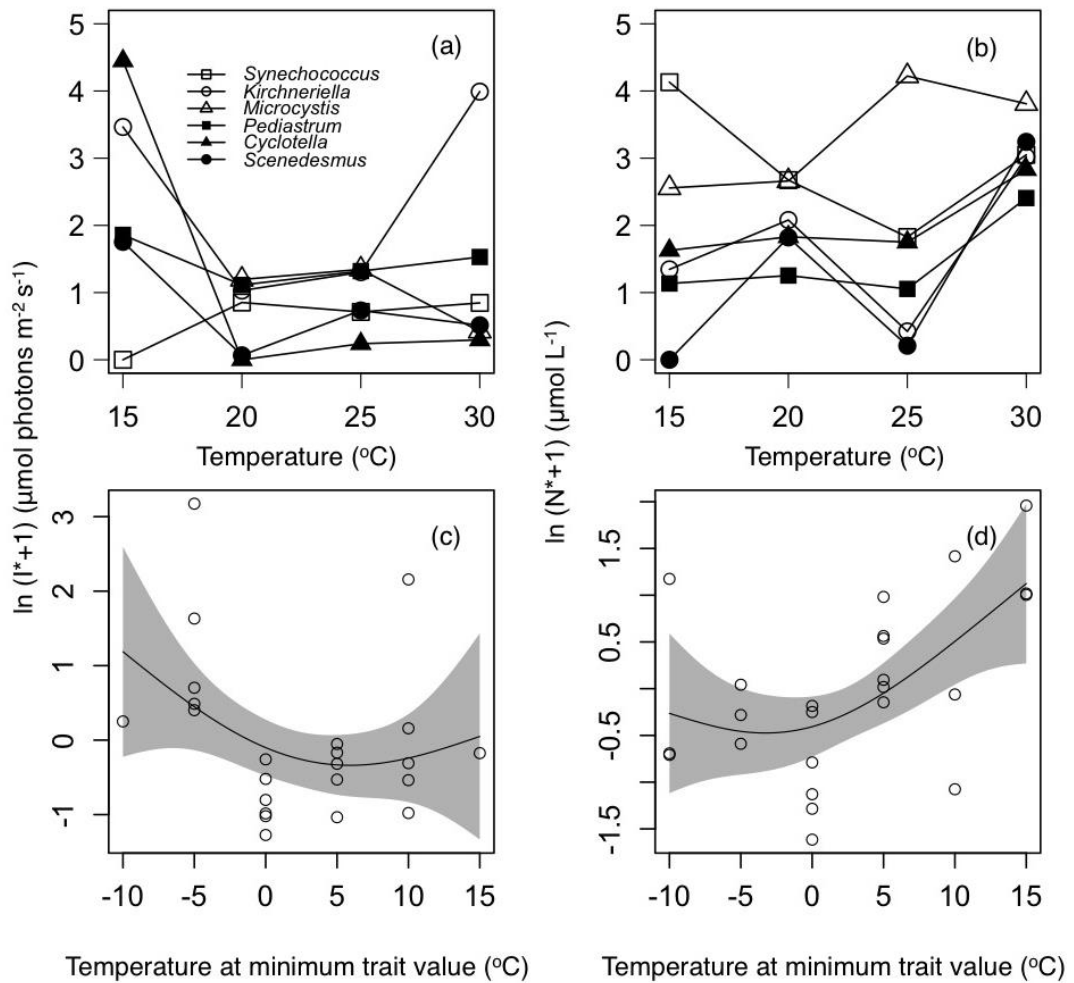


**Figure 3.1. Temperature alters minimum light ( $I^*$ ) and nitrogen ( $N^*$ ) requirements of six phytoplankton species (different symbols). (a)  $I^*$  values are lowest and least variable at intermediate experimental temperatures, (b)  $N^*$  values increase at the highest experimental temperatures. (c, d) illustrate the same data that were corrected to remove differences among species in the mean trait value across a temperature gradient. The x-axis represents temperatures standardized so that all species have their trait minimum at the same value (0  $^{\circ}\text{C}$ ). (c)  $I^*$  as a function of temperature relative to the minimum trait value, with a fitted GAMM, (d)  $N^*$  as a function of temperature relative to the minimum trait value, with a fitted GAMM.**

Despite the overall patterns in minimum resource requirements (Fig. 3.1), there were also strong interspecific differences in  $I^*$  and  $N^*$  responses to temperature (Fig. 3.2, note different y-axes). Whereas  $I^*$  and  $N^*$  showed opposite relationships with temperature for some species (e.g., *Synechococcus*, *Cyclotella*, and



*Scenedesmus*), both  $I^*$  and  $N^*$  responded consistently to temperature for other species (e.g. *Kirchneriella*). *Pediastrum* had low requirements for both resource types across the whole temperature gradient (Fig. 3.2e).

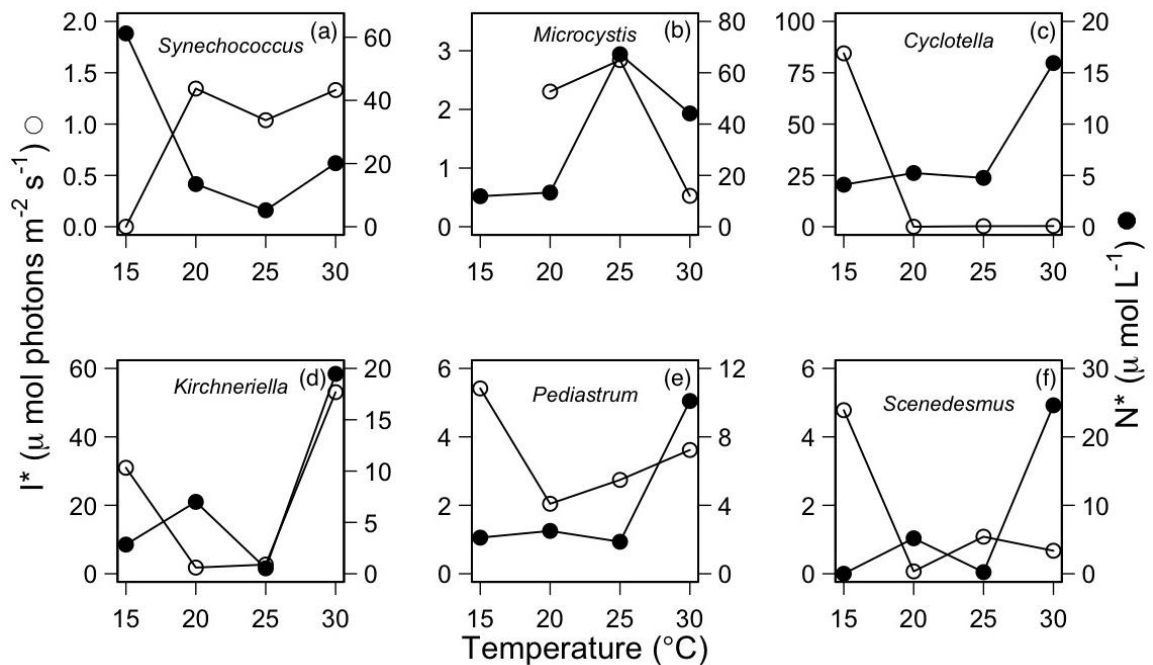


**Figure 3.2. Temperature alters within species responses to light ( $I^*$ ) and nitrogen ( $N^*$ ) limitation.**  $I^*$  and  $N^*$  show opposite relationship with temperature for some species (a, c, f), or similar trends for other species (d). Note different y-axis.

#### Temperature-dependence of other resource competition traits

Changes in  $R^*$  with temperature ultimately arise from the temperature-dependence of the traits that determine  $R^*$ . In our study, the maximum specific growth rates ( $\mu_{\max}$ ) for light and nitrogen were positively influenced by temperature, ranging from 0.09 to 1.71 day<sup>-1</sup> (Figs. 3.3a, S1, Table S3.2) and from 0.23 to 1.45 day<sup>-1</sup> (Figs. 3.3c, S3.2, Table S3.3), respectively. Whereas  $\mu_{\max}$  increased monotonically with warming in the nitrogen limitation experiment, there appeared to be an optimum temperature in the light limitation experiment, beyond which  $\mu_{\max}$  declined (Figs. 3.3b, d). The  $\mu_{\max}$  for the light limitation experiment was more sensitive to temperature than it was for the nitrogen experiment ( $Q_{10}$  for the increasing portions of the curves were 0.45 for light and 0.22 for nitrogen). The  $Q_{10}$  for the declining portion of the light curve was smaller than for the increasing portion (-0.12), indicating an asymmetric response of light  $\mu_{\max}$  to temperature around the

optimum. Across species, growth rates responded more strongly to initial increases in nitrogen than light availability ( $\alpha$ ), with larger variation across temperatures for nitrogen (Fig. 3.3e, g). Response curves for  $\alpha$  were non-monotonic under both types of resource limitation (Figs. 3.3f, h). Although the remaining traits were also temperature-dependent (i.e. the  $Q_{10}$  values differed from zero; Figs. 3i-l, Table S3.4), they showed lower sensitivity to temperature and less difference between the response to light and nitrogen in comparison to  $I^*$  and  $N^*$  (Table S3.4).

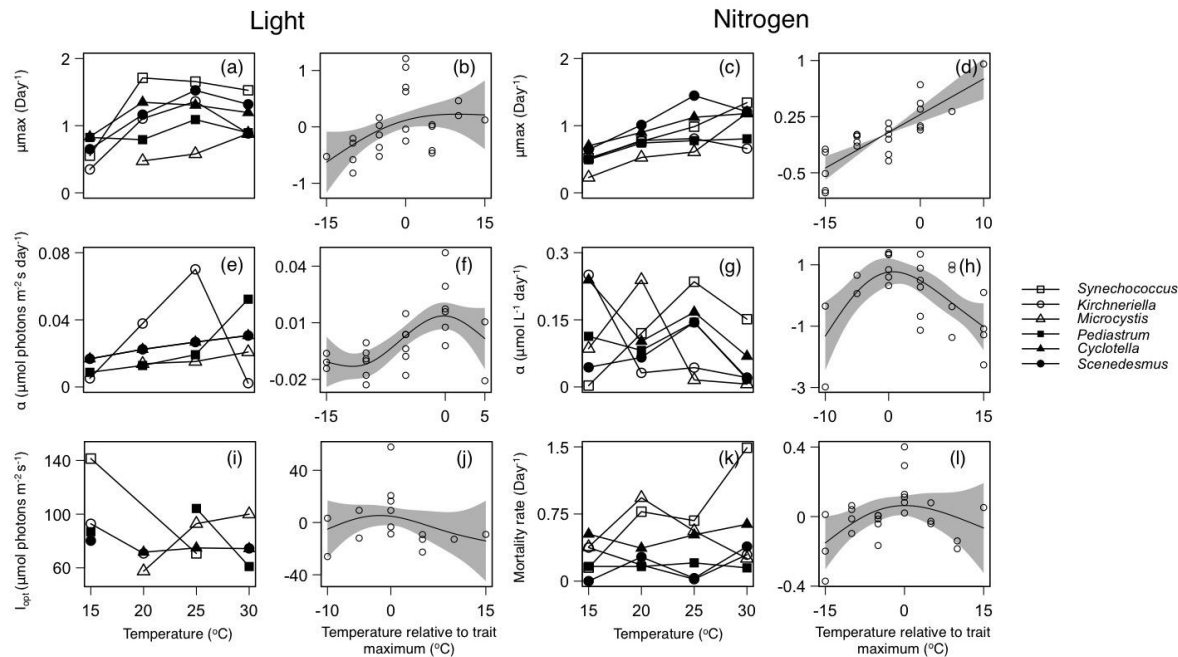


**Figure 3.3. The key traits for nitrogen and light competition depend on experimental temperature.** The effect of temperature on (a) the growth rate measured under unlimited light ( $\mu_{max}$ ) (e) the initial slope of the growth-light curve ( $\alpha$ ), (i) the optimal irradiance for growth ( $I_{opt}$ ). (c) growth rate measured under unlimited nitrate, (g) the initial slope of the growth-nitrogen curve, and (k) the specific growth rate at  $N = 0$ . The GAMMs fitted to four growth-irradiance traits modified by experimental temperature: (b)  $\mu_{max}$ , (f)  $\alpha$ , (j)  $I_{opt}$ . The GAMMs fitted to three nitrogen competition traits modified by experimental temperature: (d)  $\mu_{max}$ , (h)  $\alpha$ , and (l)  $m$ . The plotted data points are corrected to remove differences between species in the mean trait value across temperatures. The x-axis represents temperature values that have been standardized so that all species had their trait maximum at the same position (0 °C).

## **Discussion**

We provide experimental evidence that minimum resource requirements for light ( $I^*$ ) and nitrogen ( $N^*$ ) are temperature-dependent. Whereas minimum resource requirements for light tended to increase at the highest and lowest experimental temperatures, minimum resource requirement for nitrogen were more variable and on average increased with rising temperature, indicating asymmetric responses of  $R^*$  around its minimum. Species-specific differences in the temperature-dependence of  $R^*$  shifted the outcomes of competition as predicted by RCT. Empirically parameterized models illustrate how these changes in resource competition alter phytoplankton community composition and dynamics. This is in line with some previous work showing that two species of diatoms are superior competitors for silica at different temperatures (Tilman *et al.* 1981) and that temperature alters the identity of the best rotifer competitors (Stelzer 1998). The partitioning of the temperature-light niche observed in our study may enhance coexistence and biodiversity in environments with temporal or spatial variation in temperature and light (e.g. Descamps-Julien and Gonzalez 2005).

The species-specific responses of  $I^*$  and  $N^*$  to temperature indicate distinct interactive effects of temperature and light or nitrogen on each species' population growth rates. Previous tests of combined temperature and nutrient impacts on individual species (Descamps-Julien and Gonzalez 2005, Thomas *et al.* 2017) showed that temperature and nutrients could limit species ranges by decreasing individual growth rates. Moreover, temperature can also alter the supply ratio of limiting nutrients (Tilman *et al.* 1986) available in the environment, resulting in the taxonomic replacement and turnover of dominant species (Hillebrand 2011). The temperature-dependence of  $R^*$  and other competitive traits can thus alter community composition, by switching competitive hierarchies under future climate warming.

The monotonic increase in minimum nitrogen requirements with rising temperature indicates that the optimum temperature for  $N^*$  may not have been captured in the temperature range tested in our study. Maximum growth rate ( $\mu_{max}$ ) also tended to increase monotonically with temperature, whereas  $\alpha$  appeared to have a unimodal relationship with temperature for both resources. The non-linear relationship of growth traits with temperature has also been recognised in the

minimum silica requirements of two diatom species (Tilman *et al.* 1981). Furthermore, a synthesis of published light curves showed that  $\mu_{max}$ ,  $\alpha$  and  $I_{opt}$  all show unimodal relationships with temperature (Edwards *et al.* 2016) and a similar pattern of  $R^*$  across temperatures is found in models of temperature-nutrient interactions (Follows *et al.* 2007, Thomas *et al.* 2017). However, these models presently do not account for the temperature-dependence of traits such as  $\alpha$ , and may need to be modified accordingly.

Despite the potential for a temperature-dependent RCT to improve forecasting of community dynamics, experimental characterization of resource requirements for a large number of taxa is not practical (Kremer *et al.* 2017b). However, the integration of nutrient-based competition models with metabolic-based theory (Brown *et al.* 2004) may be a critical step towards understanding fundamental constraints governing community and ecosystem dynamics under changing climate (Allen and Gillooly 2009). Recent efforts to understand how temperature influences cell physiology and metabolism (e.g. synthesis of proteins and RNA) have yielded promising insights (Toseland *et al.* 2013, Daines *et al.* 2014). For instance, nitrogen-rich photosynthetic proteins are less sensitive to temperature changes than phosphorus-rich ribosomes. Consequently, the activity of ribosomes increases more rapidly with warming than that of photosynthesis proteins, requiring more photosynthetic proteins per cell with warming. This may explain temperature-induced increases in the nitrogen content of phytoplankton biomass, relative to phosphorus content (Yvon-Durocher *et al.* 2017). Such mechanistic insights may therefore allow the identification of generalities governing the temperature dependencies and sensitivities of species' resource requirement. Efforts to merge metabolic theory with RCT (Ward *et al.* 2017) have the potential to result in a more general understanding of the environmental dependence of community dynamics.

Our study demonstrates differential temperature sensitivity of competition for light and nitrogen across six phytoplankton species from varying taxonomic groups. These changes in competitive traits have the potential to reorganize ecological communities under the ongoing and accelerating climate warming. Further merging of resource competition and metabolic theory can improve the forecasts of future competitive community assembly.

## CHAPTER 4

### **Selection Drives Evolution of Minimum Resource Requirements in *Chlamydomonas reinhardtii***

#### **Abstract**

We used the model freshwater phytoplankton species *Chlamydomonas reinhardtii* to investigate whether minimum requirements for essential resources ( $R^*$ ) respond to selection by environmental reductions in local resource availability. We used ancestral populations that had been previously evolved under resource limitation in chemostat for 285 days, including low nitrogen, low phosphorus, low light, biotic (depletion of total nutrients by the growth of other phytoplankton, osmotic stress, and a crossed biotic depletion and osmotic stress treatment). We estimated population-level growth rates along gradients of light, nitrogen and phosphorus for ancestors and descendants in order to determine their  $R^*$  for these resources. Descendants displayed an adaptive response to selection under low nitrogen supply ( $N^*$ ), non-adaptive responses to low light supply and no significant trait change under low phosphate supply. Neither genotypic diversity nor additional stress consistently accelerated adaptive change, although the crossed biotic-salt treatment was the only selection treatment able to maintain the originally low ancestral light requirement. We did not observe the trade-offs between  $N^*$ ,  $P^*$  and  $I^*$  at the intraspecific level that have previously been documented across distantly related species. Species' abilities to adapt to local changes in resource supply may have consequences for the outcome of competitive community assembly in response to environmental change.

## **Introduction**

Competition is one of the major forces structuring phytoplankton communities (Tilman 1977, Tilman 1981, Sommer 1985, Huisman *et al.* 1999). Studies of phytoplankton competition show that functional traits of individual species measured in isolation can be used to predict the outcomes of competition (Tilman 1977, Tilman 1981). The hypothesis that species traits can be used to predict community assembly is attractive because it presents the possibility of successful ecological forecasting in the face of future biotic and abiotic environmental change (Keddy 1992, Petchey *et al.* 2015). However, it is unclear how the extent in which competitive traits evolve under selection imposed by levels of local resource availability.

While competition can be described in a number of ways, resource competition theory (RCT) proposes a set of competitive traits that can be used to predict the outcome of competition among species (Tilman 1982). These traits can be expressed as parameters describing the way in which population growth rates vary along gradients of resource availability (Tilman 1977, Tilman 1982). Given these parameters, and the resource-dependent growth rates along resource gradients, population dynamics and the outcome of interspecific competition can be predicted (Droop 1973, Tilman 1982, Grover 1991). A general prediction of RCT is that the species which has the lowest requirement for a given limiting resource, also commonly known as  $R^*$ , will outcompete other species in an environment with a constant supply of that resource (Tilman 1977, Tilman 1980, 1982, Miller *et al.* 2005).  $R^*$  and the other growth parameters of RCT have been used to accurately predict the outcomes of competition both in the lab and in the field (Miller *et al.* 2005, Dybzinski and Tilman 2007, Edwards *et al.* 2013). The considerable variation among species in the magnitude of these competitive traits has therefore been shown to determine the structure and diversity of communities driven by resource competition.

To date investigations of the variance and covariance of competitive traits in phytoplankton have focused on variation among species. These comparisons have been made at some of the largest taxonomic and phylogenetic scales, including variation among cyanobacteria, green, and red eukaryotic phytoplankton, and

spanning hundreds of millions of evolutionary history (Litchman *et al.* 2010, Edwards *et al.* 2011, Schwaderer *et al.* 2011, Edwards *et al.* 2013, Edwards *et al.* 2015). On these scales, there is great variation in competitive abilities for all essential resources including light, nitrogen and phosphorus (Litchman *et al.* 2007). Furthermore, there is a tendency for trade-offs among these traits (Litchman *et al.* 2007, Edwards *et al.* 2011), and some traits show evolutionary conservation (Litchman *et al.* 2010, Edwards *et al.* 2011, Schwaderer *et al.* 2011, Edwards *et al.* 2013, Edwards *et al.* 2015), where traits tend to be more similar among more taxonomically similar species. In contrast, a recent study spanning tens to hundreds of millions of years of the evolutionary history of green freshwater phytoplankton does not find evidence for phylogenetic signal of competition traits for light, nitrogen or phosphorus, suggesting that these traits may be evolutionarily labile in some clades or phylogenetic scales (Narwani *et al.* 2015).

While there are good descriptions of competitive trait variation among phytoplankton species, little is known about the extent of this trait variation within species and how it evolves. Evolution experiments have shown that phytoplankton show heritable trait variation and the potential for evolutionary adaptation in their abilities to grow along other environmental gradients including acidification (Lohbeck *et al.* 2012), warming (Schlüter *et al.* 2014) and salt stress (Lachapelle and Bell 2012). Moreover, phytoplankton can undergo rapid evolution of phenotypic traits related consumer resistance (Yoshida *et al.* 2003, Hairston *et al.* 2005, Fischer *et al.* 2014), which can fundamentally alter the strength of the consumption and the population dynamics of both the consumer and resource populations. However, phytoplankton do not show heritable phenotypic adaptation to all types of environmental change, e.g. increasing atmospheric CO<sub>2</sub> (Stinchcombe and Kirkpatrick 2012, Schaum *et al.* 2017, Yvon-Durocher *et al.* 2017). This indicates that phytoplankton growth traits may be genetically or physiologically constrained or correlated in such a way as to impose limits to or trade-offs among adaptive responses. For example, adaptations enhancing competitive ability in one environment may come at a cost, or a correlated improvement, in another environment. Trade-offs have been documented among competitive abilities for different resources at large taxonomic scales (Edwards *et al.* 2011). Yet, there is little support for trade-offs among population-level growth rate parameters within the model green alga, *Chlamydomonas reinhardtii* (Bell 1991). While the effects of



intraspecific variation and evolution on population and community-level properties and dynamics, such as primary production, have been increasingly studied (Violle *et al.* 2012), the nature and the extent of intraspecific trait variation and the mechanisms driving its evolution are still largely unknown for microbes in general. Because the evolution of resource competition traits may have strong impacts on community assembly (Vasseur and Fox 2011), it is essential to understand the potential for these traits to evolve, and the patterns of trait variance and covariance that emerge in response to selection.

Previous work in well-known model systems has shown how competition for limiting resources may lead to character displacements among species competition for substitutable resources. Evolution of niche differentiation to alleviate the negative influences of resource-limitation and competition for limiting resources has been demonstrated in Darwin's finches, sticklebacks and anolis lizards among others (Schluter and McPhail 1992, Losos *et al.* 1998, Grant and Grant 2006). Nevertheless, predictions for how trait evolution proceeds under competition for essential resources are fundamentally different: when competing for a single limiting resource, species should converge on a single optimum phenotype, which is a low requirement ( $R^*$ ) for the limiting resource (Abrams 1987, Vasseur and Fox 2011). This is because the lack of that resource cannot be compensated for by consumption or improved competitive ability for any other resource, i.e. nitrogen limitation cannot be compensated for by consumption of light or phosphorus. As such, photo-autotrophs that consume a few nutritionally essential resources including light, nitrogen and phosphorus, may be expected to converge on the same, low- $R^*$  phenotype when under selection by any type of resource limitation (Abrams 1987).

Here, we investigate the evolutionary response of competitive traits within the model alga (*Chlamydomonas reinhardtii*) to environmental reductions in local resource availability. We test the following hypotheses and expectations: (i) *Resource competition traits, in particular  $R^*$ , evolve in response to selection by limiting resources.  $R^*$  should decline in environments where the same resource is limiting. Individual populations selected under limitation by a particular resource will respond by reducing their population-level requirements for that limiting resource.* (ii) *Genetic diversity and/or stress can accelerate evolution in response to selection. A genetically diverse population will display a stronger adaptive change of  $R^*$  under resource-limitation than the isogenic clonal populations within the same*

period of selection (Hughes *et al.* 2008). Increasing the amount of stress will also impose a stronger adaptive change of  $R^*$  (Goho and Bell 2000). (iii) *Evolved variation in  $R^*$  under selection by different limiting resources results in trade-offs in competitive ability for light, nitrogen and phosphorus.* Fundamental biological constraints to adaptation results in similar trade-offs among evolved variation within a species as that which has been previously observed among species (Litchman *et al.* 2007). Alternatively, an increased competitive ability for one resource could result in a correlated improvement in the competitive ability for another (pleiotropic or correlated fitness benefits in low-resource environments) (Velicer 1999, Jeffery 2005, Lahti *et al.* 2009). The work presented in this chapter is the physiological analysis of strains previously evolved by others. This is the first study of the evolutionary change in competitive traits for essential resources in response to selection by low resource availability.

## **Methods**

### ***Evolution experiment previously performed by others***

We use the model phytoplankton strain *Chlamydomonas reinhardtii* CC1690 wild type mt+ obtained from the Chlamydomonas Centre (chlamycollection.org). The monoculture was grown in a semi-continuous liquid COMBO freshwater medium (Kilham *et al.* 1998), without vitamins, silica and animal trace elements, which are unnecessary for growing green algae. The cultures were subsequently plated onto agar. From the plates we selected four random colonies, derived from single cells (hereafter referred to as Anc 2, Anc 3, Anc 4 and Anc 5) and inoculated them into liquid COMBO freshwater medium (Fig. 4.1a). To start the selection experiment, each ancestral monoculture was transferred into seven replicate chemostats containing 30 mL of sterile COMBO medium. Each chemostat received daily sterile media replacement via an automated peristaltic pump and were continuously mixed and aerated to prevent heterogeneity in resource availability. Chemostats were maintained at 20°C and illuminated under 90  $\mu\text{mol photons m}^{-2}\text{s}^{-1}$  of light on an 18h light: 6h dark cycle.

For each ancestral population, the seven chemostats were randomly assigned to one of seven treatments: control, nitrogen limitation, phosphorus limitation, light

limitation, salt stress, biotically-depleted medium (i.e. medium previously used to grow seven other species of phytoplankton), and a combination of salt stress and biotically-depleted medium (Fig. 4.1b, Table S4.1). The biotically-depleted medium was used to infer the influence that a bio-diverse community may have on simultaneously depleting the availability of all dissolved resources. The osmotic stress treatment consisted of increasing concentrations of NaCl. We used osmotic-stress as a selection treatment to compare the adaptation under resource limitation relative to that under another type of environmental stress. The controls were maintained in full COMBO for the duration of the experiment. Resource-limitation and salt-stress increased monthly until a final, highly-stressful concentration was achieved, so that populations did not go to extinction (estimates of biomass reduction relative to the control are given in supplementary material, Fig. S4.1, Table S4.1). The experiment ran for 285 days (~285 generation), after which the evolved populations were plated onto agar.

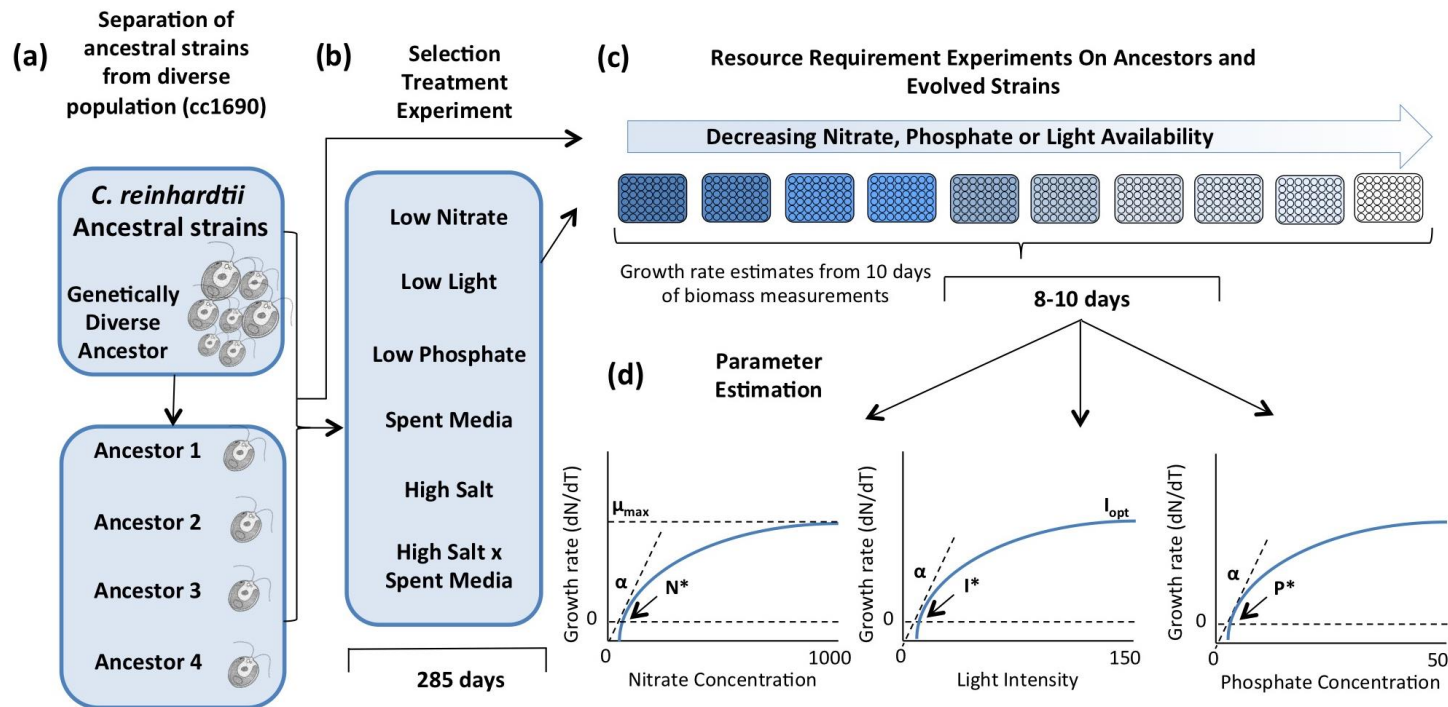


**Figure 4.1.** Conceptual diagram showing the process and timeline for (a) the isolation of ancestral populations, (b) derivation of evolved descendants by exposing ancestral populations to six different selection environments, (c) measurement of descendants' population growth rates under a gradient of light, nitrogen and phosphate availability, and (d) estimation of the competition growth parameters under light, nitrogen and phosphate resource. This work specifically performed in this chapter relate to processes (c) and (d).

### ***Resource limitation experiments***

To investigate the response of the ancestral descendant populations to light, nitrogen and phosphorus availability, we estimated their growth rates in three separate experiments in which we manipulated the supply of either light, nitrogen or phosphorus (Fig. 4.1c). Prior to each experiment, species were placed back into liquid batch culture in sterile COMBO medium, modified as described above. In each experiment, we estimated the growth rates of each species at each of ten levels of light, nitrate or phosphate. We estimated growth rates by measuring changes in population-level chlorophyll-*a* fluorescence over time using a Biotek Cytation™ 5 multi-mode plate reader. We measured chlorophyll-*a* fluorescence at excitation and emission wavelengths of 435nm and 685nm. Chlorophyll-*a* can be used as a proxy of phytoplankton biomass (Greenberg Arnold and Clesceri Lenore 1992). Although chlorophyll fluorescence is used as the main measure of chlorophyll and as a proxy for algal biomass, it is important to note that there are limitations to the use of fluorescence based measurements of *in vivo* chlorophyll in the context of the light and nutrient limitation experiments as described in both chapters 3 and 4 (Suggett *et al.* 2009). The photo physiology that affects chlorophyll fluorescence yield is known to respond to nutrient treatments, and short and long-term light exposure and this response is known to be different amongst taxonomic groups (Suggett *et al.* 2009). While chlorophyll production may respond plastically to environmental variation, we allowed all cultures to acclimate to the resource conditions prior to the experiment to allow plastic adaptation to occur before the start of the experiments. Experimental units were tissue-culture plates, which we sealed with Breathe-Easy™ membranes to prevent evaporative losses and cross-contamination between adjacent wells. To reduce the risk of contamination, all acclimation and experimental inoculation steps were performed in a laminar flow hood using sterile technique. Well-plates were randomly assigned a location within a grid in temperature-controlled incubators (Multitron, Infors HT, Switzerland), which were set to rotate at 100 rpm. Cultures were illuminated at  $140.6 \mu\text{mol photons m}^{-2}\cdot\text{s}^{-1}$  of photosynthetically active radiation (PAR), except for the light-limited treatments (see below for details), for a 18L:6D photoperiod and maintained at 20°C.

(i) *Light R\**

In the light limitation experiment, we exposed all ancestral and descendant populations to each of ten light levels (0.15, 0.95, 3.6, 6.8, 18.7, 29.3, 49.2, 77.3, 105.5, 140.6  $\mu\text{mol photons m}^{-2}\cdot\text{s}^{-1}$ ). Liquid batch cultures of all ancestors and descendants were first acclimated to the ten light levels for six days prior to the start of the experiment. Before inoculating each ancestor and descendant into the growth rate experiment, we estimated population level biomass using chlorophyll-*a* fluorescence, and aimed to equalize the starting values across all treatment combinations using dilutions. We measured raw fluorescence units (RFU) of chlorophyll-*a* by pipetting 1 mL samples of each acclimated culture into 48-well tissue-culture plates and reading the plates on a Biotek Cytation™ 5 plate reader. Dilutions were conducted to achieve a starting RFU  $\leq 1,500$ .

To estimate population-level growth rates at each light level, we inoculated 100  $\mu\text{L}$  of diluted, acclimated phytoplankton culture into 900  $\mu\text{L}$  of sterile COMBO medium into individual randomized wells of a 48-well Falcon tissue-culture plate to achieve an initial biomass of  $\leq 150$  RFU. We used neutral density filters (Solar Graphics™, Clearwater, Florida) to manipulate the total amount of light supplied without changing light spectrum. The light filters on the opaque frames prevented unmeasured light from entering the wells from the sides of the plates. Experimental light intensities under the filters were measured using a Skye PAR Quantum sensor. Each light level was replicated three times for the ancestors, but once for the descendants. We then monitored population-level chlorophyll-*a* fluorescence, as a proxy for population-level biomass, by recording RFU daily on the plate-reader over 10 days. In total, we estimated 450 growth rates from 4,500 biomass estimates.

(ii) *Nitrogen R\**

In the nitrogen limitation experiment, we exposed all ancestral and descendant populations to ten concentrations of elemental nitrogen in the form of nitrate,  $\text{NaNO}_3$  (1, 4, 6, 10, 40, 60, 100, 400, 600, 1000  $\mu\text{mol N}\cdot\text{L}^{-1}$ ). These nitrate concentrations were chosen based on previous estimates of nitrogen limitation in freshwater phytoplankton (Narwani *et al.* 2015). For comparison, standard COMBO media (Kilham *et al.* 1998) contains 1,000  $\mu\text{mol}\cdot\text{L}^{-1}$  of  $\text{NaNO}_3$ .

All ancestors and descendants were first acclimated to low-nitrate concentrations for 9 days prior to the start of the experiment (see supplementary

methodology S4.1). We first diluted the acclimated cultures to 500 RFU or less, and then inoculated 1 mL of the cultures with 9 mL of sterile COMBO containing the assigned nitrogen level into 6-well tissue culture plates, achieving an initial biomass of less than 50 RFU. We measured chlorophyll-*a* fluorescence as a proxy for population-level biomass of all populations over 8 days. This resulted in 350 growth rate estimates from a total of 3,500 biomass estimates.

*(iii) Phosphorus R\**

In the phosphorus limitation experiment, we exposed all ancestral and descendant populations to ten concentrations of elemental phosphorus in the form of phosphate, PO<sub>3</sub><sup>-</sup> (0.5, 1, 2, 4, 6, 8, 10, 20, 35, 50 μmol P·L<sup>-1</sup>). These phosphate concentrations were also chosen based on prior estimates of resource limitation of freshwater phytoplankton (Narwani *et al.* 2015). For comparison, standard COMBO media (Kilham *et al.* 1998) contains 50 μmol·L<sup>-1</sup> of PO<sub>3</sub><sup>-</sup>.

All ancestors and descendants were first acclimated to low-phosphate concentrations for 9 days prior to the start of the experiment (see supplementary methodology S4.1). We first diluted the acclimated cultures to 500 RFU or less, and then inoculated 1 mL of the cultures with 9 mL of sterile COMBO containing the assigned phosphate level into 6-well tissue culture plates, achieving an initial biomass of less than 50 RFU. We measured chlorophyll-*a* fluorescence as a proxy for population-level biomass of all populations over 8 days. This resulted in 350 growth rate estimates from a total of 3,500 biomass estimates.

***Population growth estimates***

As in Chapter 3, we described variation in light-dependent growth using the Eilers-Peeters model (Eilers and Peeters 1988):

$$\mu(I) = \frac{\mu_{max}I}{\frac{\mu_{max}}{\alpha I_{opt}^2} I^2 + \left(1 - 2\frac{\mu_{max}}{\alpha I_{opt}}\right)I + \frac{\mu_{max}}{\alpha}}, \quad (1)$$

where  $\mu$  is the specific growth rate (per day) as a function of irradiance  $I$  (in μmol photons m<sup>-2</sup> s<sup>-1</sup>),  $I_{opt}$  is the optimal irradiance for growth,  $\mu_{max}$  is the maximum specific growth rate and  $\alpha$  is the initial slope of the curve.

As in Chapter 3, we described variation in nitrogen-dependent and phosphate-dependent growth using a modified version of the Monod equation (Monod 1949):

$$\mu(NP) = \frac{\mu_{\max}NP}{NP + \frac{\mu_{\max}}{\alpha}} - m, \quad (2)$$

where  $\mu$  is the specific growth rate (per day) as a function of nitrogen concentration  $N$  or phosphate concentration  $P$  (in  $\mu\text{mol}\cdot\text{L}^{-1}$ ),  $\alpha$  is the initial slope of the curve,  $m$  is the background mortality rate (i.e. the specific growth rate at  $N$  or  $P = 0$ ), and  $\mu_{\max}$  is the maximum growth rate only when  $m = 0$ . We modified the Monod equation by including the  $m$  parameter, which accounts for mortality in the absence of any nutrients. The estimated maximum growth rate ( $\mu_{\max}$ ) is therefore the sum of  $\mu_{\max}$  and  $m$ .

We fit equations (1) and (2) to our experimental data and used the resulting parameters to numerically estimate  $R^*$  values (the irradiance, nitrate and phosphate levels where each species' net growth rate equaled zero,  $I^*$ ,  $N^*$  and  $P^*$  respectively).

### ***Statistical analyses***

We analysed the independent effects of the selection treatment and ancestral identity for each descendant on: i) the minimum resource requirement for light ( $I^*$ ), nitrogen ( $N^*$ ) and phosphate ( $P^*$ ), and ii) the initial rate of response of the population-level growth rate to increases in resource availability ( $\alpha$ ), representing the slope of the curve at low resource-availability.

To illustrate the effects of the selection treatments and investigate whether the descendants differed significantly from the ancestor, we used linear models (LM) with selection treatment as a fixed effect. To investigate whether the genotypically diverse ancestor displayed a stronger adaptive change of  $R^*$  under resource-limitation than the isogenic clonal populations within the same period of selection, we used LM with ancestor as a fixed effect. All analyses were performed in R 3.2.3 (R Development Core Team 2016), using the function *lm* in the package *lme4*.

To reveal whether evolved variation in  $R^*$  under selection by different limiting resources results in trade-offs in competitive ability for light, nitrogen and phosphorus, we applied Principle Component Analysis (PCA) and Redundancy



Analysis (RDA) on the combined  $R^*$  and  $\alpha$  data from all three experiments. PCA and RDA were performed using the function *dudi.pca* and *rda* in the package *vegan*. We also tested whether different histories of low-resource selection result in trade-offs or associated fitness benefits across different contemporary low-resource environments.

## **Results**

### **(a) Selection experiment**

Minimum light ( $I^*$ ) and nitrogen ( $N^*$ ) requirements evolved in response to experimental selection by different limiting resources (Figs. 4.2a, b, Table S4.5). Compared to the ancestors,  $I^*$  increased significantly for all descendants selected under the biotic, light, nitrogen and salt treatments (LM,  $F_{6,29} = 11.13$ ,  $P < 0.05$ ; Figs. 4.2a, Table S4.5), but  $I^*$  did not change significantly for descendants selected under phosphate or the combined biotic x salt treatment ( $F_{6,29} = 11.13$ ,  $P = 0.193$ ,  $0.999$ , respectively; Figs. 4.2a, Table S4.5). Overall, the ancestors had the lowest mean requirement for light ( $I^* = 0.03$ , Fig. 4.2a, Table S4.2), indicating a low requirement for light in the ancestral populations. The combined biotic and salt selection environment resulted in the lowest mean requirement for light out of all descendants ( $I^* = 0.18$ , Fig. 4.2a, Table S4.2). The salt-stress and the biotic treatments alone resulted in the highest mean requirements for light ( $I^* = 7.14$ , respectively, Fig. 4.2a, Table S4.2) and therefore did not accelerate the adaptive change in minimum resource requirements.

In comparison to the ancestors,  $N^*$  decreased significantly for descendants selected under low light and low nitrogen ( $F_{6,26} = 1.92$ ,  $P < 0.05$ ; Figs. 4.2b, Table S4.5), but it did not change significantly for descendants selected under the biotic, biotic x salt, phosphate or salt treatments ( $F_{6,26} = 1.92$ ,  $P = 0.119$ ,  $0.115$ ,  $0.953$  and  $0.385$  respectively; Figs. 4.2b, Table S4.5). Overall, the low nitrogen selection treatment resulted in the lowest mean nitrogen requirement ( $N^* = 2.64$ , Fig. 4.2b, Table S4.3), whereas the low phosphate selection treatment resulted in the highest mean requirement for nitrogen ( $N^* = 11.21$ , Fig. 4.2b, Table S4.3). Minimum phosphate requirements ( $P^*$ ) did not respond significantly to any of the selection environments measured in this study ( $F_{6,27} = 0.69$ ,  $P = 0.660$ , Fig. 4.2c, Table S4.5).

The response of descendants to initial increases in light ( $\alpha$ ) were affected by the selection treatment (Figs. 4.2e, Table S4.5). Compared to the ancestors,  $\alpha$  decreased significantly for all descendants regardless of the selection environment ( $F_{5,30} = 0.94$ ,  $P < 0.05$ , Fig. 4.2e, Table S4.5). The response of descendants to initial increases in phosphate ( $\alpha$ ) were also mediated by the selection treatment, although due to large variation among ancestors for this trait, the biotic and nitrogen treatments only marginally reduced  $\alpha$  in relative to the ancestor ( $F_{5,30} = 0.94$ ,  $P = 0.06$ , 0.041, Fig. 4.2g, Table S4.5). The response of ancestors and descendants to initial increases in nitrogen was not significantly effected by the selection treatment ( $F_{6,26} = 1.03$ ,  $P = 0.430$ , Fig. 4.2f, Table S4.5).

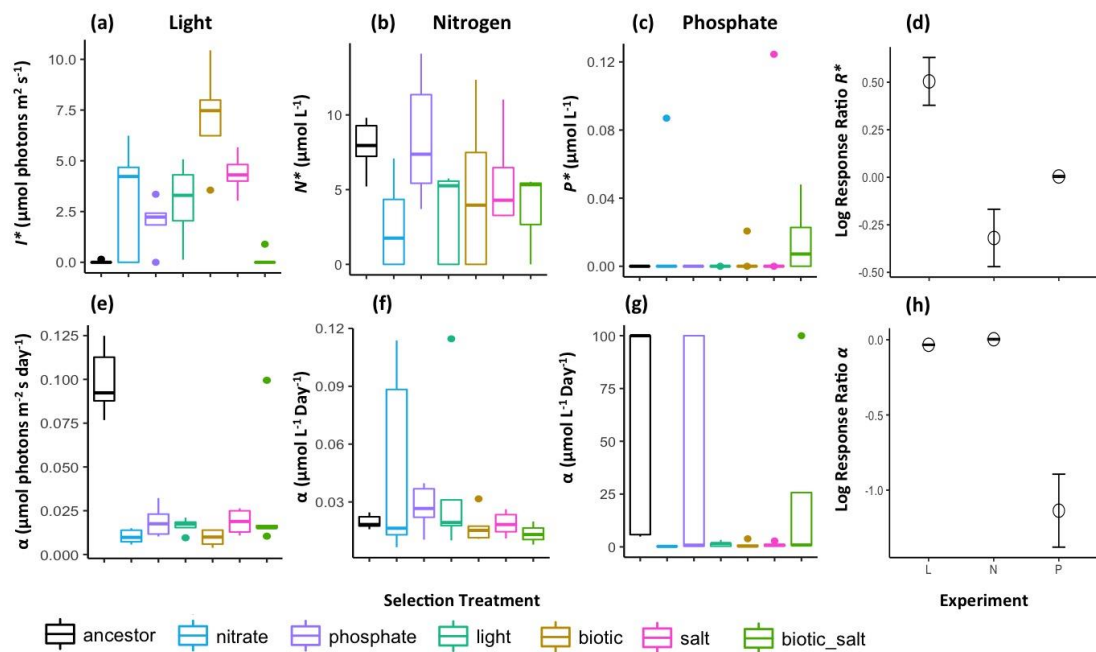


**Figure 4.2.** Minimum resource requirements evolve in response to selection environment and depend on the type of limiting resource. (a-c) The ancestral and environmentally-selected descendant minimum light ( $I^*$ ), nitrogen ( $N^*$ ) and phosphate requirements ( $P^*$ ). (d) Variation in the descendants'  $R^*$  for light, nitrogen and phosphate measured as the log response ratio of each descendant relative to its ancestor for each limiting resource. (e-g) The ancestral and environmentally selected descendants initial growth response ( $\alpha$ ) to increasing light, nitrogen and phosphate resource. (h) Variation in the descendants'  $\alpha$  for light, nitrogen and phosphate measured as the log response ratio of each descendant relative to its ancestor for each limiting resource.

### **(b) Ancestral genotype**

While the selection treatment was a better predictor for  $R^*$  than the ancestral identity for most descendants under light and phosphorus limitation (Figs. 4.3a,c, Table S4.5), the identity of the ancestral population was marginally more important in explaining the response of the descendant  $N^*$ s to environmental selection ( $F_{4,28} = 2.35$ ,  $P = 0.079$ , Fig. 4.3b, Table S4.5). Anc 2's minimum nitrogen requirement were significantly larger than Anc 3 and Anc 4 ( $F_{4,28} = 2.35$ ,  $P < 0.05$ , Fig. 4.3b, Table S4.5) under all selection treatments, and marginally higher than Anc 5 and the diverse population ancestor CC 1690 ( $F_{4,28} = 2.35$ ,  $P = 0.0632$ ,  $0.0690$ , Fig. 4.3b, Table S4.5), under certain selection treatments (Fig. 3), suggesting a possible genotype by environment interaction (as indicated by the crossover of ancestral lines). Overall, the genotypically diverse ancestor did not consistently accelerate the adaptive change in  $N^*$  (Fig. 4.3b).

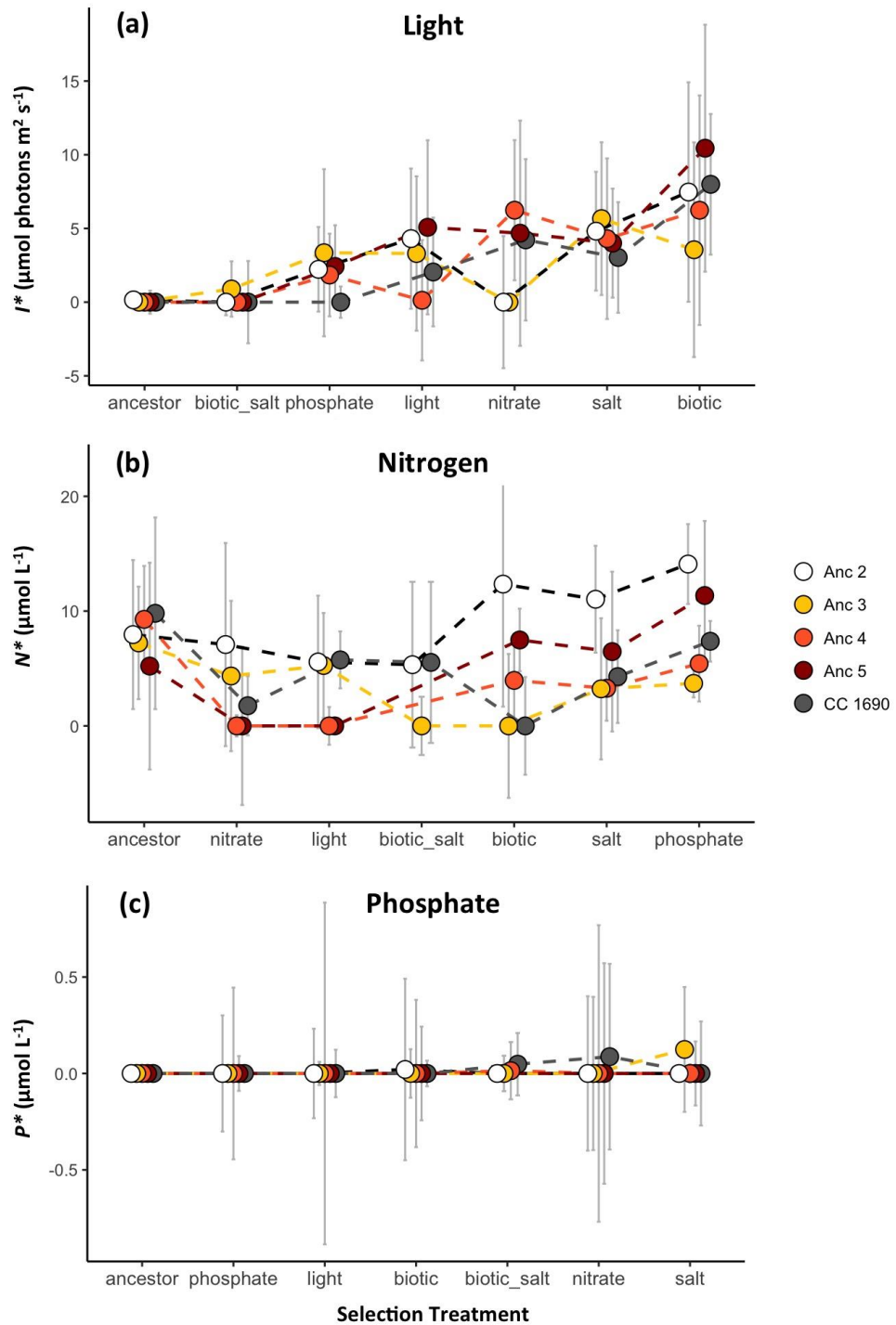


**Figure 4.3.** Ancestral genotypes only explain variation in descendant's response to nitrogen. The ancestral and environmentally-selected descendant minimum (a) light ( $I^*$ ), (b) nitrogen ( $N^*$ ) and (c) phosphate requirements ( $P^*$ ), coloured by ancestral genotype for each selection treatment.

### (c) Trade-offs in competitive ability

We did not find support for our hypothesis that there are trade-offs among the minimum requirements for light, nitrogen and phosphate. Variation in  $I^*$  and  $N^*$  was oriented orthogonally according to variation in the first two axes of a principal components analysis, suggesting that variation in these traits among ancestors and descendants of the selection experiment was largely independent ( $\rho = -0.28$ ,  $P = 0.112$ , Fig. 4.4a). There was relatively little variation in  $P^*$  observed (Fig. 4.2e), and overall, there was no evidence of a negative trade-off between  $P^*$  and  $N^*$  ( $\rho = -0.23$ ,  $P = 0.204$ ) or between  $P^*$  and  $I^*$  ( $\rho = 0.36$ ,  $P = 0.042$ ). Principal components analysis showed that 89.94% of the variation in these three traits is explained by the first two PC axes (Fig. 4.4a). The first axis (64.81% of the variation) corresponds primarily to variation associated with nitrogen requirements, and the second axis (25.13% of the variation) corresponds primarily to variation associated with light requirements. Minimum phosphate requirements did not correspond to the first two axes and was primarily associated with the third axis (PC3 = 9.06%, Fig. 4.4a, Table S4.6). An increase in light requirement explains most of the variance in the evolution of the descendants away from the ancestors, and the selection treatment explains more of the variation in nitrogen and phosphate requirements of the descendants (Fig. 4.4a, Table S4.6).

There was a clear separation of the ancestor and descendants' initial response to increases in resource ( $\alpha$ ). Principal components analysis shows that 94.73% of the variation in  $\alpha$  for all resources is explained by the first two PC axes (Fig. 4.4b). The first axis (81.73% of the variation) corresponds primarily to variation associated with the initial response to increases in phosphate, and the second axis (13% of the variation) corresponds primarily to variation associated with the initial response to increases in light and nitrogen (Fig. 4.4b, Table S4.6). The RDA constrained by selection treatment indicates a possible trade-off between  $R^*$  and  $\alpha$  (Fig. 4.4c). There was a weak, but significant negative correlation between  $R^*$  and  $\alpha$  ( $R^2 = 0.13$ ,  $P < 0.05$ , Fig. 4.4c), suggesting the existence of trade-off between the requirements of a resource and its initial growth response to increasing resource availability.

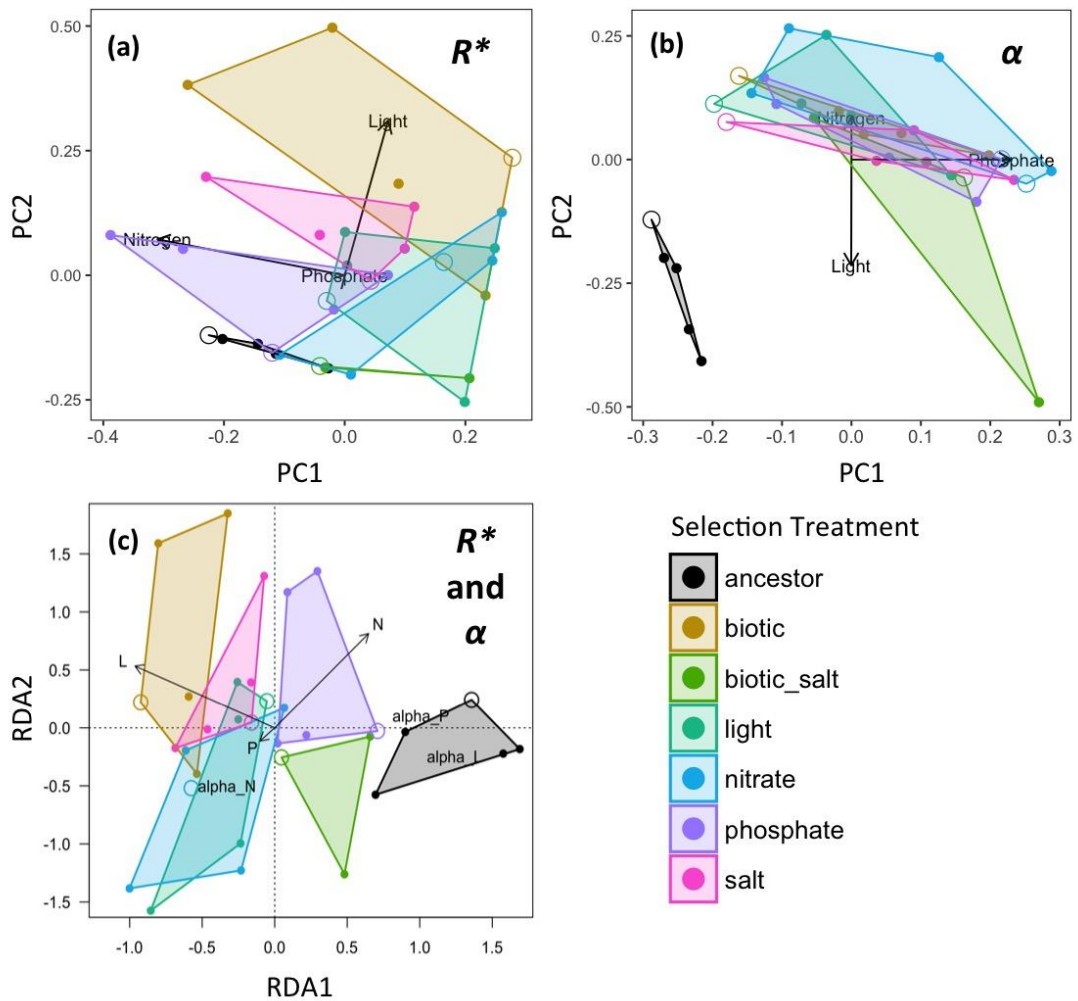


**Figure 4.4.** (a) Principle components analysis (PCA) showing the separation of the descendants and ancestors minimum resource requirements for light ( $I^*$ ), nitrogen ( $N^*$ ) and phosphate ( $P^*$ ) depending on the selection treatment onto the first two PC axes of a PCA. The first axis (64.81% of the variation) corresponds primarily to variation associated with nitrogen requirements, and the second axis (25.13% of the variation) corresponds primarily to variation associated with light requirements. Minimum phosphate requirements did not correspond to the first two axes and was primarily associated with the third axis (9.06% of the variation). (b) PCA showing clear separation of the ancestor and descendants' initial response to increases in resource ( $\alpha$ ). The first axis (81.73% of the variation) corresponds primarily to variation associated with the initial response to increases in phosphate, and the second axis (13% of the variation) corresponds primarily to variation associated with the initial response to increases in light and nitrogen. (c) An RDA constrained by selection treatment indicates a possible trade-off between  $R^*$  and  $\alpha$  (Note  $R^*$  and  $\alpha$  loading onto opposite orthogonal axes for each resource). The scores for the

genetically diverse ancestor *CC1690* under each selection treatment are plotted as open circles to distinguish from the isoclinal ancestors. The percentage of variation explained by each axis was 58% and 21% for axis 1 and axis 2 respectively.

Finally, we tested whether evolved differences in  $R^*$  were also associated with differences in low-resource fitness. Here we were focused only on nitrogen and light limitation because we observed minimal variation in  $P^*$  in the descendants of the selection experiment. The reaction norms provide evidence that all descendants have reduced fitness under low light relative to the ancestors, but greater fitness under low-nitrogen (Fig. S4.9a-f), consistent with the  $R^*$  results. This suggests that selection under nitrogen limitation increased fitness more than selection under light limitation (Figs. S4.1, S4.9g). The nitrogen selection treatment was also the most stressful treatment in chemostat at the end of the evolution experiment relative to the control, indicating that it imposed a greater selective pressure compared to the other selection environments (Fig. S4.1). The genotypically diverse ancestor evolved a greater relative fitness benefit under low nitrogen than the other descendants evolved from isoclinal ancestors.

## **Discussion**

The requirements of *C. reinhardtii* for three essential resources responded to selection under low resource availability and osmotic stress in all possible ways: adaptive evolutionary trait change, non-adaptive change and no change. Nitrogen requirements were reduced in low-nitrogen environments, demonstrating the approach to an adaptive phenotypic trait optimum (lower  $N^*$ ). Light requirements moved away from an ancestral trait optimum (shown by the increase in  $I^*$ ), even when selected under low light. Finally, phosphorus requirements did not change significantly as a result of selection in any environment, potentially due to a constraint on trait variation (indicated by the lack of variation in  $P^*$ ). Counter to our predictions, neither stress nor genotypic diversity significantly nor consistently increased the magnitude of adaptive change. We also did not find support for the emergence of trade-offs among competitive abilities across descendant genotypes as has been observed among species across much larger taxonomic scales.

All of the descendants evolved a lower resource requirement for nitrogen regardless of the selection history. In agreement with our hypothesis, descendants selected under low nitrogen decreased their requirements for nitrogen the most compared to the ancestor. The opposite has been demonstrated in isolates of natural fungi (Goddard and Bradford 2003), where isolates did not adapt to nitrogen-limitation but did so when limited by carbon, as a result of greater adaptation to nitrogen- than carbon-limitation in the ancestral populations. The fact that the ancestral population had higher requirements for nitrogen than the descendants in our study suggests that selection may result in advantageous mutations in competitive traits towards a trait optimum, but will do little for populations that are already close to their adaptive optimum for a particular resource. The population growth rate response of descendants to initial increases in nitrogen supply ( $\alpha$ ) was not altered by the selection treatment and therefore did not evolve in the same direction as  $N^*$ . These outcomes differ from previous findings of multiple trait adaptation to fish predation, where most traits evolved towards their new optima (Stoks *et al.* 2016). Therefore, although strong selection may cause rapid evolution in some competitive traits, our results suggest that not all traits determining competitive ability for a resource will respond to selection.

In contrast to the nitrogen experiment, the ancestral populations originally started with near-zero requirements for light. The lowest level of light imposed under the low-light selection ( $5 \mu\text{mol photons}\cdot\text{m}^{-2}\cdot\text{s}^{-1}$ ) may therefore not have imposed strong light limitation (Figs.4.1a, S4.1, Table S4.1), effectively representing a case of relaxed selection (Lahti *et al.* 2009). The environment that combined biotic and salt stress however maintained the low ancestral light requirement. This likely resulted from a stronger selective pressure on  $I^*$  (although not by directly limiting light), keeping descendants on the ancestral low-light trait optimum. This suggests that the combined biotic and salt stress selection treatment may have been most similar to the growth conditions of this *Chlamydomonas* strain in the culture collection, where cultures are maintained under relatively low light, on agar with a Yeast-Acetate (YA) medium which includes organic carbon from yeast extract and acetate, as well as inorganic mineral salts (Sueoka 1960). Similar conditions can result in the evolution of *Chlamydomonas* into efficient heterotrophs through adaptation to low light and the supply of an organic substrate (acetate) (Bell 2013). This may explain the ancestral low light requirements observed in this study. The increase in light



requirement observed in many of the treatments may also have occurred via selection on another, genetically correlated, trait via antagonistic pleiotropy or linkage disequilibrium (Velicer 1999, Jeffery 2005, Lahti *et al.* 2009). Selection may therefore have occurred on an unmeasured trait that is negatively associated with  $I^*$ . One possibility, given our knowledge of the historical growth environment, could be selection for an increase in growth rate in chemostat. Cultures were previously maintained on agar plates and sub cultured only once every few months, allowing for slow growth rates, but in chemostats a growth rate higher than the dilution rate is necessary to maintain a viable population. More light may also then be required to maintain this higher-than ancestral growth rate, especially given the absence of organic carbon substrates in the selection medium.

The lack of adaptation to phosphorus limitation may be explained by the adaptive constraint resulting from the low genotypic variation in  $P^*$  among the populations, or by the stabilizing selection on this trait either directly, or indirectly (via selection on a correlated trait) across all selection treatments. The ancestral populations may also have already been at their trait optimum for phosphorus, where the descendants remained. A previous study was also unable to detect specific evolutionary adaptation to elevated  $\text{CO}_2$  (Low-Décarie *et al.* 2013) due to conservation in the ability to utilize carbon. However, there was large variation in the response of the ancestors to increasing amounts of phosphate ( $\alpha$ ). Phosphate is the most biologically available form of phosphorus for most phytoplankton and is usually found in low concentrations in aquatic ecosystems (Maloney *et al.* 1972), therefore even slight increases in phosphate can produce large increases in the growth rate.

We also tested whether different ancestral genotypes affected the response of the environmentally selected descendants to limiting light, nitrogen and phosphate. There were differences among ancestral genotypes in the evolution of  $R^*$  only when they were limited by nitrogen. In particular Anc 2 had the largest requirements for nitrogen depending on the type of environmental selection. However, the genetically diverse population (CC1690) did not consistently show a stronger adaptive change in  $N^*$ , contrary to our prediction (Hughes *et al.* 2008), which may have been due to clonal interference slowing the adaptive potential of the genotypically diverse population (Gerrish and Lenski 1998). In a previous study, the impact of nitrogen limitation on CC1690, Anc 3 and Anc 5, showed that the genetically diverse

population maintained higher single-cell multi-dimensional phenotypic variation for three phenotypes (high chlorophyll, high membrane lipid and high storage lipid) over time (Krismer *et al.* 2016). This suggests that although, genetic diversity can result in greater individual-level variation in some phenotypic responses in *C. reinhardtii*, it does not necessarily translate into a greater adaptive potential for  $R^*$  under selection by limiting resources. To test how genotypic diversity affects the evolution of competitive abilities, competition experiments between all descendants and ancestors, with clear variation in  $R^*$  traits for nitrogen or light could be carried out, while tracking the changes in frequency of all genotypes, to show whether the genotype with the lowest  $R^*$  wins, and is fixed in a population under low resource availability.

An adaptive decline in resource requirements for light did not come at a reduced competitive ability for nitrogen, as previously hypothesized, and variation in these traits among ancestors and descendants were largely independent. Although such a trade-off has been found for light and nitrogen resource across large taxonomic groups (Litchman and Klausmeier 2001, Litchman *et al.* 2007), we find that the same trade-off does not occur within a species. This suggests that the trade-offs among species result from long-term adaptation and speciation that are not observed at the intraspecific level. Moreover, the trade-offs may not be due to genetic or biophysical constraints of trade-offs (Via and Lande 1985, Houle 1991). Despite the lack of intraspecific trade-off for  $R^*$  between resources, we found a negative trade-off between the minimum resource requirement and the initial growth response ( $\alpha$ ) to low resource availability across light and nitrogen resource. There is other evidence for trade-offs occurring between the maximum growth rate, equilibrium competitive ability and ability to store phosphorus between species (Edwards *et al.* 2011), indicating that different strategies are favoured under different conditions of nutrient supply. A negative relationship between  $R^*$  and  $\alpha$  therefore suggests that when resources are limiting, populations may evolve a lower requirement for a resource by increasing their initial growth response to increasing amounts of resource.

Although we provide novel and valuable insights into the evolutionary potential of resource requirements, the experimental work used only one species of phytoplankton. Although *C. reinhardtii* is a well-established model species used for the study of evolutionary adaptation (Bell 1991, 2013), different phytoplankton

species have markedly different life cycles and growth strategies that may alter their responses to limiting nutrients (Litchman *et al.* 2015). For example, smaller phytoplankton grow particularly well under low resource availability because of their high surface area to volume ratio, enabling rapid assimilation of nitrate (Hein *et al.* 1995). The intraspecific patterns in trade-offs identified in this chapter are also limited to a single species. Therefore the findings of an adaptive response to resource limitation or the evidence of intraspecific trade-offs cannot be directly generalised to other species. A promising avenue for future work would be to investigate the evolutionary changes of multiple species (including those studied in Chapter 3), to assess generality of these findings.

Although genetic diversity did not result in a stronger adaptive change in the minimum resource requirements for light, nitrogen and phosphate, the genetically diverse population of *C. reinhardtii* may have a lower resource requirement compared to the isoclonal populations at higher temperatures (as shown by the temperature dependence of resource requirements in Chapter 3). Currently it is not clear whether an adaptation for improved competitive ability in one environment at higher temperature will come at a cost in another, and whether genetic diversity may alleviate the phenotypic constraint on the response. It would therefore be interesting to empirically test the minimum resource requirements of environmentally adapted population from the genetically diverse ancestors and isoclonal ancestors to see whether the adaptive response varies across a temperature gradient.

Despite these limitations, we show that the adaptive potential of some resource requirements may be constrained or may undergo correlated evolution, which could limit the degree of adaptive convergence in  $R^*$  of competitors, or may even show non-adaptive selection or drift away from the trait optimum. This contradicts the theory predicting that adaptation under essential resource limitation should lead to convergence of competitive abilities among competitors when limited by the same resource (Fox and Vasseur 2008). A promising venue for future studies would experimentally test whether and how the evolution of competitive traits alters ecological dynamics. Characterizing the adaptive potential of a species' competitive ability is therefore a necessary first step with important consequences for predicting the effects of evolution on the competitive outcomes in response to environmental change.

## CHAPTER 5

### General Conclusions

The main aim of my research was to investigate how freshwater planktonic species, communities and ecosystem are governed by abiotic environmental change. The results presented in this thesis connect the main ideas outlined in the Introduction Chapter (Chapter 1). I used freshwater planktonic communities as experimental model systems and measured the response of individual species and functional traits to provide novel mechanistic insights into the effects of warming and resource availability on population and community structure.

In Chapter 2, a microcosm experiment of the combined effects of temperature and non-resource diversity revealed that both temperature and diversity independently reduced CO<sub>2</sub> concentration, with a dramatic reduction only at the highest diversity treatment. This work is the first to demonstrate the pivotal role of high diversity of inedible resources in reducing CO<sub>2</sub> concentrations, with the potential to mitigate the impact of on-going and accelerating climate warming. The identity of the species that comprised the high diversity treatments was also important for determining the functional response of the community to changes in the environmental temperature (Chapter 2). Indeed it is well known that individual functional groups within phytoplankton communities can respond differentially to global warming (Litchman *et al.* 2015, Thomas *et al.* 2016). In Chapter 3 I demonstrated that the key functional traits governing interspecific phytoplankton competition for light and nitrogen are strongly temperature- and species-dependent, and can subsequently explain the distributions of species under different temperature regimes. In particular, I found that under light and nitrogen limitation, resource requirements are generally lowest at intermediate temperatures, and that changes in temperature may therefore alter the competitive hierarchy amongst species.

The turnover in the identity and abundance of a particular species within a community characterised in Chapters 2 and 3 may also result from nutrient limitation favouring particular populations of a single species that have selective advantages in different environments. In Chapter 4, I find that local adaptation to different environmental stressors is critical for predicting the outcomes of competition under

resource limitation. Using *Chlamydomonas reinhardtii* as a model green alga, I showed that populations are able to evolve their resource requirements to respond to low-resource availability. In particular, I revealed that populations evolve lower requirements for nitrogen when limited by nitrogen, allowing *C. reinhardtii* populations to approach an adaptive-trait optimum. Populations can also move away from an optimum of ancestral populations established under light limitation, thus increasing the requirement for light in descendant populations. There may also be no adaptive response in competition traits to phosphate limitation, presumably due to a highly conserved constraint for phosphate requirements present in ancestral populations, perhaps because phosphate is usually found in low concentrations in aquatic ecosystems (Maloney *et al.* 1972). Increasing environmental stressors may therefore select for particular populations depending on the type of adaptation to the most limiting resource, therefore influencing overall ecosystem functioning (chapter 2) in a multitude of ways (Litchman *et al.* 2015).

Species are constantly adjusting to changes in local environmental conditions. Where phenotypic plasticity or genetic adaptations cannot cope with the environmental change, the species can either move to a more favourable environment or go locally extinct. My thesis identifies some of the main mechanisms underlying co-existence within plankton communities within a variable abiotic environment. I identified the relative importance of adaptation, and the role of temperature in governing the interactions of freshwater plankton communities. This work thus improves our mechanistic understanding of the pivotal role of species diversity and thus improving the forecasts of community dynamics in a changing world.

# SUPPLEMENTARY MATERIAL

## Supplementary Chapter 2

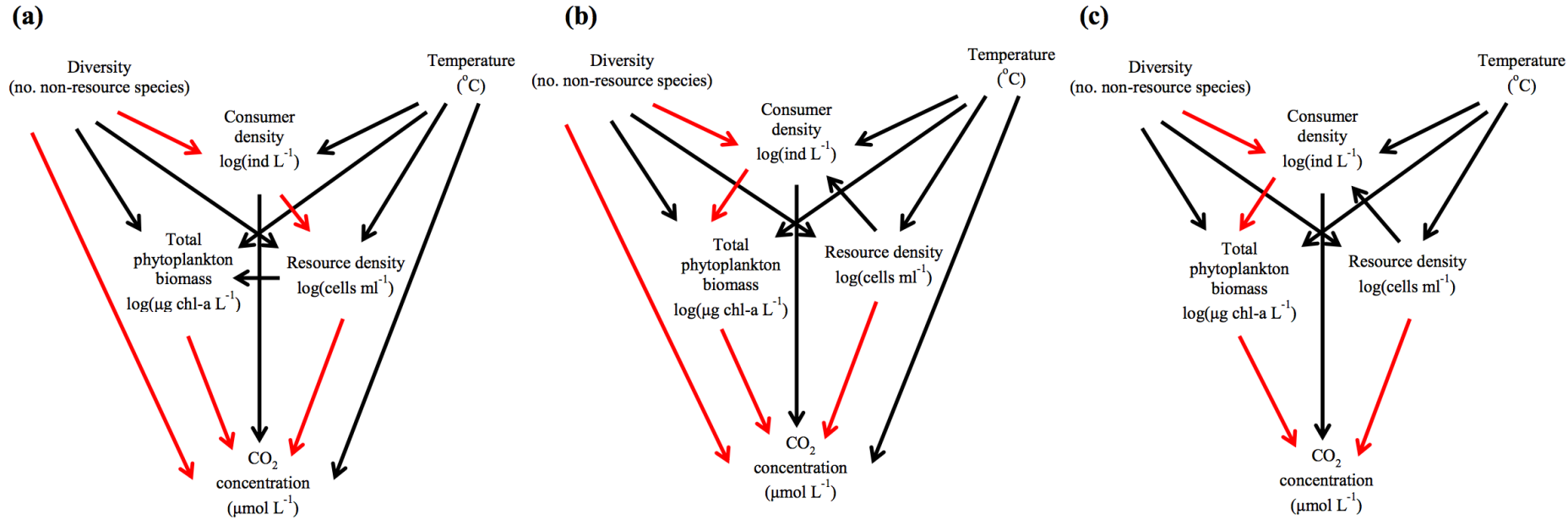


**Figure S2.1.** Conceptual path diagram illustrating the alternative hypotheses based on the models presented in Table S2.5, of how warming ( $^{\circ}\text{C}$ ) and phytoplankton diversity (number of non-resource species), may affect consumer density, resource density, total phytoplankton biomass (total chlorophyll-a concentration) and  $\text{CO}_2$  concentration. Red and black colors indicate negative and positive effects respectively. All models, (a) model 1 and 2, (b) model 3, (c) Model 4, reflect our hypotheses that (i) high temperature would directly increase consumer density, resource density and total phytoplankton biomass; (ii) high diversity would reduce consumer density, increase resource density and total phytoplankton biomass; (iii) consumers increase  $\text{CO}_2$  concentration whilst total phytoplankton biomass and resource density reduces  $\text{CO}_2$  concentration in the water. (iv) at high temperature, high diversity would reduce consumer density, increase resource density and total phytoplankton biomass, and reduce  $\text{CO}_2$  concentration; (v) at high temperature, low diversity would increase consumer density, decrease resource density, decrease total phytoplankton biomass but increase  $\text{CO}_2$  concentration. We composed models with (model 1 2 and 3) or without (model 4) a direct effect of temperature and diversity on  $\text{CO}_2$  concentration, and with biologically relevant combinations of direct links of consumer, resource densities and total phytoplankton biomass. Model 2 included phytoplankton composition as a random factor.

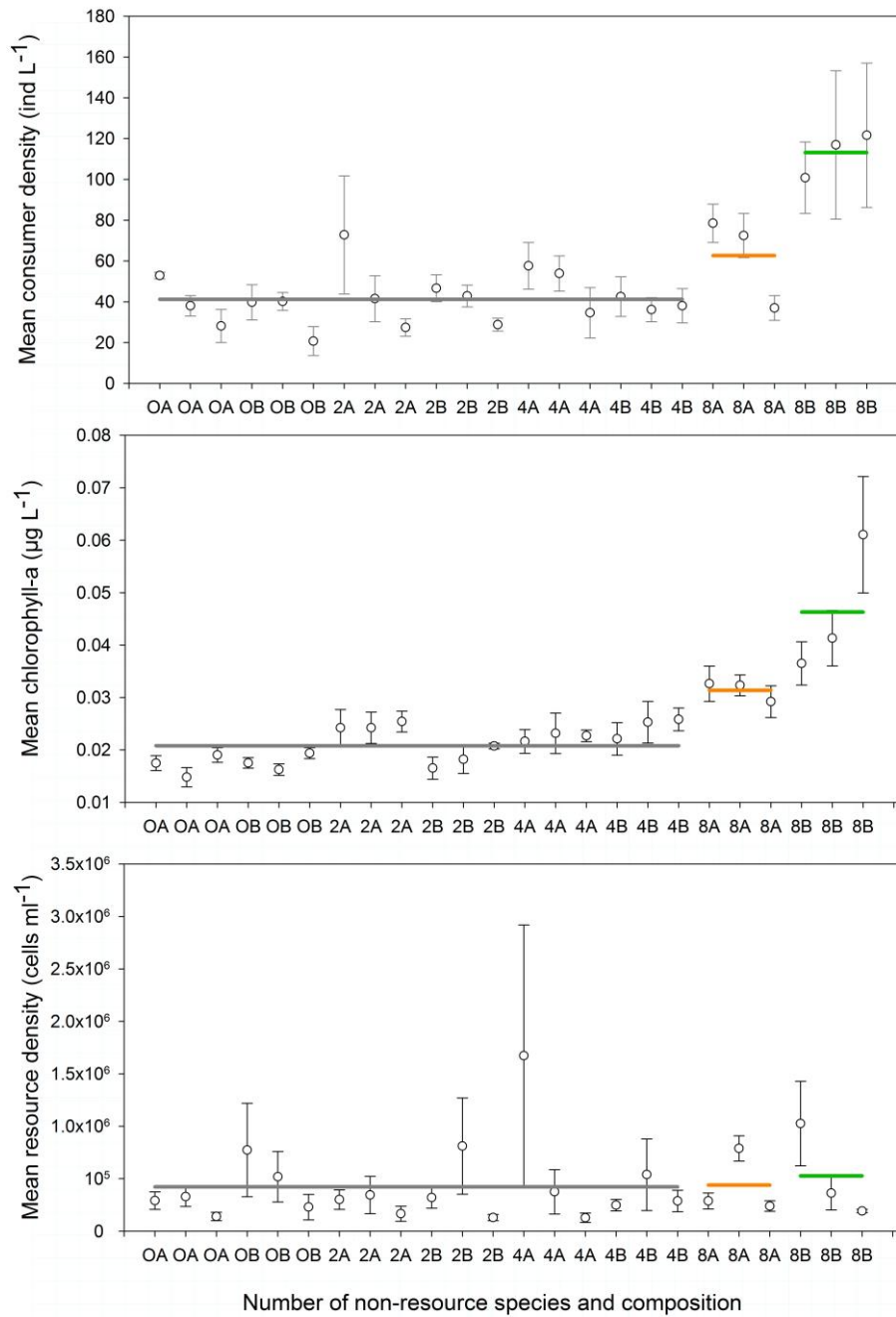


**Figure S2.2.** Mean consumer density, chlorophyll-*a* concentration (total phytoplankton biomass) and resource density over the over the experimental duration for different diversity levels and community compositions (error bars are  $\pm 1$  standard error, N=4). Horizontal lines are means of each diversity category (grey for all 0, 2 and 4 non-resource diversity treatments combined, orange for 8 non-resource composition A and green for 8 non- resource composition B).



**Table S2.1.** Inocula of phytoplankton species that originated from the Experimental Phycology and Culture Collection of Algae at the University of Göttingen (EPSAG) and the Culture Collection of Algae of Charles University in Prague (CAUP). Cell diameter and biovolume estimates were determined from an average sample size of 30 cells calculated using a stage micrometer. Cell diameters are mean  $\pm$  1 SD. Biovolumes for each species were calculated using equations based on the body shape and cell size of each species (Hillebrand *et al.* 1999). The last column indicates the number of lakes each phytoplankton species occurs across North America as found in the US EPA's National Lakes Assessment survey (2007).

Species	Source & Identifier	Cell Diameter ( $\mu\text{m}$ ) ( $\pm$ SD) <b>Biovolume (<math>\mu\text{m}^3</math>)</b>	No. lakes each species occurs
<i>Chlorella vulgaris</i>	EPSAG 211-11b	4 $\pm$ 0.44 <b>33.49</b>	
<i>Cosmarium botrytis</i>	EPSAG 612-5	43 $\pm$ 1.6 <b>41608.66</b>	161
<i>Closterium acerosum</i>	EPSAG 126.8	333 $\pm$ 7.52 <b>109089</b>	545
<i>Mougeotia sp.</i>	EPSAG 650-1	1494 $\pm$ 67.06 <b>269181.69</b>	366
<i>Eremosphaera viridis</i>	EPSAG 228-1	182 $\pm$ 1.42 <b>3154950.59</b>	2
<i>Staurastrum pingue</i>	EPSAG 5.94	56 $\pm$ 3.3 <b>11084</b>	70
<i>Pediastrum duplex</i>	EPSAG 84.8	27 $\pm$ 6.52 <b>140</b>	360
<i>Eudorina elegans</i>	EPSAG 29.87	38 $\pm$ 2.83 <b>2467.7</b>	545
<i>Closterium littorale</i>	EPSAG 611-7	146 $\pm$ 7.74 <b>3750</b>	366
<i>Ankistrodesmus falcatus</i>	EPSAG 202-2	44 $\pm$ 1.58 <b>363.2</b>	2
<i>Volvox aureus</i>	EPSAG 88-1	159 $\pm$ 13.34 <b>7563.1</b>	139
<i>Micrasterias crux-melitensis</i>	CAUP K602	98 $\pm$ 98- 1.13 <b>5670.6</b>	511

**Table S2.2.** Chemical composition of Volvic Mineral Water used as experimental media.

Mineral:	Composition (mg l <sup>-1</sup> ):
Calcium (Ca)	12
Sulphates (SO <sub>4</sub> )	9
Magnesium (Mg)	8
Sodium (Na)	12
Bicarbonates (HCO <sub>3</sub> )	74
Potassium (K)	6
Silica (SiO <sub>2</sub> )	32
Chlorides (Cl <sup>-</sup> )	15
Nitrates (NO <sub>3</sub> )	7.3

**Table S2.3.** Linear mixed effects (LMEs) model summary statistics illustrating the independent and combined effects of non-resource diversity and environmental temperature on the time averaged response variables: (i) consumer density (number of *D. pulex* per sample), (ii) resource density (number of *C. vulgaris* cells per sample), (iii) total phytoplankton biomass (aggregated biomass of all phytoplankton taxa in the community) and (iv) concentration of CO<sub>2</sub> (amount of CO<sub>2</sub> in the water uncorrected for the difference in solubility at each temperature). Temperature and non-resource diversity were treated as fixed effects. We accounted for the temporal blocks, non-resource community composition and position of the microcosms in the incubators (nested in time) as random effects. We used the *varIdent* function to improve homogeneity of variance in the model fit (Zuur *et al.* 2009).

	d.f.	<i>F</i> value	R <sup>2</sup> (cond)	R <sup>2</sup> (marg)	<i>P</i>
(a) CO <sub>2</sub> uncorrected			0.938	0.565	
Diversity	1,89	9.719			0.0025
Temperature	1,89	48.942			<0.0001
Diversity*Temperature	1,89	0.042			0.838
(b) Phytoplankton biomass			0.609	0.236	
Diversity	1,89	60.931			<0.0001
Temperature	1,89	3.788			0.050
Diversity*Temperature	1,89	0.732			0.395
(c) Consumer			0.414	0.219	
Diversity	1,89	13.333			0.0004
Temperature	1,89	20.358			<0.0001
Diversity*Temperature	1,89	0.462			0.498
(d) Resource			0.638	0.099	
Diversity	1,89	1.309			0.256
Temperature	1,89	10.023			0.002
Diversity*Temperature	1,89	0.353			0.554

**Table S2.4.** Linear mixed effects (LMEs) model summary statistics illustrating the independent and combined effects of non-resource diversity and environmental temperature on four response variables: (i) consumer density (number of *D. pulex* per sample), (ii) resource density (number of *C. vulgaris* cells per sample), (iii) total phytoplankton biomass (aggregated biomass of all phytoplankton taxa in the community) and (iv) concentration of CO<sub>2</sub> (amount of CO<sub>2</sub> in the water uncorrected for the difference in solubility at each temperature). This model was fit to the whole time series data. Temperature and non-resource diversity were treated as fixed effects. We accounted for the temporal blocks, non-resource community composition and position of the microcosms in the incubators (nested in time) as random effects. We used the *varIdent* function to improve homogeneity of variance in the model fit (Zuur *et al.* 2009).

	d.f.	<i>F</i> value	R <sup>2</sup> (cond)	R <sup>2</sup> (marg)	<i>P</i>
(a) CO <sub>2</sub> uncorrected			0.855	0.052	
Diversity	1,191	18.161			<0.0001
Temperature	1,1308	119.005			<0.0001
Diversity*Temperature	1,1308	0.008			0.931
(b) Phytoplankton biomass			0.899	0.174	
Diversity	1,191	125.591			<0.0001
Temperature	1,1310	9.995			0.002
Diversity*Temperature	1,1310	3.686			0.055
(c) Consumer			0.799	0.046	
Diversity	1,191	29.691			<0.0001
Temperature	1,1310	28.164			<0.0001
Diversity*Temperature	1,1310	0.976			0.323
(d) Resource			0.858	0.008	
Diversity	1,191	1.911			0.169
Temperature	1,1310	13.612			0.0002
Diversity*Temperature	1,1310	0.627			0.429

**Table S2.5.** A comparison of different structural equations models (SEMs) used to explain patterns of covariance among variables analyzed in this experiment (Lefcheck 2016). We compared the models with (models 1,2 and 3) or without (model 4) a direct effect of temperature (T) and diversity (D) on CO<sub>2</sub> concentration, and with biologically relevant combinations of direct links of consumer (C), resource (R) densities and total phytoplankton biomass (Chl). The best model (model 1) was also compared to a model with phytoplankton composition as a random factor (model 2) to test whether species compositions contributed to any variation in the data. We also simplified the model by removing individual pathway predictors (models 5 and 6) but model 1 described the data best, as indicated by the lowest AIC and non-significant Fisher C. For each model we report the degrees of freedom, Fisher C, P value, *n* (number of samples) and *K* (number of model parameters). We selected the model with the lowest AIC score, representing the best fit to our data. All SEMs incorporated a random effect of block, time and position within the incubator. The degrees of freedom were extracted directly from the analyses summary statistics using the *sem.fit* function from the PiecewiseSEM package in R. Notes: The best model is in bold font.

<b>Model</b>	<b>Description</b>	<b>d.f.</b>	<b>Fisher C</b>	<b>P</b>	<b>n</b>	<b>K</b>	<b>AIC</b>
<b>1</b>	<b>CO<sub>2</sub> ~ T + D + Chl + C + R</b> <b>Chl ~ T + D + R</b> <b>R ~ T + D + C</b> <b>C ~ T + D</b>	<b>2</b>	<b>3.20</b>	<b>0.202</b>	<b>1536</b>	<b>33</b>	<b>69.2</b>
2	Model 1 with composition as random factor	2	3.38	0.184	1536	37	77.38
3	CO <sub>2</sub> ~ T + D + Chl + C + R Chl ~ T + D + C R ~ T + D C ~ T + D + R	2	31.19	0	1536	33	97.19
4	CO <sub>2</sub> ~ Chl + C + R Chl ~ T + D + C R ~ T + D C ~ T + D + R	6	39.06	0	1536	31	101.06
5	CO <sub>2</sub> ~ T + D + Chl + C + R Chl ~ T + D + R R ~ T + C C ~ T + D	4	9.40	0.052	1536	32	73.4
6	CO <sub>2</sub> ~ T + D + Chl + C + R Chl ~ T + D + R R ~ T C ~ T + D + R	4	8.66	0.070	1536	32	72.66

### Supplementary Chapter 3

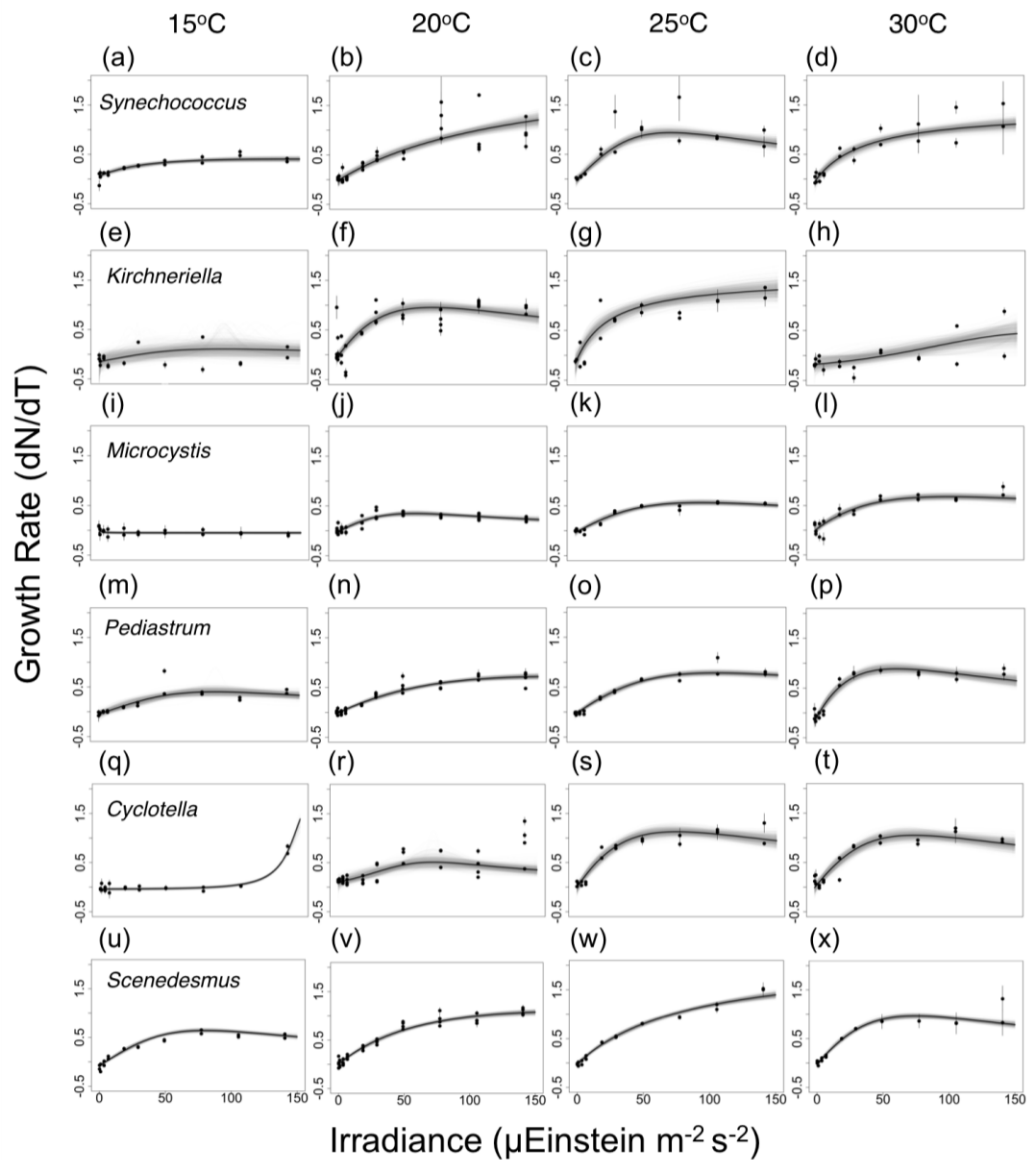


**Figure S3.1.** The interactive effect of temperature and light on growth rate of six freshwater phytoplankton species. Fitted models are of equation (1). (a-d) *Synechococcus*, sp. (e-h) *Kirchneriella subcapitata*, (i-l) *Microcystis*, (m-p) *Pediastrum boryanum*, (q-t) *Cyclotella meneghiniana*, (u-x) *Scenedesmus acuminatus*. Growth rate estimates were weighted based on the uncertainty in each point. The grey lines represent represents the 95% confidence interval of the curve using 1000 bootstrapped values.

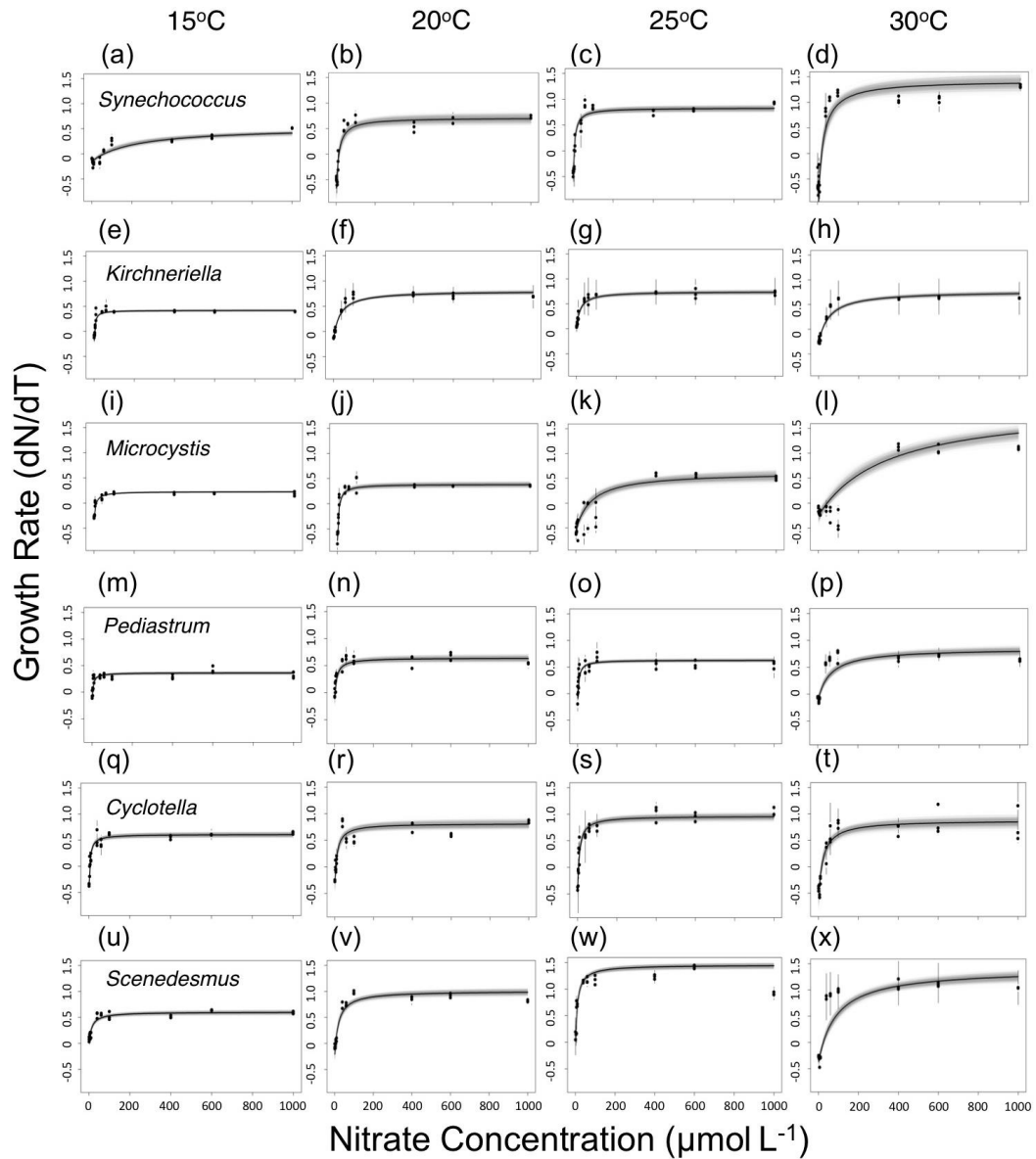


**Figure S3.2.** The interactive effect of temperature and nitrate concentration ( $\mu\text{mol L}^{-1}$ ) on growth rate of six freshwater phytoplankton species. Fitted models are of equation (2). (a-d) *Synechococcus*, sp. (e-h) *Kirchneriella subcapitata*, (i-l) *Microcystis*, (m-p) *Pediastrum boryanum*, (q-t) *Cyclotella meneghiniana*, (u-x) *Scenedesmus acuminatus*. Growth rate estimates were weighted based on the uncertainty in each point. The grey lines represent represents the 95% confidence interval of the curve using 1000 bootstrapped values.



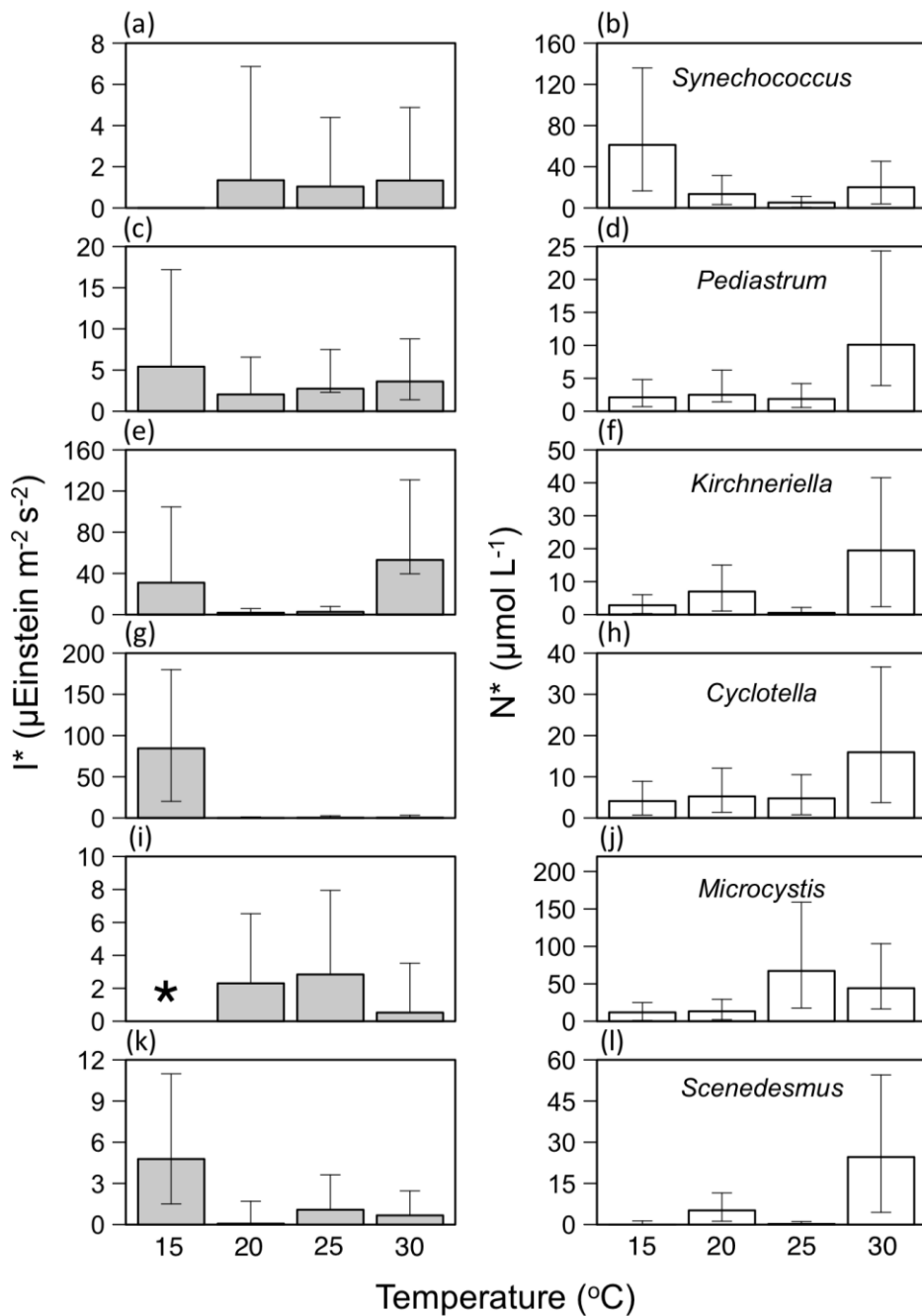


**Figure S3.3.** Within species comparisons of the estimated minimum resource requirements for light ( $I^*$ ) and nitrogen ( $N^*$ ) across a gradient of temperature for (a-b) *Synechococcus* sp., (c-d) *P. boryanum*, (e-f) *K. subcapitata*, (g-h) *C. meneghiniana*, (i-j) *M. aeruginosa* and (k-l) *S. acuminatus*. It was observed that *M. aeruginosa* did not grow at 15°C and therefore  $I^*$  could not be estimated (denoted by the \*).

**Table S3.1.** The list of phytoplankton taxa used for both, the light and nitrogen competition experiments. The culture collection names are abbreviations: SAG = Sammlung von Algenkulturen Göttingen (Göttingen, Germany), CCAP = the Culture Collection of Algae and Protozoa (Oban, Scotland). Temperature optima ( $T_{opt}$ ) were obtained from (Thomas *et al.* 2016) and approximated based on different measurements from multiple strains. These taxa can be found naturally in lakes across North America, as described in the US EPA’s National Lakes Assessment survey ((USEPA) 2009).

Species	Culture Collection	Strain Number	$T_{Opt}$ (°C)
<i>Scenedesmus acuminatus</i>	SAG	38.81	29
<i>Pediastrum boryanum</i>	SAG	87.81	19
<i>Kirchneriella subcapitata</i>	SAG	12.81	24-26
<i>Cyclotella meneghiniana</i>	SAG	1020.1a	24
<i>Synechococcus sp.</i>	CCAP	1479.10	31
<i>Microcystis aeruginosa</i>	Lab Strain	-	28-33

**Table S3.2.** Light limitation experimental parameter estimates for six freshwater phytoplankton species.  $\alpha$  is the species' initial response to elevated resource availability,  $\mu_{max}$  is the maximum growth rate under non-limiting light conditions,  $I_{opt}$  is the optimal irradiance for growth and  $I^*$  is the species minimum light requirement. Parameter uncertainty (in parentheses) was measured as the 95% confidence width estimated from 1000 bootstrap values.

Species	Temp (°C)	$\alpha$	$\mu_{max} \pm SE$	$I_{opt}$	$I^*$ [ $\mu\text{mol photons m}^{-2}\text{s}^{-2}$ ]
<i>Scenedesmus acuminatus</i>	15	0.02 (0.01-0.02)	0.65 ± 0.0000 3	80.24 (75.67-87.29)	4.78 (3.27-6.20)
	20	0.02 (0.02-0.03)	1.16 ± 0.02	194.73 (194.73-194.73)	0.07 (0-1.63)
	25	0.03 (0.02-0.03)	1.53 ± 0.04	9049.78 (9049.8-9049.8)	1.08 (0-2.54)
	30	0.03 (0.02-0.07)	1.32 ± 0.27	74.50 (68.42-83.51)	0.67 (0-1.78)
<i>Pediastrum boryanum</i>	15	0.01 (0.003-0.03)	0.82 ± 0.05	86.88 (70.47-951.56)	5.42 (0-11.77)
	20	0.01 (0.01-0.02)	0.79 ± 0.09	168.69 (168.69-168.69)	2.05 (0-4.52)
	25	0.02 (0.01-0.03)	1.10 ± 0.11	104.23 (92.38-123.65)	2.74 (0.44-4.76)
	30	0.05 (0.03-0.09)	0.90 ± 0.09	60.98 (52.17-77.86)	3.62 (2.21-5.17)
<i>Kirchneriella subcapitata</i>	15	0.01 (0.0001-1)	0.35 ± 0.01	92.85 (35.31-8402.34)	30.97 (0-73.69)
	20	0.04 (0.02-0.08)	1.10 ± 0.07	70.74 (57.99-110.84)	1.80 (0-4.01)
	25	0.07 (0.03-0.18)	1.36 ± 0.004	10000 (10000-10000)	2.68 (0-5.14)
	30	0.002 (0.0001-0.02)	0.88 ± 0.08	175.50 (175.50-175.50)	53.06 (13.41-77.77)
<i>Cyclotella meneghiniana</i>	15	0.0001 (0.0001-0.0001)	0.84 ± 0.05	156.13 (156.11-156.19)	84.46 (64.28-95.56)
	20	0.01 (0.0001-0.06)	1.35 ± 0.08	71.66 (52.88-3986.30)	0 (0-1.24)
	25	0.04 (0.02-0.07)	1.31 ± 0.19	74.84 (62.73-113.52)	0.27 (0-2.32)
	30	0.03 (0.02-0.07)	1.20 ± 0.20	74.33 (62.08-104.20)	0.34 (0-2.92)
<i>Synechococcus</i>	15	0.01 (0.01-0.03)	0.55 ± 0.06	141.40 (141.40-141.40)	0 (0-0)
	20	0.02 (0.01-0.03)	1.71 ± 0.04	1421.90 (1421.9-1421.9)	1.35 (0-5.52)
	25	0.03 (0.02-0.05)	1.66 ± 0.48	70.77 (61.58-88.69)	1.04 (0-3.34)

	30	0.04 (0.02-0.07)	1.53 ± 0.45	9838.23 (9838.2-9838.2)	1.33 (0-3.55)
<i>Microcystis aeruginosa</i>	15	1.000 (0.02-1)	0.09 ± 0.10	0.22 (0.09-0.45)	0.05 (0.02-0.12)
	20	0.01 (0.01-0.03)	0.48 ± 0.03	57.53 (50.14-68.77)	2.30 (0-4.22)
	25	0.02 (0.01-0.03)	0.58 ± 0.02	92.90 (84.50-120.53)	2.84 (0-5.12)
	30	0.02 (0.01-0.04)	0.88 ± 0.10	99.99 (79.56-1190.55)	0.53 (0-3)

**Table S3.3.** Nitrate limitation experimental parameter estimates for six freshwater phytoplankton species.  $\alpha$  is the species' initial response to elevated resource availability,  $\mu_{max}$  is the maximum growth rate under non-limiting nitrate conditions,  $m$  is the specific growth rate at  $N = 0$  and  $N^*$  is the species minimum nitrate requirement. Parameter uncertainty (in parentheses) was measured as the 95% confidence intervals estimated from 1000 bootstraps.

Species	Temp (°C)	$\alpha$	$\mu_{max} \pm SE$	$m$	$N^*$ [ $\mu\text{mol L}^{-1}$ ]
<i>Scenedesmus acuminatus</i>	15	0.04 (0.03-0.08)	$0.64 \pm 0.01$	0 (0-0.07)	0 (0-1.34)
	20	0.07 (0.05-0.10)	$1.01 \pm 0.03$	0.27 (0.18-0.37)	5.18 (3.95-6.36)
	25	0.14 (0.12-0.20)	$1.45 \pm 0.0005$	0.03 (0-0.15)	0.23 (0-0.87)
	30	0.02 (0.01-0.03)	$1.21 \pm 0.34$	0.39 (0.31-0.48)	24.61 (20.17-29.89)
<i>Pediastrum boryanum</i>	15	0.11 (0.06-0.22)	$0.49 \pm 0.02$	0.16 (0.08-0.27)	2.11 (1.42-2.70)
	20	0.08 (0.04-0.17)	$0.74 \pm 0.04$	0.16 (0.05-0.32)	2.50 (1.07-3.74)
	25	0.14 (0.09-0.22)	$0.78 \pm 0.18$	0.20 (0.11-0.30)	1.87 (1.30-2.32)
	30	0.02 (0.01-0.03)	$0.80 \pm 0.05$	0.15 (0.08-0.23)	10.10 (6.21-14.23)
<i>Kirchneriella subcapitata</i>	15	0.25 (0.17-0.38)	$0.50 \pm 0.13$	0.38 (0.29-0.48)	2.84 (2.51-3.20)
	20	0.03 (0.03-0.04)	$0.78 \pm 0.18$	0.18 (0.14-0.22)	7.00 (5.93-8.02)
	25	0.04 (0.03-0.06)	$0.81 \pm 0.19$	0.02 (0-0.09)	0.53 (0-1.66)
	30	0.02 (0.02-0.03)	$0.66 \pm 0.40$	0.30 (0.26-0.34)	19.47 (17.07-22.09)
<i>Cyclotella meneghiniana</i>	15	0.24 (0.14-0.41)	$0.70 \pm 0.18$	0.53 (0.37-0.71)	4.09 (3.38-4.80)
	20	0.10 (0.05-0.20)	$0.90 \pm 0.08$	0.37 (0.21-0.57)	5.23 (3.86-6.83)
	25	0.17 (0.12-0.26)	$1.13 \pm 0.07$	0.52 (0.36-0.69)	4.76 (3.97-5.76)
	30	0.07 (0.04-0.12)	$1.18 \pm 0.05$	0.64 (0.49-0.81)	15.94 (12.21-20.72)
<i>Synechococcus</i>	15	0.003 (0.002-0.01)	$0.52 \pm 0.02$	0.15 (0.12-0.20)	61.21 (44.65-74.74)
	20	0.12 (0.06-0.22)	$0.77 \pm 0.09$	0.78 (0.58-1.03)	13.50 (10.16-18.08)
	25	0.24 (0.15-0.37)	$0.99 \pm 0.09$	0.68 (0.51-0.87)	5.21 (4.40-6.06)
	30	0.15 (0.10-0.24)	$1.34 \pm 0.13$	1.49 (1.23-1.76)	20.12 (16.16-25.13)

<i>Microcystis aeruginosa</i>	15	0.09 (0.07-0.12)	0.23 ± 0.0001	0.38 (0.35-0.42)	11.89 (10.90-13.13)
	20	0.24 (0.15-0.38)	0.53 ± 0.11	0.93 (0.79-1.11)	13.31 (11.23-15.97)
	25	0.02 (0.01-0.03)	0.61 ± 0.04	0.56 (0.46-0.67)	67.21 (49.52-91.74)
	30	0.01 (0.004-0.01)	1.19 ± 0.01	0.25 (0.15-0.38)	44.15 (27.72-59.46)

---

**Table S3.4.**  $Q_{10}$  values calculated from the fitted slope of a linear model fit to the log-transformed response of each trait estimate to temperature.  $Q_{10}$  values represent the temperature sensitivity of the change in the trait value due to an increase by  $10^{\circ}\text{C}$ .

<b>Parameter</b>	<b>Adjusted temperature range (<math>^{\circ}\text{C}</math>)</b>	<b><math>Q_{10}</math></b>	<b>95% Confidence width</b>
<i>Light</i>			
$I^*$	Below 0	-2.25	0.22
	Above 0	0.70	0.09
$\mu_{\max}$	Below 0	0.45	0.02
	Above 0	-0.12	0.03
$\alpha$	Below 0	0.02	0.001
	Above 0	-0.05	0.01
$I_{\text{opt}}$	Below 0	0.31	0.03
	Above 0	-0.25	0.03
<i>Nitrogen</i>			
$N^*$	Below 0	-1.01	0.15
	Above 0	0.45	0.06
$\mu_{\max}$	Across entire x-axis	0.22	0.01
$\alpha$	Below 0	0.14	0.01
	Above 0	-0.08	0.005
$m$	Below 0	0.18	0.02
	Above 0	-0.25	0.03

### **S3.1. Supplementary Methodology**

#### **Acclimation to nitrogen**

To allow for acclimatization, the phytoplankton were maintained at the assigned nitrate concentration and experimental temperature, for 13 days prior to the start of the experiment. 100ml batch cultures of each species were first placed into temperature-controlled incubators set to one of the four experimental temperatures (Multitron, Infors HT, Switzerland). After 7 days, 12ml of each phytoplankton culture was centrifuged at 3,000rpm for 12 minutes and re-suspended in COMBO medium containing their respective target nitrate concentration. This allowed cultures acclimate to their assigned experimental nitrate concentrations. This resuspension was repeated on the third and fifth day of the acclimation to ensure complete removal of excess nitrate from the culture medium while also preventing starvation due to depletion. The phytoplankton pellet was then once again re-suspended in fresh and sterile COMBO medium with the assigned nitrate concentration.

#### **Parameter estimation**

We estimated population growth rates ( $r$ ) as the slope of the log-transformed population-level pigment fluorescence (chlorophyll- $a$  for eukaryotes, phycocyanin for cyanobacteria) against time (Simis *et al.* 2012). We used a minimum of three time points selected from the period during which growth was exponential (determined visually).

We used a maximum likelihood approach to fit equation (1) and equation (2) to the light-dependent and nitrogen-dependent growth rate estimates of each species at all experimental temperatures. We accounted for uncertainty in individual growth rate estimates by weighting each point by the reciprocal of the standard error. In addition to estimating the parameters of equation (1), we also numerically estimated the  $R^*$  (i.e.  $I^*$  and  $N^*$ ) values, or the irradiance and nitrogen levels at which the



population growth rate is equal to zero, by solving the parameterized growth functions. We then quantified the uncertainty in each parameter estimate, while accounting for the uncertainty in the individual growth rate estimates.

For each fitted curve, we simulated 1000 new datasets with the same number of points as the original fit, and at exactly the same irradiance levels. Residuals were randomly drawn and based on the variance in the original fit, but adjusted for bias in maximum likelihood estimates of variance (Gelman and Hill 2007). We then refit equations (1) and (2) to each of these 1000 simulated datasets and calculated the 95% confidence intervals in each parameter estimate. We followed this approach to account for the weighting of individual points by their uncertainty, and to capture uncertainty in  $R^*$ , which was not a parameter included in the equation (and therefore precluded a likelihood profile-based approach). The parameters were estimate using R 3.3.3. (R Development Core Team 2014). Maximum likelihood fits were performed using the package *bbmle* (Bolker 2016).

## Supplementary Chapter 4

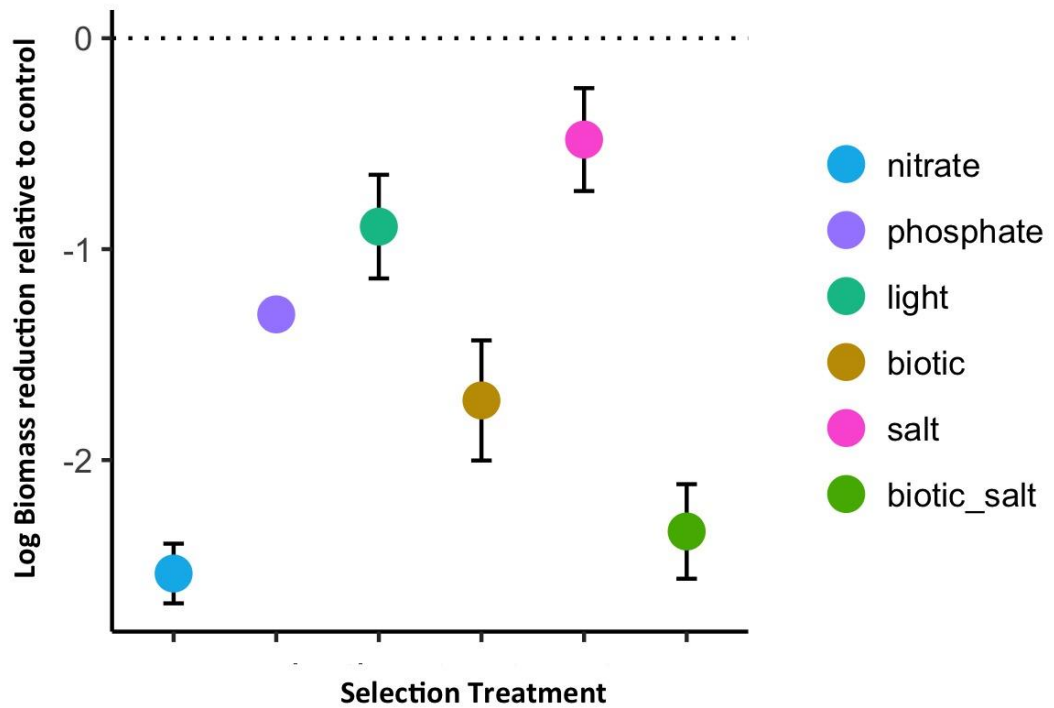


**Figure S4.1.** Estimates of biomass reduction of all ancestral strains assigned to each selection treatment relative to the control (indicated by the dotted line). Estimates of biomass reduction for each treatment were calculated by taking the log response ratio of the mean biomass estimate (RFU) of the last 4 time points of the selection experiment relative to the last 4 time points of the control.

Treatment: Ancestor

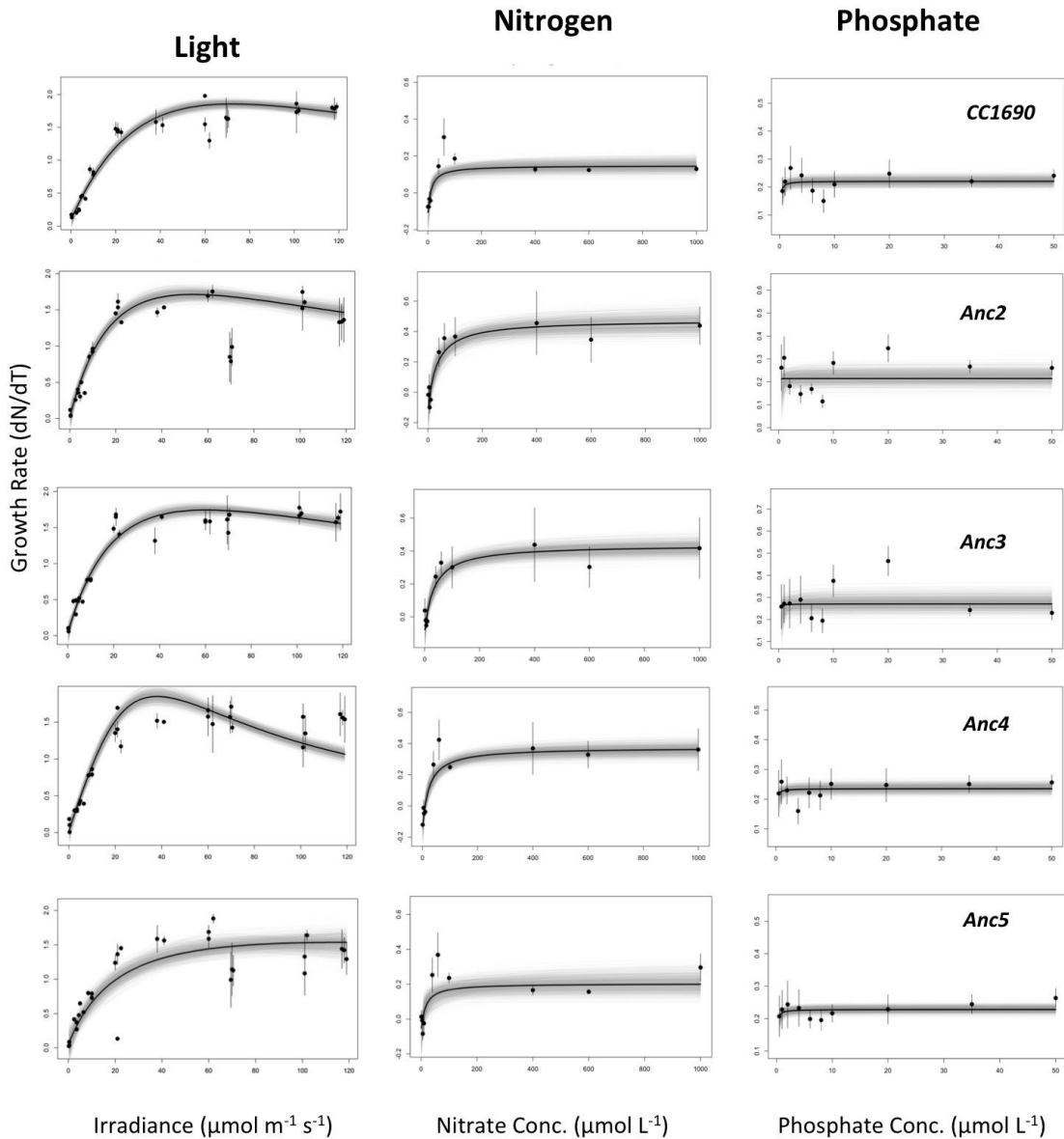


**Figure S4.2.** Growth curves of all ancestors under limiting light, nitrogen and phosphate resource. Rows demonstrate the response of each descendant's ancestral history to each limiting resource. Growth rate estimates were weighted based on the uncertainty in each point. The grey lines represent represents the 95% confidence interval of the curve using 1000 bootstrapped values.

Treatment: Biotic

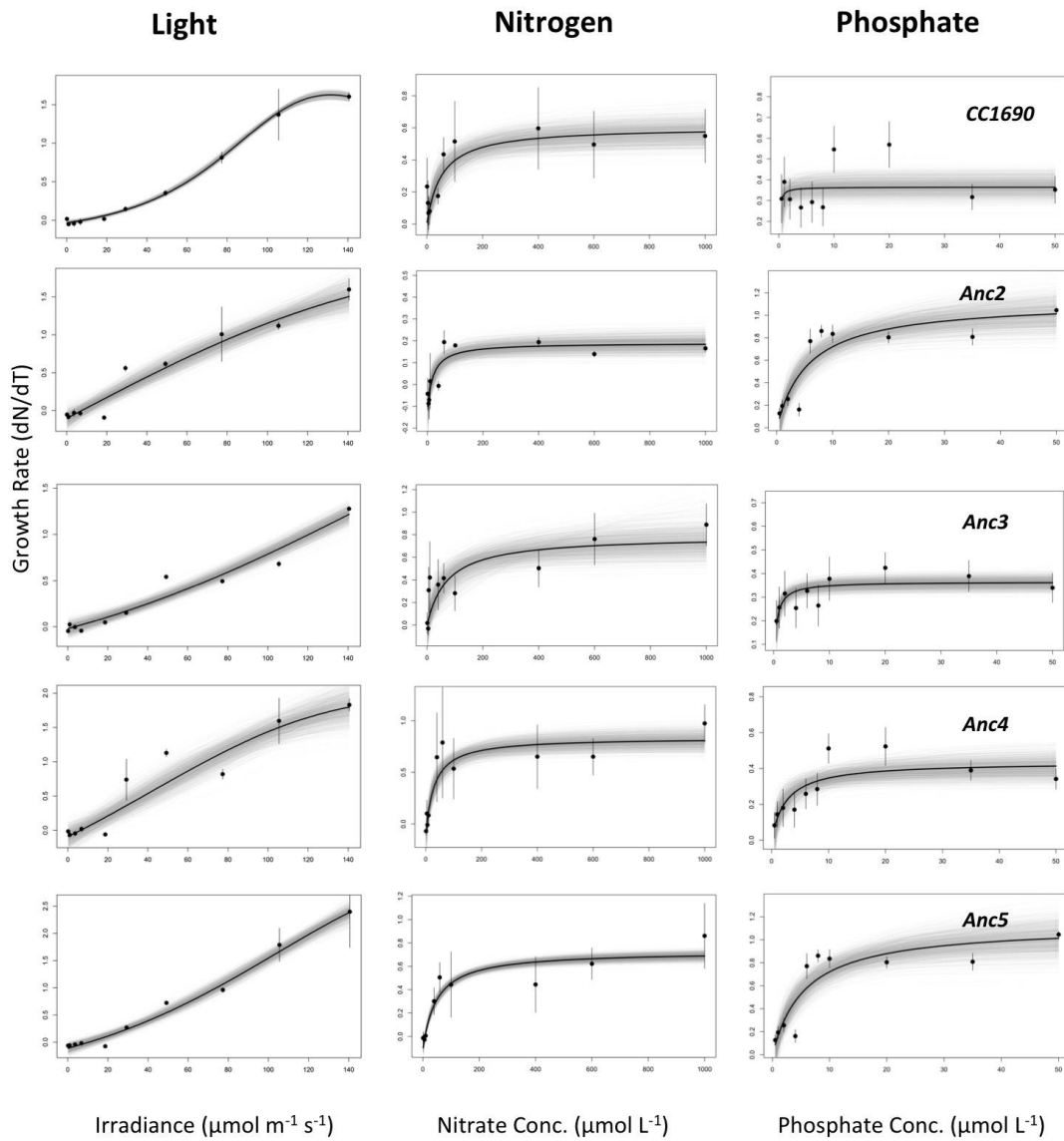


**Figure S4.3.** Growth curves of all descendants selected under the biotic treatment, for limiting light, nitrogen and phosphate resource. Rows demonstrate the response of each descendant's ancestral history to each limiting resource. Growth rate estimates were weighted based on the uncertainty in each point. The grey lines represents the 95% confidence interval of the curve using 1000 bootstrapped values.

Treatment: Light

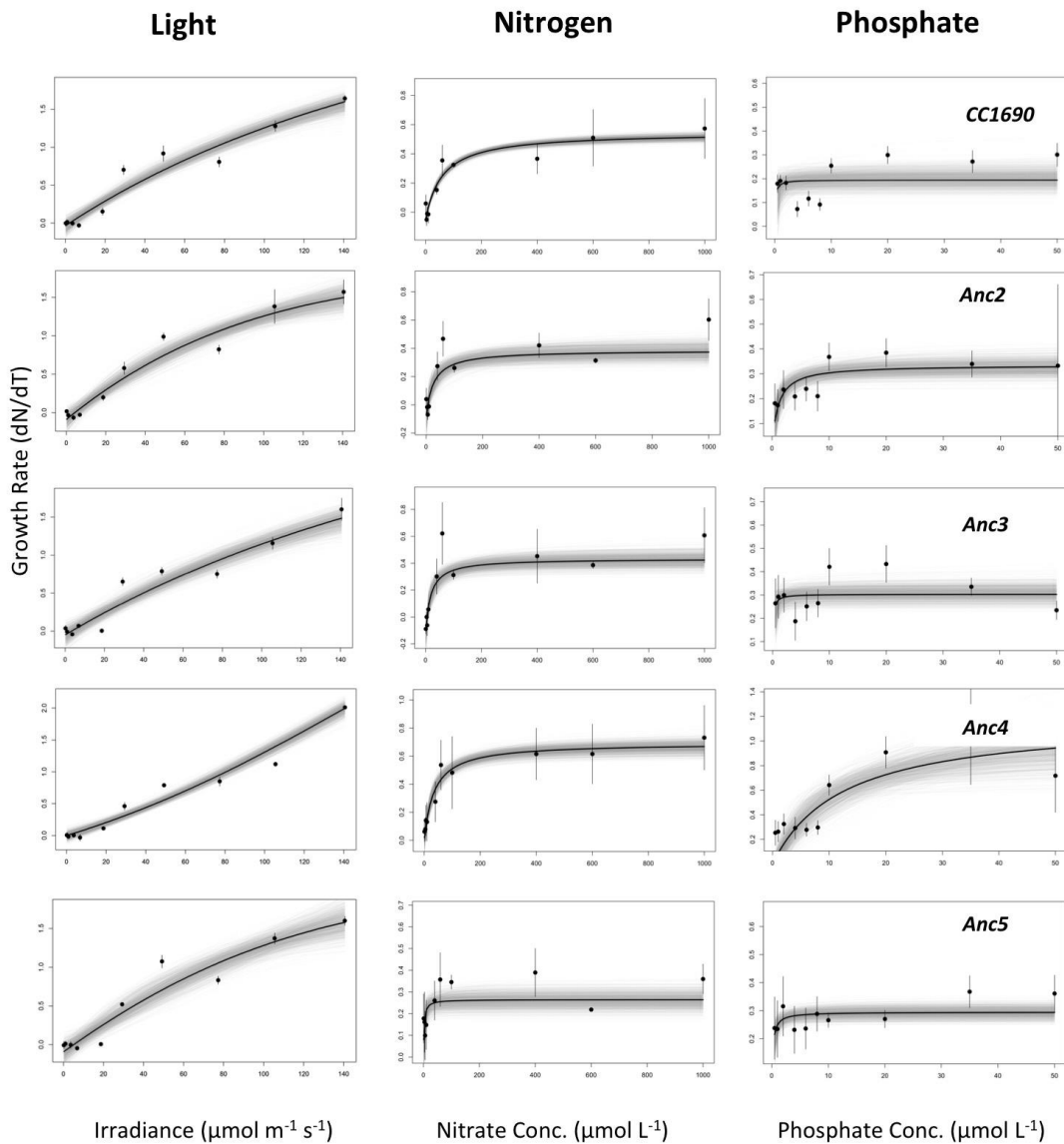


**Figure S4.4.** Growth curves of all descendants selected under the biotic treatment, for limiting light, nitrogen and phosphate resource. Rows demonstrate the response of each descendant's ancestral history to each limiting resource. Growth rate estimates were weighted based on the uncertainty in each point. The grey lines represents the 95% confidence interval of the curve using 1000 bootstrapped values.

Treatment: Nitrogen

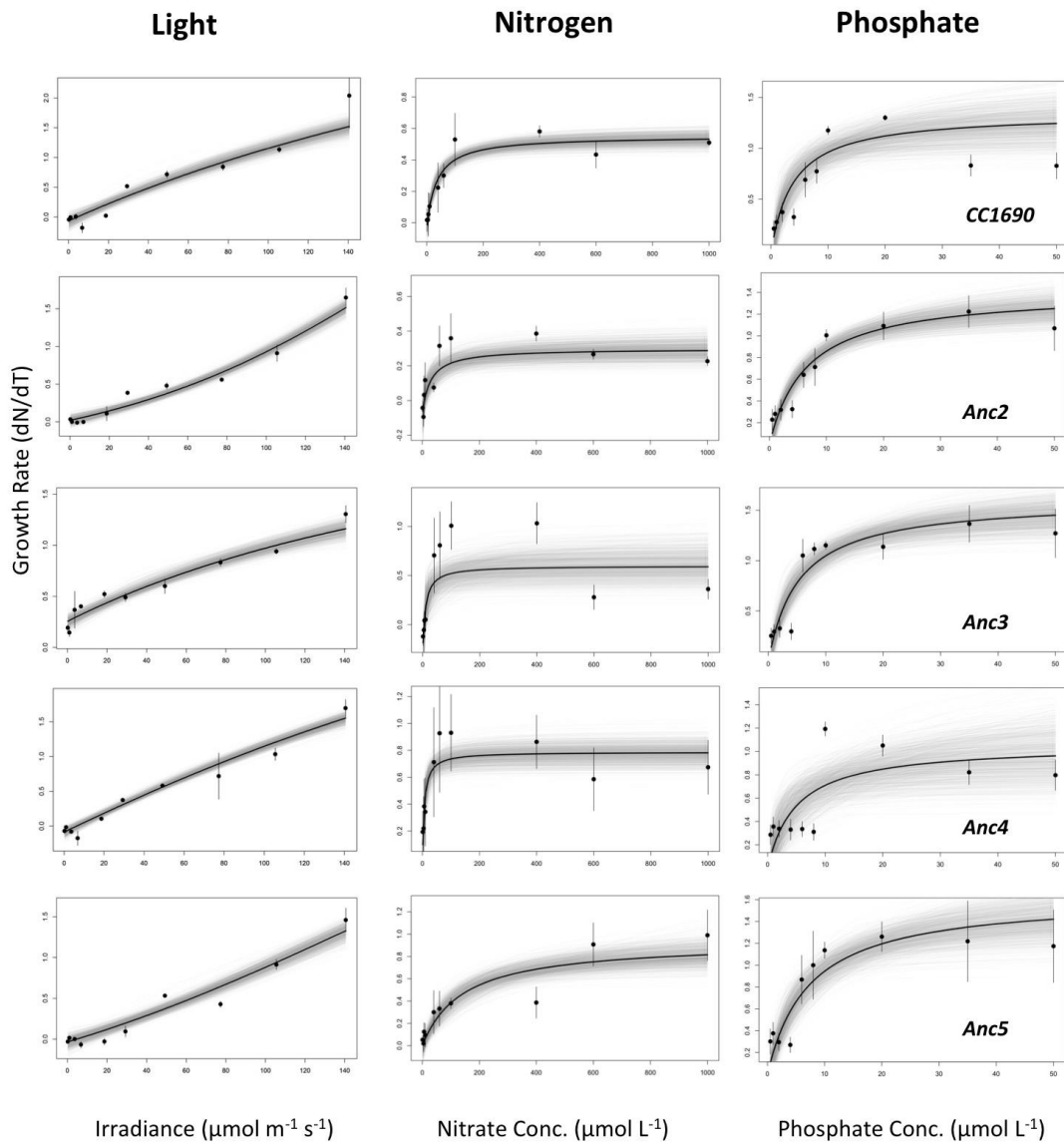


**Figure S4.5.** Growth curves of all descendants selected under the biotic x salt treatment, for limiting light, nitrogen and phosphate resource. Rows demonstrate the response of each descendant's ancestral history to each limiting resource. Growth rate estimates were weighted based on the uncertainty in each point. The grey lines represent the 95% confidence interval of the curve using 1000 bootstrapped values.

Treatment: Phosphate

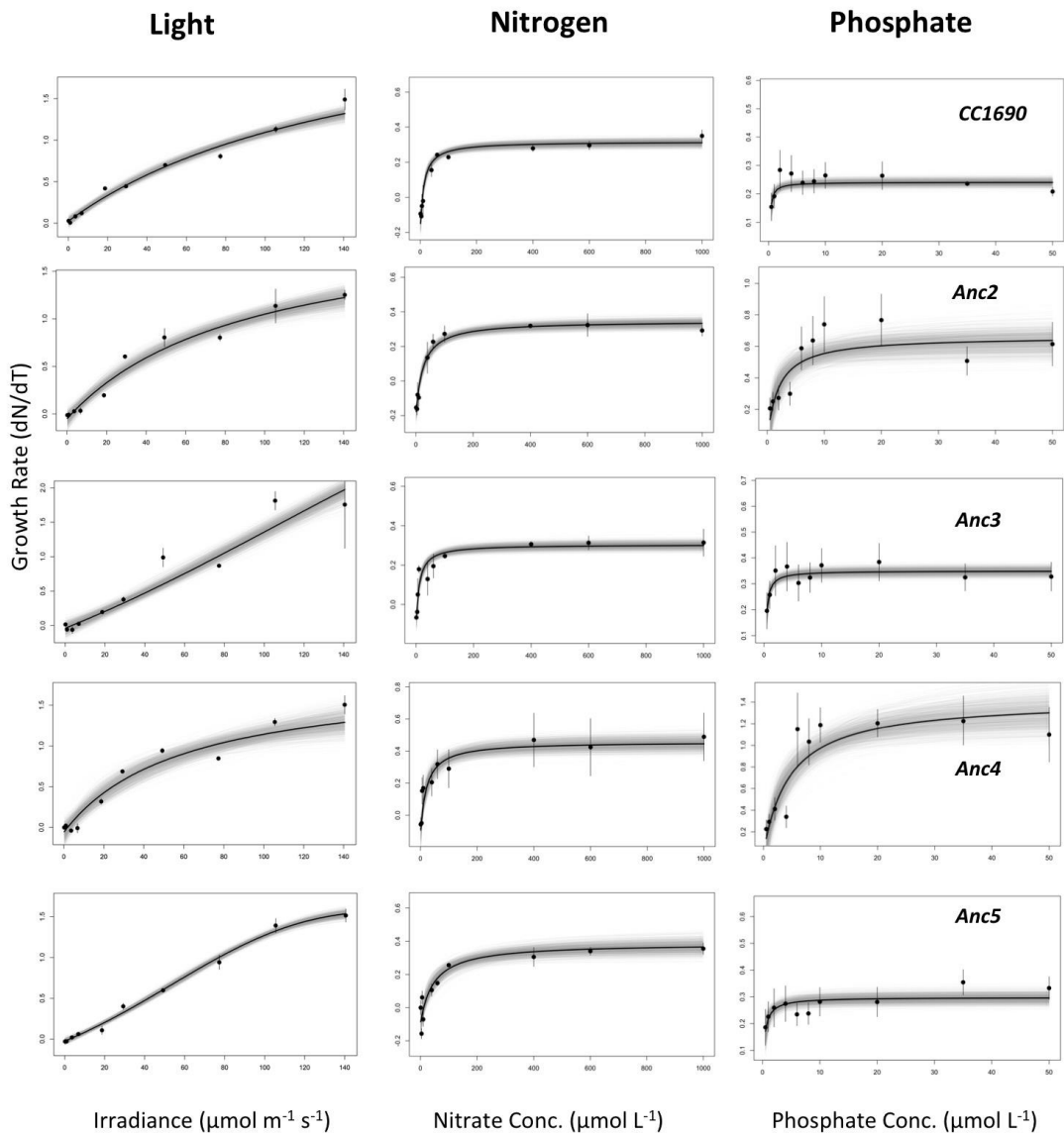


**Figure S4.6.** Growth curves of all descendants selected under the low phosphate treatment, for limiting light, nitrogen and phosphate resource. Rows demonstrate the response of each descendant's ancestral history to each limiting resource. Growth rate estimates were weighted based on the uncertainty in each point. The grey lines represent the 95% confidence interval of the curve using 1000 bootstrapped values.

Treatment: Salt

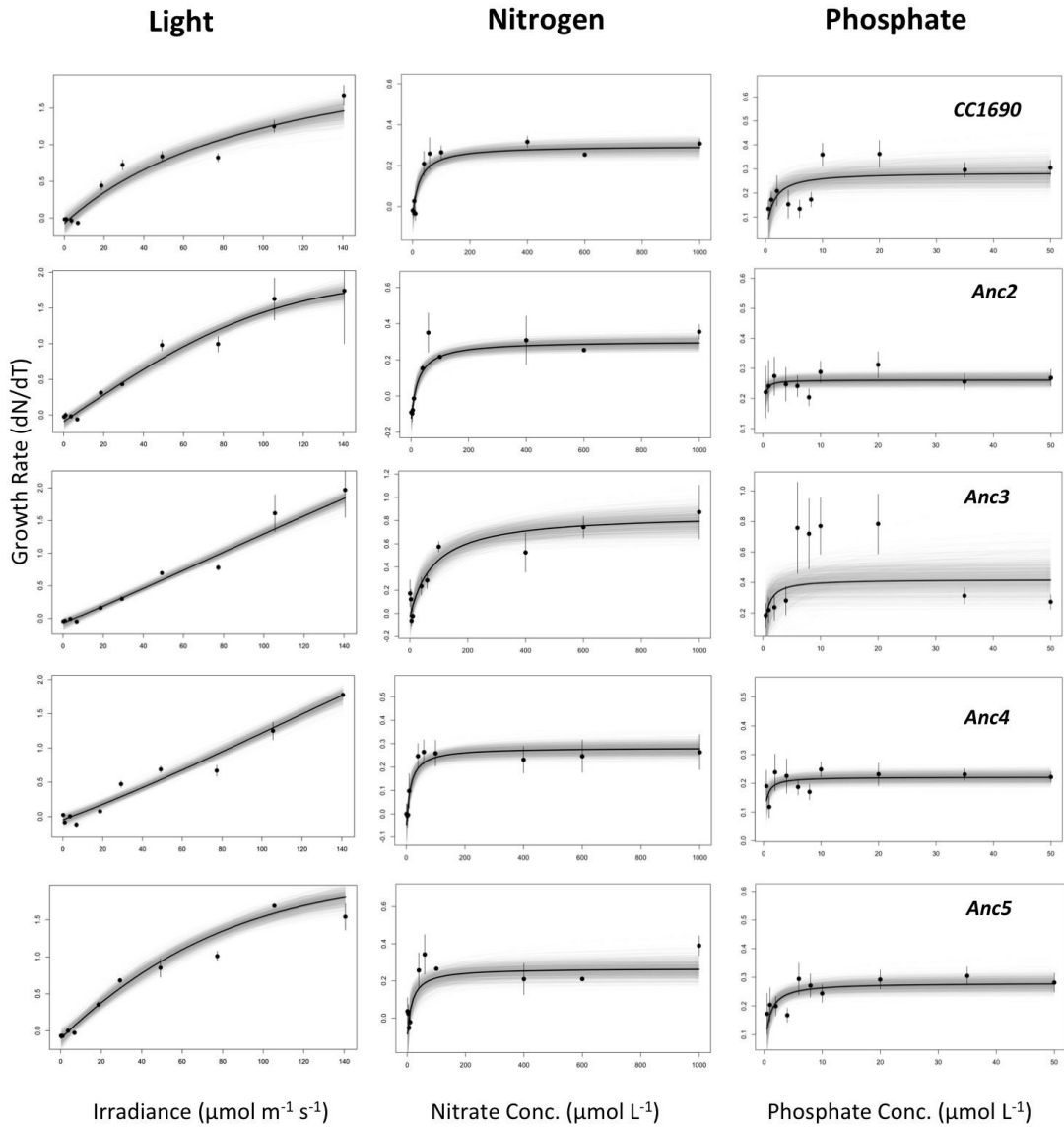


**Figure S4.7.** Growth curves of all descendants selected under the high osmotic stress (salt) treatment, for limiting light, nitrogen and phosphate resource. Rows demonstrate the response of each descendant's ancestral history to each limiting resource. Growth rate estimates were weighted based on the uncertainty in each point. The grey lines represent the 95% confidence interval of the curve using 1000 bootstrapped values.



Treatment: Biotic x Salt

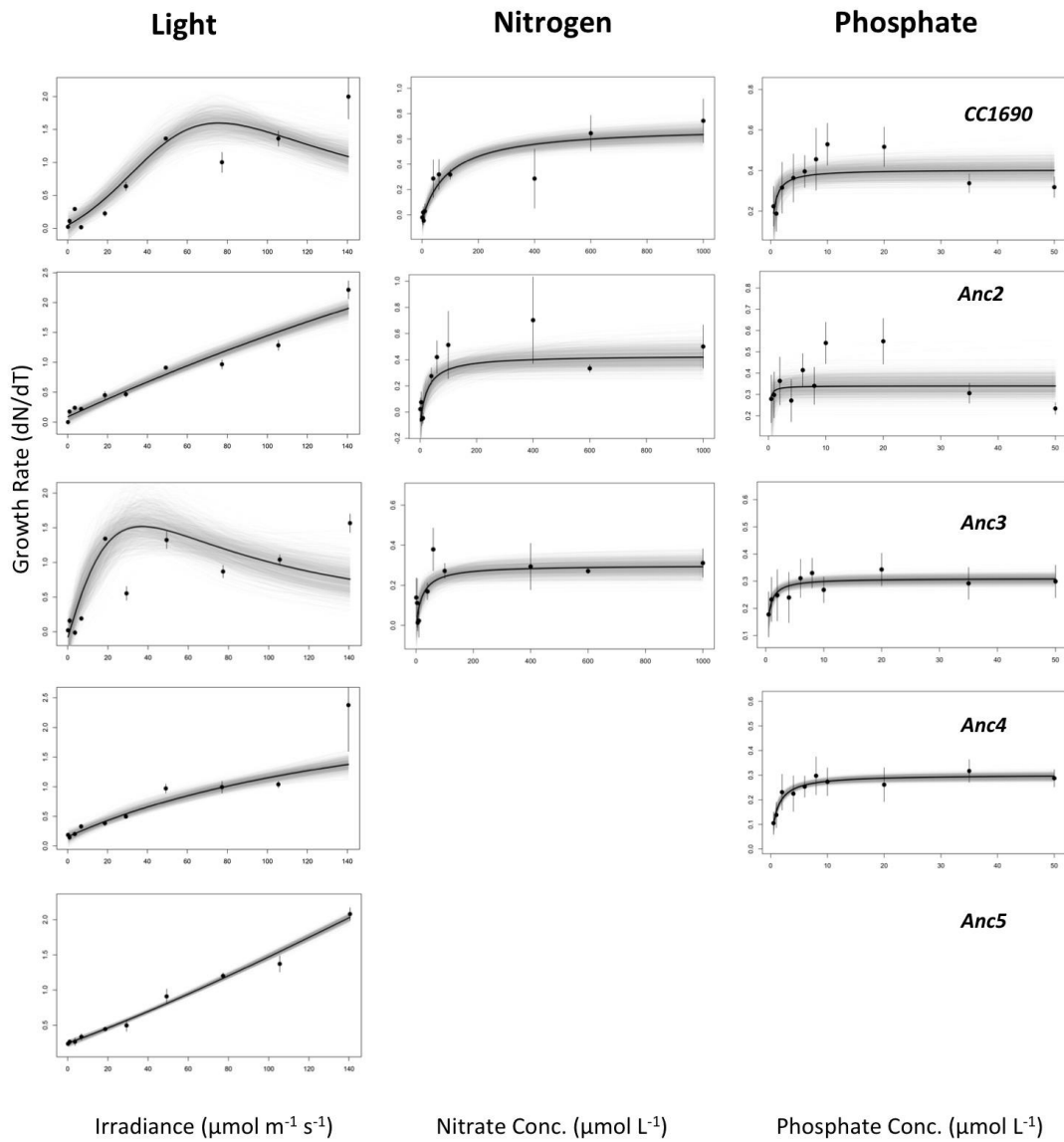


**Figure S4.8.** Growth curves of all descendants selected under the biotic x salt treatment, for limiting light, nitrogen and phosphate resource. Rows demonstrate the response of each descendant's ancestral history to each limiting resource. Growth rate estimates were weighted based on the uncertainty in each point. The grey lines represent the 95% confidence interval of the curve using 1000 bootstrapped values.

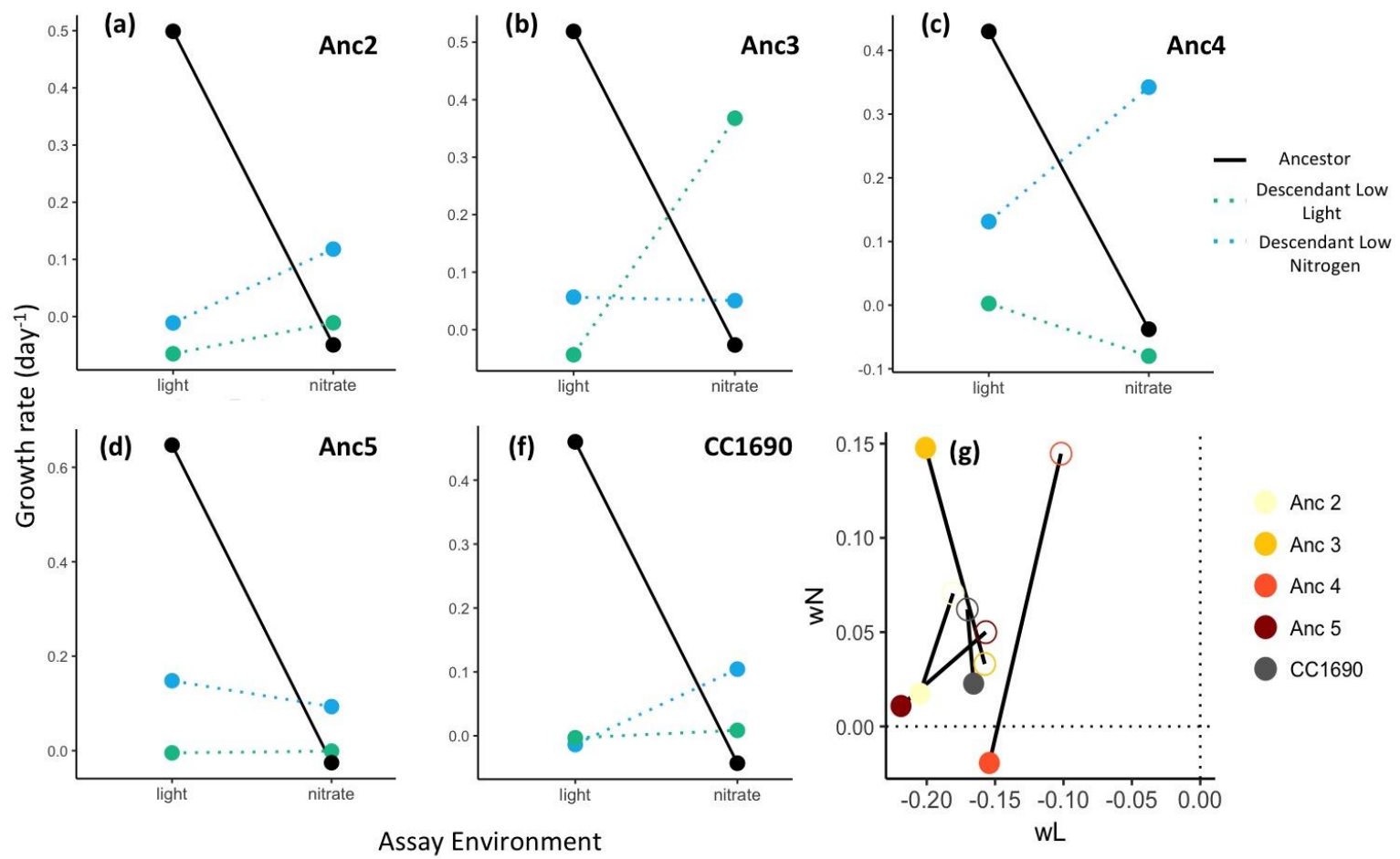


**Figure S4.9. (a-f)** Reaction norms of absolute fitness of each descendant and its ancestor; green = selected under low light, blue = selected under low nitrogen and red = ancestor). Lines connect the fitness of the descendants or ancestor in each assay environment. **(g)** Trade-offs in fitness resulting from divergent selection. Lines connect a pair of evolved descendants from their common ancestor selected in one of two environments (filled circles: selected in low light (wL); open circle: selected in low nitrogen (wN)). Values are expressed as relative fitness calculated as the Log response ratio of each environmentally selected descendant to its relative ancestor. The fitness of the ancestor is by definition given by the intersection of the two dashed lines in the figure.

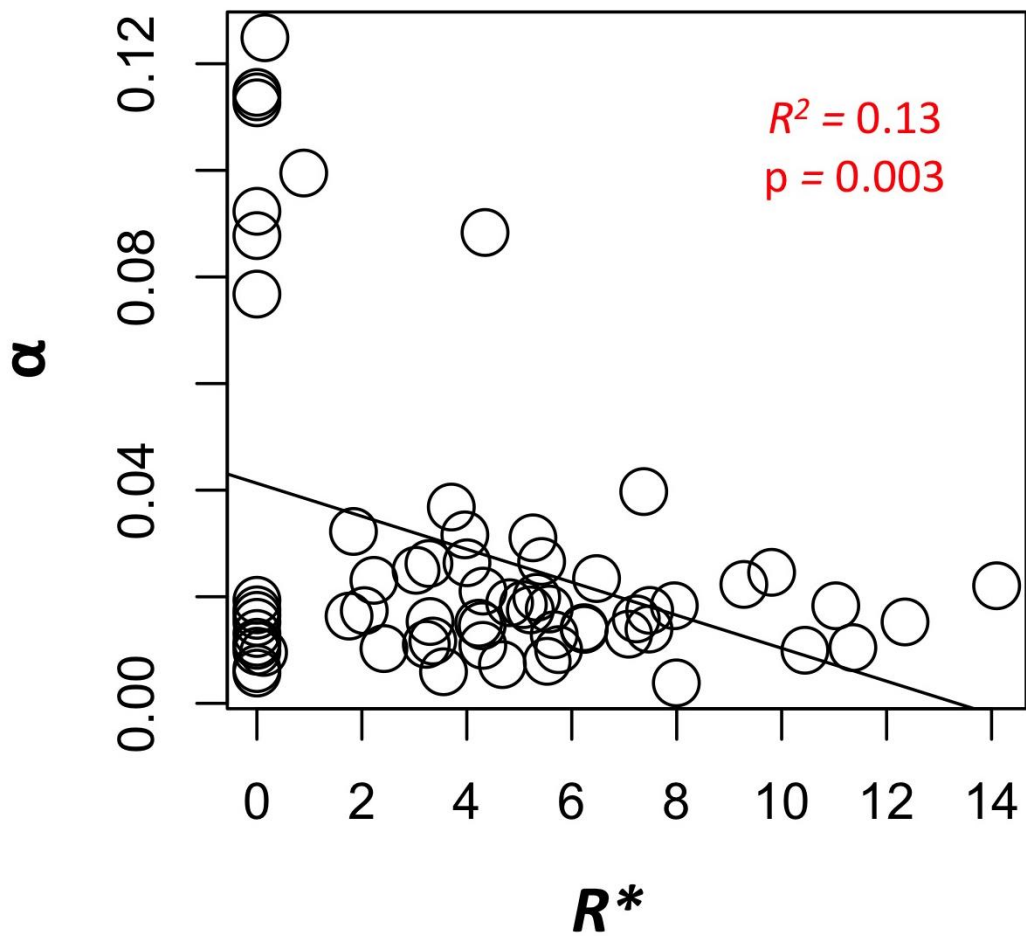


**Figure S4.10.** The weak, but significant negative correlation between  $R^*$  and  $\alpha$ , indicating a negative trade-off between the requirements of a resource and its initial growth response to increasing resource availability. Due to little variation in  $P^*$  observed in this experiment, we use only the  $R^*$  and  $\alpha$  estimates from the light and nitrogen experiments.

**Table S4.1.** Experimental treatments applied monthly during the evolution experiment performed previous to the experiments carried in Chapter 5. All treatments are resource depletion treatments, except for the control and the NaCl treatments. The NaCl treatment consisted of increasing concentrations of salt in order to impose an osmotic stress. Competition medium was first made by allowing seven species of other freshwater green phytoplankton to grow on and deplete the resource from standard COMBO medium, and then mixing that medium together with some proportion of standard (full) COMBO. The proportions shown are the proportions of the media made up of biotically depleted COMBO (i.e. 1 is completely depleted, or spent COMBO).

Month	NaNO <sub>3</sub> ( $\mu\text{mol L}^{-1}$ )	K <sub>2</sub> HPO <sub>4</sub> ( $\mu\text{mol L}^{-1}$ )	Competition (Proportion)	Light ( $\mu\text{mol photons m}^{-2}\text{s}^{-1}$ )	NaCl (g/L)	Competition x NaCl	
1	1000	50	0	100	0	0	0
2	100	5	0.01	70	1	0.01	1
3	100	5	0.1	50	2	0.1	2
4	10	0.5	0.4	20	4	0.4	4
5	10	0.5	0.75	15	6	0.75	6
6	10	0.5	0.95	5	8	0.95	8
7	10	0.5	1	5	8	1	8
8	10	0.5	1	5	8	1	8

**Table S4.2.** Light limitation experimental parameter estimates for descendants under each selection treatment.  $\alpha$  is the species' initial response to elevated resource availability,  $\mu_{max}$  is the maximum growth rate under non-limiting light conditions,  $I_{opt}$  is the optimal irradiance for growth and  $I^*$  is the species minimum light requirement. Parameter uncertainty (in parentheses) was measured as the 95% confidence width estimated from 1000 bootstrap values.

Treatment	Ancessor	$\alpha$	$\mu_{max} \pm SE$	$I_{opt}$	$I^*$ [ $\mu\text{mol photons m}^{-2}\text{s}^{-2}$ ]
<b>Ancestor</b>					
	Anc2	0.12 (0.08-0.19)	1.75 $\pm$ 0.09	53.43 (46.99-65.25)	0.15 (0-0.85)
	Anc3	0.11 (0.08-0.16)	1.77 $\pm$ 0.23	60.25 (53.51-73.93)	0 (0-0.65)
	Anc4	0.09 (0.06-0.13)	1.71 $\pm$ 0.14	38.06 (35.46-40.77)	0 (0-0.94)
	Anc5	0.09 (0.03-0.18)	1.88 $\pm$ 0.07	118.80 (62.89-10000)	0 (0-1.53)
	CC 1690	0.08 (0.06-0.11)	1.98 $\pm$ 0.03	72.38 (63.95-89.45)	0 (0-0.11)
<b>Biotic</b>					
	Anc2	0.01 (0.008-0.03)	1.59 $\pm$ 0.14	297.68 (297.68-297.68)	7.47 (0-14.59)
	Anc3	0.01 (0.005-0.008)	1.28 $\pm$ 0.02	341.54 (341.54-351.54)	3.56 (0-14.27)
	Anc4	0.01 (0.007-0.03)	1.83 $\pm$ 0.09	190.93 (190.92-190.93)	6.24 (0-15.26)
	Anc5	0.01 (0.008-0.01)	2.40 $\pm$ 0.66	217.68 (217.67-217.68)	10.44 (0.94-17.37)
	CC 1690	0.004 (0.003-0.004)	1.61 $\pm$ 0.05	131.45 (131.45-131.46)	7.99 (2.76-12.11)
<b>Light</b>					
	Anc2	0.02 (0.01-0.04)	1.57 $\pm$ 0.16	285.62 (285.62-285.62)	4.31 (0-9.32)
	Anc3	0.02 (0.01-0.03)	1.26 $\pm$ 0.15	971.21 (971.21-971.21)	3.30 (0-10.26)
	Anc4	0.01 (0.008-0.01)	2.01 $\pm$ 0.004	335.38 (335.38-335.39)	0.13 (0-8.00)
	Anc5	0.02 (0.009-0.04)	1.60 $\pm$ 0.06	289.27 (289.26-289.27)	5.08 (0-11.57)
	CC 1690	0.02 (0.01-0.03)	1.64 $\pm$ 0.04	1049.37 (1049.37-1049.37)	2.05 (0-7.22)
<b>Nitrogen</b>					
	Anc2	0.01 (0.005-0.01)	1.65 $\pm$ 0.13	305.97 (305.97-305.97)	0 (0-8.78)
	Anc3	0.01 (0.008-0.02)	1.31 $\pm$ 0.09	1652.41 (1652.41-1652.41)	0 (0-0)
	Anc4	0.01 (0.01-0.02)	1.69 $\pm$ 0.13	651.91 (651.91-651.92)	6.24 (1.49-10.81)

	Anc5	0.01 (0.006-0.01)	1.46 ± 0.15	382.35 (382.35-382.36)	4.68 (0-14.97)
	CC 1690	0.02 (0.01-0.02)	2.04 ± 0.55	1457.37 (1457.37- 1457.37)	4.23 (0-10.73)
<b>Phosphate</b>					
	Anc2	0.02 (0.02-0.04)	1.25 ± 0.05	3468.74 (3468.74- 3468.74)	2.23 (0-5.63)
	Anc3	0.01 (0.009-0.02)	1.81 ± 0.14	353.45 (353.45-353.46)	3.35 (0-11.11)
	Anc4	0.03 (0.02-0.07)	1.51 ± 0.11	8937.91 (8937.91- 8937.91)	1.84 (0-5.49)
	Anc5	0.01 (0.009-0.01)	1.51 ± 0.08	161.69 (161.69-161.69)	2.42 (0-5.48)
	CC 1690	0.02 (0.01-0.02)	1.49 ± 0.13	5876.22 (5876.22- 5876.22)	0 (0-2.08)
<b>Salt</b>					
	Anc2	0.02 (0.01-0.03)	1.74 ± 0.74	196.80 (196.80-196.80)	4.82 (0.41-8.30)
	Anc3	0.01 (0.01-0.02)	1.97 ± 0.42	460.90 (460.90-460.90)	5.67 (0.23-10.39)
	Anc4	0.01 (0.009-0.02)	1.78 ± 0.008	390.18 (390.18-390.19)	4.30 (0-10.68)
	Anc5	0.03 (0.02-0.04)	1.69 ± 0.02	238.73 (238.73-238.73)	4.00 (0-7.24)
	CC 1690	0.02 (0.02-0.04)	1.67 ± 0.14	9727.47 (9727.47- 9727.47)	3.03 (0-7.36)
<b>Biotic x Salt</b>					
	Anc2	0.02 (0.01-0.02)	2.21 ± 0.15	844.99 (844.99-844.99)	0 (0-1.75)
	Anc3	0.10 (0.02-0.41)	1.57 ± 0.14	37.04 (26.02-54.69)	0.89 (0-3.67)
	Anc4	0.02 (0.01-0.03)	2.38 ± 0.78	4306.02 (4306.02- 4306.02)	0 (0-0)
	Anc5	0.01 (0.009-0.01)	2.08 ± 0.09	445.66 (445.66-445.66)	0 (0-0)
	CC 1690	0.02 (0.008-0.04)	2.00 ± 0.34	75.74 (65.09-95.68)	0 (0-5.47)

**Table S4.3.** Nitrogen limitation experimental parameter estimates for descendants under each selection treatment.  $\alpha$  is the species' initial response to elevated resource availability,  $\mu_{max}$  is the maximum growth rate under non-limiting nitrate conditions,  $m$  is the specific growth rate at  $N = 0$  and  $N^*$  is the species minimum nitrate requirement. Parameter uncertainty (in parentheses) was measured as the 95% confidence intervals estimated from 1000 bootstraps

<b>Treatment</b>	<b>Ancestor</b>	<b><math>\alpha</math></b>	<b><math>\mu_{max} \pm</math> SE</b>	<b><math>m</math></b>	<b><math>N^*</math> [<math>\mu\text{mol L}^{-1}</math>]</b>
<b>Ancestor</b>					
	Anc2	0.02 (0.01-0.07)	0.46 $\pm$ 0.21	0.12 (0.01-0.28)	7.95 (1.73-14.45)
	Anc3	0.02 (0.01-0.04)	0.44 $\pm$ 0.22	0.09 (0.02-0.19)	7.23 (2.29-11.89)
	Anc4	0.02 (0.01-0.06)	0.42 $\pm$ 0.13	0.15 (0.07-0.26)	9.28 (5.47-14.59)
	Anc5	0.02 (0.002-0.64)	0.37 $\pm$ 0.13	0.07 (0-0.47)	5.21 (0-17.65)
	CC 1690	0.02 (0.004-0.15)	0.30 $\pm$ 0.10	0.13 (0.04-0.29)	9.81 (4.59-20.95)
<b>Biotic</b>					
	Anc2	0.02 (0.004-0.09)	0.19 $\pm$ 0.02	0.12 (0.04-0.26)	12.35 (5.09-26.00)
	Anc3	0.01 (0.004-0.06)	0.89 $\pm$ 0.19	0 (0-0.24)	0.00002 (0-12.28)
	Anc4	0.03 (0.01-0.09)	0.97 $\pm$ 0.18	0.11 (0-0.31)	3.96 (0-7.84)
	Anc5	0.02 (0.01-0.03)	0.86 $\pm$ 0.28	0.11 (0.06-0.17)	7.48 (4.73-10.07)
	CC 1690	0.01 (0.01-0.05)	0.60 $\pm$ 0.26	0 (0-0.17)	0.00002 (0-8.34)
<b>Light</b>					
	Anc2	0.02 (0.01-0.09)	0.60 $\pm$ 0.15	0.08 (0-0.25)	5.57 (0-11.31)
	Anc3	0.03 (0.01-0.11)	0.62 $\pm$ 0.23	0.13 (0.003-0.30)	5.26 (0.25-9.21)
	Anc4	0.02 (0.01-0.04)	0.73 $\pm$ 0.23	0 (0-0.09)	0.00002 (0-3.22)
	Anc5	0.11 (0.03-100)	0.39 $\pm$ 0.11	0 (0-3.66)	0.00002 (0-1.35)
	CC 1690	0.01 (0.007-0.01)	0.57 $\pm$ 0.21	0.05 (0.03-0.08)	5.75 (3.27-8.13)
<b>Nitrogen</b>					
	Anc2	0.01 (0.003-0.11)	0.39 $\pm$ 0.04	0.07 (0-0.27)	7.08 (0-17.33)
	Anc3	0.09 (0.007-4.48)	1.03 $\pm$ 0.21	0.28 (0-2.24)	4.35 (0-12.83)
	Anc4	0.11 (0.06-1.08)	0.93 $\pm$ 0.29	0 (0-0.69)	0.00002 (0-1.81)
	Anc5	0.007 (0.004-0.02)	0.99 $\pm$ 0.23	0 (0-0.13)	0.00002 (0-13.51)
	CC 1690	0.02 (0.01-0.04)	0.58 $\pm$ 0.04	0.03 (0-0.11)	1.76 (0-5.05)
<b>Phosphate</b>					



	Anc2	0.02 (0.01-0.04)	0.32 ± 0.07	0.20 (0.15-0.25)	14.10 (10.83-17.65)
	Anc3	0.04 (0.02-0.07)	0.31 ± 0.07	0.10 (0.05-0.17)	3.70 (2.53-4.93)
	Anc4	0.03 (0.01-0.07)	0.49 ± 0.15	0.12 (0.03-0.23)	5.43 (1.99-8.46)
	Anc5	0.01 (0.004-0.02)	0.36 ± 0.03	0.10 (0.03-0.17)	11.36 (5.57-18.29)
	CC 1690	0.04 (0.02-0.07)	0.35 ± 0.03	0.18 (0.13-0.25)	7.37 (5.84-9.30)
<b>Salt</b>					
	Anc2	0.02 (0.009-0.04)	0.35 ± 0.04	0.14 (0.08-0.22)	11.03 (7.06-16.19)
	Anc3	0.01 (0.006-0.03)	0.88 ± 0.23	0.03 (0-0.19)	3.23 (0-12.05)
	Anc4	0.03 (0.009-0.09)	0.26 ± 0.05	0.07 (0-0.19)	3.28 (0-5.55)
	Anc5	0.02 (0.004-0.20)	0.39 ± 0.05	0.11 (0-0.36)	6.47 (0-13.64)
	CC 1690	0.01 (0.006-0.04)	0.32 ± 0.03	0.05 (0-0.15)	4.29 (0-7.91)
<b>Biotic x Salt</b>					
	Anc2	0.02 (0.004-0.16)	0.70 ± 0.33	0.09 (0-0.34)	5.33 (0-14.15)
	Anc3	0.01 (0.006-0.10)	0.38 ± 0.11	0 (0-0.14)	0.00002 (0-4.97)
	CC 1690	0.008 (0.004-0.02)	0.74 ± 0.17	0.04 (0-0.14)	5.53 (0-13.76)

**Table S4.4.** Phosphate limitation experimental parameter estimates for descendants under each selection treatment.  $\alpha$  is the species' initial response to elevated resource availability,  $\mu_{max}$  is the maximum growth rate under non-limiting phosphate conditions,  $m$  is the specific growth rate at  $P = 0$  and  $P^*$  is the species minimum phosphate requirement. Parameter uncertainty (in parentheses) was measured as the 95% confidence intervals estimated from 1000 bootstraps.

<b>Treatment</b>	<b>Ancestor</b>	<b><math>\alpha</math></b>	<b><math>\mu_{max} \pm</math> SE</b>	<b><math>m</math></b>	<b><math>P^*</math> [<math>\mu\text{mol L}^{-1}</math>]</b>
<b>Ancestor</b>					
	Anc2	100 (99.98-100)	0.27 $\pm$ 0.08	0.92 (0 -1.89)	0 (0-0)
	Anc3	4.87 (4.14-100)	0.26 $\pm$ 0.03	0 (0-0.19)	0 (0-0)
	Anc4	5.80 (5.79-100)	0.26 $\pm$ 0.07	0 (0-0.28)	0 (0-0)
	Anc5	100 (99.99-100)	0.46 $\pm$ 0.07	0.46 (0-2.63)	0 (0-0)
	CC 1690	100 (99.99-100)	0.35 $\pm$ 0.07	0 (0-2.66)	0 (0-0)
<b>Biotic</b>					
	Anc2	3.85 (0.66-100)	0.57 $\pm$ 0.11	0 (0-3.13)	0 (0-0.13)
	Anc3	0.17 (0.08-100)	0.52 $\pm$ 0.11	0 (0-3.74)	0.00002 (0-0.75)
	Anc4	0.20 (0.12-1.03)	1.05 $\pm$ 0.02	0.004 (0-0.49)	0.02 (0-0.92)
	Anc5	0.34 (0.16-100)	0.45 $\pm$ 0.08	0 (0-3.84)	0.00002 (0-0.48)
	CC 1690	0.75 (0.43-100)	0.42 $\pm$ 0.07	0 (0-3.30)	0.00002 (0-0.25)
<b>Light</b>					
	Anc2	1.63 (0.16-100)	0.30 $\pm$ 0.05	0 (0-2.76)	0.00002 (0-0.24)
	Anc3	3.35 (0.58-100)	0.43 $\pm$ 0.08	0 (0-2.63)	0 (0-0.12)
	Anc4	1.60 (0.69-100)	0.36 $\pm$ 0.06	0 (0-2.48)	0.00002 (0-0.08)
	Anc5	0.09 (0.05-0.40)	1.08 $\pm$ 0.43	0 (0-0.37)	0.00002 (0-1.74)
	CC 1690	0.33 (0.16-100)	0.38 $\pm$ 0.06	0 (0-3.50)	0.00002 (0-0.45)
<b>Nitrogen</b>					
	Anc2	0.23 (0.13-0.97)	1.26 $\pm$ 0.14	0 (0-0.59)	0.00002 (0-1.12)
	Anc3	0.30 (0.20-1.17)	1.37 $\pm$ 0.18	0 (0-0.55)	0.00002 (0-0.78)
	Anc4	0.22 (0.08-54.31)	1.19 $\pm$ 0.06	0 (0-5)	0.00002 (0-1.51)
	Anc5	0.36 (0.17-11.18)	1.30 $\pm$ 0.03	0.03 (0-2.24)	0.09 (0-0.94)
	CC 1690	0.22 (0.15-0.57)	1.22 $\pm$ 0.15	0 (0-0.36)	0.00002 (0-0.78)
<b>Phosphate</b>					

	Anc2	100 (99.99-100)	0.38 ± 0.07	2.50 (1.94-3.02)	0 (0-0)
	Anc3	0.81 (0.46-100)	0.35 ± 0.05	0 (0-2.82)	0.00002 (0-0.18)
	Anc4	0.34 (0.18-88.31)	0.77 ± 0.17	0 (0-4.14)	0.00002 (0-0.59)
	Anc5	0.31 (0.20-1.56)	1.22 ± 0.23	0 (0-0.66)	0.00002 (0-0.87)
	CC 1690	100 (99.99-100)	0.28 ± 0.07	1.75 (1.04-2.33)	0 (0-0)
<hr/>					
	<b>Salt</b>				
	Anc2	0.27 (0.10-100)	0.36 ± 0.06	0 (0-3.34)	0.00002 (0-0.53)
	Anc3	0.42 (0.23-100)	0.30 ± 0.03	0 (0-2.77)	0.00002 (0-0.33)
	Anc4	0.78 (0.38-100)	0.25 ± 0.03	0 (0-2.25)	0.00002 (0-0.09)
	Anc5	2.81 (1.43-100)	0.31 ± 0.04	0 (0-1.57)	0 (0-0.07)
	CC 1690	1.14 (0.11-0.04)	0.78 ± 0.20	0.11 (0-5)	0.12 (0-0.63)
<hr/>					
	<b>Biotic x Salt</b>				
	Anc2	100 (99.97-100)	0.55 ± 0.11	1.23 (0-3.51)	0 (0-0)
	Anc3	0.81 (0.53-100)	0.34 ± 0.06	0 (0-2.76)	0.00002 (0-0.18)
	Anc4	0.32 (0.24-3.44)	0.32 ± 0.05	0.005 (0-0.43)	0.01 (0-0.29)
	CC 1690	0.96 (0.29-100)	0.53 ± 0.10	0.04 (0-3.88)	0.05 (0-0.32)

**Table S4.5.** Linear model (LM) summary statistics illustrating the independent effects of selection treatment and ancestor on six response variables: (a) descendants minimum light requirements ( $I^*$ ), (b) descendants minimum nitrogen requirements ( $N^*$ ), (c) descendants minimum phosphate requirements ( $P^*$ ), (d) descendants initial response to elevated light availability ( $\alpha$ ), (e) descendants initial response to elevated nitrogen availability ( $\alpha$ ) and (f) descendants initial response to elevated phosphate availability ( $\alpha$ ). Either the selection treatment or the ancestral genotype was treated as fixed effects.

Trait	d.f.	<i>F</i> value	AIC	<i>P</i>
(a) sqrt ( $I^* + 1$ )				
<b>Selection treatment</b>	<b>6,29</b>	<b>11.13</b>	<b>62.411</b>	<b>&lt;0.0001</b>
Ancestor	5,30	2.16	86.529	0.086
(b) sqrt ( $N^* + 1$ )				
Selection treatment	6,26	1.92	88.546	0.115
<b>Ancestor</b>	<b>4,28</b>	<b>2.35</b>	<b>88.071</b>	<b>0.079</b>
(c) sqrt ( $P^* + 1$ )				
Selection treatment	6,27	0.69		0.660
Ancestor	5,28	0.88		0.508
(d) sqrt ( $\alpha$ light +1)				
<b>Selection treatment</b>	<b>6,29</b>	<b>20.82</b>	<b>-158.59</b>	<b>&lt;0.0001</b>
Ancestor	5,30	0.94	-125.52	0.472
(e) sqrt ( $\alpha$ nitrogen +1)				
Selection treatment	6,26	1.03	-125.46	0.430
Ancestor	4,28	0.81	-141.70	0.527
(f) sqrt ( $\alpha$ phosphate +1)				
<b>Selection treatment</b>	<b>6,27</b>	<b>3.10</b>	<b>160.47</b>	<b>0.019</b>
Ancestor	4,29	1.11	173.86	0.372

**Table S4.6.** Results for the Principle Component Analysis evaluating the variation in  $R^*$  and  $\alpha$  under selection by limiting light, nitrogen and phosphate resource.

Analysis	PC1	PC2	PC3
<b>(a) <math>R^*</math></b>			
Eigenvalue	0.725	0.277	0.099
Variance explained (%)	65.810	25.125	9.064
<i>Light</i>	0.226	0.974	0.001
<i>Nitrogen</i>	-0.974	0.226	-0.001
<i>Phosphate</i>	0.001	0.001	-0.999
<b>(b) <math>\alpha</math></b>			
Eigenvalue	1.191	0.189	0.077
Variance explained (%)	81.732	13.004	5.265
<i>Light</i>	-0.001	-0.928	-0.372
<i>Nitrogen</i>	0.00003	0.372	-0.92
<i>Phosphate</i>	0.999	-0.001	-0.001

## **S4.1. Supplementary Methodology**

### **Acclimation to nitrogen and phosphorus**

To allow for acclimatization, the descendants and ancestors were maintained at the assigned nitrate or phosphate concentration listed in the table below, for 13 days prior to the start of the experiment. Batch cultures of each population were firstly transferred from agar into 100ml of standard COMBO media and cultured at 20°C on a 16:8 hour light-dark cycle for two weeks. 12ml of each batch culture were then centrifuged at 3,000rpm for 12 minutes and re-suspended into COMBO medium containing one of five nitrate or phosphate concentrations (Table S4.7). This allowed cultures to acclimate to their assigned experimental nitrate or phosphate concentrations. This re-suspension was repeated on the fourth and seventh day of the acclimation to ensure complete removal of excess nitrate or phosphate from the culture medium while also preventing starvation due to depletion. The phytoplankton pellet was then once again re-suspended in fresh and sterile COMBO medium with the assigned nitrate or phosphate concentration.

**Table S4.7.** Assigned acclimation concentrations for experimental nitrogen and phosphorus concentrations.

Experimental Concentration		Acclimation Concentration	
<b>Nitrate</b>	<b>Phosphate</b>	<b>Nitrate</b>	<b>Phosphate</b>
( $\mu\text{mol N}\cdot\text{L}^{-1}$ )	( $\mu\text{mol P}\cdot\text{L}^{-1}$ )	( $\mu\text{mol N}\cdot\text{L}^{-1}$ )	( $\mu\text{mol P}\cdot\text{L}^{-1}$ )
1	0.5	1	0.5
4	1	1	0.5
6	2	6	2
10	4	6	2
40	6	40	6
60	8	40	6
100	10	100	10
400	20	100	10
600	35	600	35
1000	50	600	35

### Parameter estimation

We estimated population growth rates ( $r$ ) as the slope of the log-transformed population-level pigment fluorescence (chlorophyll-*a*) against time (Simis *et al.* 2012). We used a minimum of three time points selected from the period during which growth was exponential (determined visually).

We used a maximum likelihood approach to fit equation (1) and equation (2) to the light-dependent, nitrogen-dependent and phosphate-dependent growth rate estimates of each ancestor and descendant for all selection treatments. We accounted for uncertainty in individual growth rate estimates by weighting each point by the reciprocal of the standard error. In addition to estimating the parameters of equation (1), we also numerically estimated the  $R^*$  (i.e.  $I^*$ ,  $N^*$  and  $P^*$ ) values, or the irradiance, nitrogen or phosphate levels at which the population growth rate is equal to zero, by solving the parameterized growth functions. We then quantified the

uncertainty in each parameter estimate, while accounting for the uncertainty in the individual growth rate estimates.

For each fitted curve, we simulated 1000 new datasets with the same number of points as the original fit, and at exactly the same irradiance levels. Residuals were randomly drawn and based on the variance in the original fit, but adjusted for bias in maximum likelihood estimates of variance (Gelman and Hill 2007). We then refit equations (1) and (2) to each of these 1000 simulated datasets and calculated the 95% confidence intervals in each parameter estimate. We followed this approach to account for the weighting of individual points by their uncertainty, and to capture uncertainty in  $R^*$ , which was not a parameter included in the equation (and therefore precluded a likelihood profile-based approach). The parameters were estimate using R 3.3.3. (R Development Core Team 2014). Maximum likelihood fits were performed using the package *bbmle* (Bolker 2016).



## REFERENCES

- Abrams, P. A. 1987. Alternative models of character displacement and niche shift. I. Adaptive shifts in resource use when there is competition for nutritionally nonsubstitutable resources. *Evolution* **41**:651-661.
- Allen, A. P., and J. F. Gillooly. 2009. Towards an integration of ecological stoichiometry and the metabolic theory of ecology to better understand nutrient cycling. *Ecology Letters* **12**:369-384.
- Allen, A. P., J. F. Gillooly, and J. H. Brown. 2005. Linking the global carbon cycle to individual metabolism. *Functional Ecology* **19**:202-213.
- Altermatt, F., E. A. Fronhofer, A. Garnier, A. Giometto, F. Hammes, *et al.* 2015. Big answers from small worlds: A user's guide for protist microcosms as a model system in ecology and evolution. *Methods in Ecology and Evolution* **6**:218-231.
- Anderson, D. M., P. M. Glibert, and J. M. Burkholder. 2002. Harmful algal blooms and eutrophication: Nutrient sources, composition, and consequences. *Estuaries* **25**:704-726.
- Atwood, T. B., E. Hammill, H. S. Greig, P. Kratina, J. B. Shurin, *et al.* 2013. Predator-induced reduction of freshwater carbon dioxide emissions. *Nature Geoscience* **6**:191-194.
- Atwood, T. B., E. Hammill, P. Kratina, H. S. Greig, J. B. Shurin, *et al.* 2015. Warming alters food web-driven changes in the CO<sub>2</sub> flux of experimental pond ecosystems. *Biology Letters* **11**.
- Behl, S., and H. Stibor. 2015. Prey diversity and prey identity affect herbivore performance on different time scales in a long term aquatic food-web experiment. *Oikos* **124**:1192-1202.
- Bell, G. 1991. The ecology and genetics of fitness in *Chlamydomonas* iii. Genotype-by-environment interaction within strains. *Evolution* **45**:668-679.
- Bell, G. 2013. Experimental evolution of heterotrophy in a green alga. *Evolution* **67**:468-476.
- Bell, T., A. K. Lilley, A. Hector, B. Schmid, L. Kind, *et al.* 2009. A linear model method for biodiversity–ecosystem functioning experiments. *The American Naturalist* **174**:836-849.
- Bolker, B. 2016. Bblme: Tools for general maximum likelihood estimation. R package version 1.0.18.

- Brown, J. H., J. F. Gillooly, A. P. Allen, V. M. Savage, and G. B. West. 2004. Toward a metabolic theory of ecology. *Ecology* **85**:1771-1789.
- Bulling, M. T., P. C. White, D. Raffaelli, and G. J. Pierce. 2006. Using model systems to address the biodiversity–ecosystem functioning process. *Marine Ecology Progress Series* **311**:295-309.
- Burns, C. W., and J. J. Gilbert. 1986. Effects of daphnid size and density on interference between daphnia and *keratella cochlearis*. *Limnology and Oceanography* **31**:848-858.
- Butchart, S. H. M., M. Walpole, B. Collen, A. van Strien, J. P. W. Scharlemann, *et al.* 2010. Global biodiversity: Indicators of recent declines. *Science* **328**:1164-1168.
- Butman, D., and P. A. Raymond. 2011. Significant efflux of carbon dioxide from streams and rivers in the united states. *Nature Geoscience* **4**:839-842.
- Cardinale, B. J., K. L. Matulich, D. U. Hooper, J. E. Byrnes, E. Duffy, *et al.* 2011. The functional role of producer diversity in ecosystems. *American Journal of Botany* **98**:572-592.
- Carpenter, S. R. 1996. Microcosm experiments have limited relevance for community and ecosystem ecology. *Ecology* **77**:677-680.
- Carpenter, S. R. 1999. Microcosm experiments have limited relevance for community and ecosystem ecology: Reply. *Ecology* **80**:1085-1088.
- Carpenter, S. R., J. J. Cole, J. R. Hodgson, J. F. Kitchell, M. L. Pace, *et al.* 2001. Trophic cascades, nutrients, and lake productivity: Whole-lake experiments. *Ecological Monographs* **71**:163-186.
- Chase, J. M., and M. A. Leibold. 2003. *Ecological niches: Linking classical and contemporary approaches*. University of Chicago Press, Chicago.
- Chesson, P. 2000. Mechanisms of maintenance of species diversity. *Annual Review of Ecology and Systematics* **31**:343-366.
- Cole, J. J., and N. F. Caraco. 1998. Atmospheric exchange of carbon dioxide in a low-wind oligotrophic lake measured by the addition of sf<sub>6</sub>. *Limnology and Oceanography* **43**:647-656.
- Cole, J. J., Y. T. Prairie, N. F. Caraco, W. H. McDowell, L. J. Tranvik, *et al.* 2007. Plumbing the global carbon cycle: Integrating inland waters into the terrestrial carbon budget. *Ecosystems* **10**:171-184.
- Cross, W. F., J. M. Hood, J. P. Benstead, A. D. Huryn, and D. Nelson. 2015. Interactions between temperature and nutrients across levels of ecological organization. *Global Change Biology* **21**:1025-1040.

- Daines, S. J., J. R. Clark, and T. M. Lenton. 2014. Multiple environmental controls on phytoplankton growth strategies determine adaptive responses of the n : P ratio. *Ecology Letters* **17**:414-425.
- Dalsgaard, T., Nielsen, L.P., Brotas, V., Viaroli, P., Underwood, G.J.C., Nedwell, D.B., Sundback, K., Rysgaard, S., Miles, A., Bartoli, M., Dong, L., Thornton, D.C.O., Ottosen, L.D.M., Castaldelli, G., Risgaard-Petersen, N. 2000. Protocol handbook for nice-nitrogen cycling in estuaries: A project under the eu research programme. *Marine science and technology (mast iii)*. Page 62. National Environmental Research Institute, Silkeborg, Denmark.
- Davidson, E. A., and I. A. Janssens. 2006. Temperature sensitivity of soil carbon decomposition and feedbacks to climate change. *Nature* **440**:165-173.
- Davidson, T. A., J. Audet, J. C. Svenning, T. L. Lauridsen, M. Sondergaard, *et al.* 2015. Eutrophication effects on greenhouse gas fluxes from shallow-lake mesocosms override those of climate warming. *Global Change Biology* **21**:4449-4463.
- Dell, A. I., S. Pawar, and V. M. Savage. 2011. Systematic variation in the temperature dependence of physiological and ecological traits. *Proceedings of the National Academy of Sciences of the United States of America* **108**:10591-10596.
- Descamps-Julien, B., and A. Gonzalez. 2005. Stable coexistence in a fluctuating environment: An experimental demonstration. *Ecology* **86**:2815-2824.
- Drake, J. M., and A. M. Kramer. 2012. Mechanistic analogy: How microcosms explain nature. *Theoretical ecology* **5**:433-444.
- Droop, M. R. 1973. Some thoughts on nutrient limitation in algae<sup>1</sup>. *Journal of Phycology* **9**:264-272.
- Duffy, J. E., J. P. Richardson, and E. A. Canuel. 2003. Grazer diversity effects on ecosystem functioning in seagrass beds. *Ecology Letters* **6**:637-645.
- Dybzinski, R., and D. Tilman. 2007. Resource use patterns predict long-term outcomes of plant competition for nutrients and light. *American Naturalist* **170**:305-318.
- Edwards, K. F., C. A. Klausmeier, and E. Litchman. 2011. Evidence for a three-way trade-off between nitrogen and phosphorus competitive abilities and cell size in phytoplankton. *Ecology* **92**:2085-2095.
- Edwards, K. F., C. A. Klausmeier, and E. Litchman. 2015. Nutrient utilization traits of phytoplankton. *Ecology* **96**:2311-2311.
- Edwards, K. F., E. Litchman, and C. A. Klausmeier. 2013. Functional traits explain phytoplankton responses to environmental gradients across lakes of the united states. *Ecology* **94**:1626-1635.

- Eilers, P. H. C., and J. C. H. Peeters. 1988. A model for the relationship between light-intensity and the rate of photosynthesis in phytoplankton. *Ecological Modelling* **42**:199-215.
- Eklöf, J. S., J. N. Havenhand, C. Alsterberg, and L. Gamfeldt. 2015. Community-level effects of rapid experimental warming and consumer loss outweigh effects of rapid ocean acidification. *Oikos* **124**:1040-1049.
- Eppley, R. W. 1972. Temperature and phytoplankton growth in the sea. *Fish. Bull* **70**:1063-1085.
- Falkowski, P. G., R. T. Barber, and V. Smetacek. 1998. Biogeochemical controls and feedbacks on ocean primary production. *Science* **281**:200-206.
- Falkowski, P. G., and M. J. Oliver. 2007. Mix and match: How climate selects phytoplankton. *Nature reviews. Microbiology* **5**:813.
- Field, C. B., M. J. Behrenfeld, J. T. Randerson, and P. Falkowski. 1998. Primary production of the biosphere: Integrating terrestrial and oceanic components. *Science* **281**:237-240.
- Finlay, K., R. J. Vogt, M. J. Bogard, B. Wissel, B. M. Tutolo, *et al.* 2015. Decrease in CO<sub>2</sub> efflux from northern hardwater lakes with increasing atmospheric warming. *Nature* **519**:215-218.
- Fischer, B. B., M. Kwiatkowski, M. Ackermann, J. Krismer, S. Roffler, *et al.* 2014. Phenotypic plasticity influences the eco-evolutionary dynamics of a predator-prey system. *Ecology* **95**:3080-3092.
- Follows, M. J., S. Dutkiewicz, S. Grant, and S. W. Chisholm. 2007. Emergent biogeography of microbial communities in a model ocean. *Science* **315**:1843-1846.
- Fox, J. W., and D. A. Vasseur. 2008. Character convergence under competition for nutritionally essential resources. *The American Naturalist* **172**:667-680.
- Fussmann, K. E., F. Schwarzmüller, U. Brose, A. Jousset, and B. C. Rall. 2014. Ecological stability in response to warming. *Nature Climate Change* **4**:206-210.
- Gause, G. F. 1934. Experimental analysis of Vito Volterra's mathematical theory of the struggle for existence. *Science* **79**:16-17.
- Gelman, A., and J. Hill. 2007. *Data analysis using regression and multilevel/hierarchical models*. Cambridge University Press.
- Gerrish, P. J., and R. E. Lenski. 1998. The fate of competing beneficial mutations in an asexual population. *Genetica* **102**:127.
- Gliwicz, Z., and E. Siedlar. 1980. Food size limitation and algae interfering with food collection in daphnia. *Arch. Hydrobiol* **88**:155-177.

- Goddard, M. R., and M. A. Bradford. 2003. The adaptive response of a natural microbial population to carbon- and nitrogen-limitation. *Ecology Letters* **6**:594-598.
- Goho, S., and G. Bell. 2000. Mild environmental stress elicits mutations affecting fitness in *chlamydomonas*. *Proceedings of the Royal Society of London B: Biological Sciences* **267**:123-129.
- Gonzalez, A., and E. J. Chaneton. 2002. Heterotroph species extinction, abundance and biomass dynamics in an experimentally fragmented microecosystem. *Journal of Animal Ecology* **71**:594-602.
- Grant, P. R., and B. R. Grant. 2006. Evolution of character displacement in darwin's finches. *Science* **313**:224-226.
- Greenberg Arnold, E., and S. Clesceri Lenore. 1992. Standard methods for the examination of water and wastewater. USA: American Public Health Association; ISBN 0-87553-207-1.
- Grover, J. P. 1991. Dynamics of competition among microalgae in variable environments: Experimental tests of alternative models. *Oikos* **62**:231-243.
- Grover, J. P. 1997. Resource competition. Springer Science & Business Media.
- Hairston, N. G., S. P. Ellner, M. A. Geber, T. Yoshida, and J. A. Fox. 2005. Rapid evolution and the convergence of ecological and evolutionary time. *Ecology Letters* **8**:1114-1127.
- Hammill, E., P. Kratina, M. Vos, O. L. Petchey, and B. R. Anholt. 2015. Food web persistence is enhanced by non-trophic interactions. *Oecologia* **178**:549-556.
- Hardin, G. 1960. The competitive exclusion principle. *Science* **131**:1292-1297.
- Harley, C. D. G. 2011. Climate change, keystone predation, and biodiversity loss. *Science* **334**:1124-1127.
- Hasler, C. T., D. Butman, J. D. Jeffrey, and C. D. Suski. 2016. Freshwater biota and rising pco<sub>2</sub>? *Ecology Letters* **19**:98-108.
- Hastings, A. 2012. Temporally varying resources amplify the importance of resource input in ecological populations. *Biology letters* **8**:1067-1069.
- Hein, M., M. F. Pedersen, and K. Sand-Jensen. 1995. Size-dependent nitrogen uptake in micro-and macroalgae. *Marine Ecology Progress Series*:247-253.
- Hillebrand, H. 2011. Temperature mediates competitive exclusion and diversity in benthic microalgae under different n:P stoichiometry. *Ecological Research* **26**:533-539.
- Hillebrand, H., T. Burgmer, and E. Biermann. 2012. Running to stand still: Temperature effects on species richness, species turnover, and functional community dynamics. *Marine Biology* **159**:2415-2422.

- Hillebrand, H., and B. J. Cardinale. 2004. Consumer effects decline with prey diversity. *Ecology Letters* **7**:192-201.
- Hillebrand, H., C. D. Durselen, D. Kirschtel, U. Pollinger, and T. Zohary. 1999. Biovolume calculation for pelagic and benthic microalgae. *Journal of Phycology* **35**:403-424.
- Hillebrand, H., J. Soininen, and P. Snoeijs. 2010. Warming leads to higher species turnover in a coastal ecosystem. *Global Change Biology* **16**:1181-1193.
- Hoffmann, A. A., and C. M. Sgrò. 2011. Climate change and evolutionary adaptation. *Nature* **470**:479.
- Houle, D. 1991. Genetic covariance of fitness correlates: What genetic correlations are made of and why it matters. *Evolution* **45**:630-648.
- Huertas, I. E., M. Rouco, V. López-Rodas, and E. Costas. 2011. Warming will affect phytoplankton differently: Evidence through a mechanistic approach. *Proceedings of the Royal Society of London B: Biological Sciences*.
- Hughes, A. R., B. D. Inouye, M. T. Johnson, N. Underwood, and M. Vellend. 2008. Ecological consequences of genetic diversity. *Ecology Letters* **11**:609-623.
- Huisman, J., R. R. Jonker, C. Zonneveld, and F. J. Weissing. 1999. Competition for light between phytoplankton species: Experimental tests of mechanistic theory. *Ecology* **80**:211-222.
- Hutchinson, G. E. 1961. The paradox of the plankton. *The American Naturalist* **95**:137-145.
- IPCC. 2014. *Climate change 2014: Impacts, adaptation, and vulnerability.*, Cambridge (United Kingdom) and New York.
- Ives, A. R., and S. R. Carpenter. 2007. Stability and diversity of ecosystems. *Science* **317**:58-62.
- Jeffery, W. 2005. Adaptive evolution of eye degeneration in the mexican blind cavefish. *Journal of Heredity* **96**:185-196.
- Karl, T. R., A. Arguez, B. Y. Huang, J. H. Lawrimore, J. R. McMahon, *et al.* 2015. Possible artifacts of data biases in the recent global surface warming hiatus. *Science* **348**:1469-1472.
- Keddy, P. 2002. *Competition*. 2nd Edition edition. Kluwer Academic Publisher, London.
- Keddy, P. A. 1992. Assembly and response rules: Two goals for predictive community ecology. *Journal of Vegetation Science* **3**:157-164.
- Kilham, S. S., D. A. Kreeger, S. G. Lynn, C. E. Goulden, and L. Herrera. 1998. Combo: A defined freshwater culture medium for algae and zooplankton. *Hydrobiologia* **377**:147-159.

- Kingsolver, J. G. 2009. The well-temperated biologist. *American Naturalist* **174**:755-768.
- Klausmeier, C. A., E. Litchman, T. Daufresne, and S. Levin. 2008. Phytoplankton stoichiometry. *Ecological Research* **23**:479-485.
- Kratina, P., H. S. Greig, P. L. Thompson, T. S. A. Carvalho-Pereira, and J. B. Shurin. 2012. Warming modifies trophic cascades and eutrophication in experimental freshwater communities. *Ecology* **93**:1421-1430.
- Kratina, P., E. Hammill, and B. R. Anholt. 2010. Stronger inducible defences enhance persistence of intraguild prey. *Journal of Animal Ecology* **79**:993-999.
- Kratina, P., M. Vos, and B. R. Anholt. 2007. Species diversity modulates predation. *Ecology* **88**:1917-1923.
- Kremer, C. T., M. K. Thomas, and E. Litchman. 2017a. Temperature- and size-scaling of phytoplankton population growth rates: Reconciling the eppley curve and the metabolic theory of ecology. *Limnology and Oceanography* **62**:1658-1670.
- Kremer, C. T., A. K. Williams, M. Finiguerra, A. A. Fong, A. Kellerman, *et al.* 2017b. Realizing the potential of trait-based aquatic ecology: New tools and collaborative approaches. *Limnology and Oceanography* **62**:253-271.
- Krismer, J., M. Tamminen, S. Fontana, R. Zenobi, and A. Narwani. 2016. Single-cell mass spectrometry reveals the importance of genetic diversity and plasticity for phenotypic variation in nitrogen-limited chlamydomonas. *The ISME Journal* **11**:988.
- Lachapelle, J., and G. Bell. 2012. Evolutionary rescue of sexual and asexual populations in a deteriorating environment. *Evolution* **66**:3508-3518.
- Lahti, D. C., N. A. Johnson, B. C. Ajie, S. P. Otto, A. P. Hendry, *et al.* 2009. Relaxed selection in the wild. *Trends in Ecology & Evolution* **24**:487-496.
- Lefcheck, J. S. 2016. Piecewissem: Piecewise structural equation modelling in r for ecology, evolution, and systematics. *Methods in Ecology and Evolution* **7**:573-579.
- Lehman, C., xa, L, D. Tilman, and D. G. Associate Editor: Steven. 2000. Biodiversity, stability, and productivity in competitive communities. *The American Naturalist* **156**:534-552.
- Li, W., and M. H. H. Stevens. 2017. Community temporal variability increases with fluctuating resource availability. *Scientific Reports* **7**:45280.
- Litchman, E., and C. A. Klausmeier. 2001. Competition of phytoplankton under fluctuating light. *The American Naturalist* **157**:170-187.

- Litchman, E., and C. A. Klausmeier. 2008. Trait-based community ecology of phytoplankton. *Annual Review of Ecology Evolution and Systematics* **39**:615-639.
- Litchman, E., C. A. Klausmeier, O. M. Schofield, and P. G. Falkowski. 2007. The role of functional traits and trade-offs in structuring phytoplankton communities: Scaling from cellular to ecosystem level. *Ecology Letters* **10**:1170-1181.
- Litchman, E., P. D. Pinto, C. A. Klausmeier, M. K. Thomas, and K. Yoshiyama. 2010. Linking traits to species diversity and community structure in phytoplankton. *Hydrobiologia* **653**:15-28.
- Litchman, E., P. Tezanos Pinto, K. F. Edwards, C. A. Klausmeier, C. T. Kremer, *et al.* 2015. Global biogeochemical impacts of phytoplankton: A trait - based perspective. *Journal of Ecology* **103**:1384-1396.
- Lohbeck, K. T., U. Riebesell, and T. B. H. Reusch. 2012. Adaptive evolution of a key phytoplankton species to ocean acidification. *Nature Geoscience* **5**:346.
- Lopez-Urrutia, A., E. San Martin, R. P. Harris, and X. Irigoien. 2006. Scaling the metabolic balance of the oceans. *Proceedings of the National Academy of Sciences of the United States of America* **103**:8739-8744.
- Losos, J. B., T. R. Jackman, A. Larson, K. d. Queiroz, and L. Rodríguez-Schettino. 1998. Contingency and determinism in replicated adaptive radiations of island lizards. *Science* **279**:2115-2118.
- Low-Décarie, E., G. Bell, and G. F. Fussmann. 2015. CO<sub>2</sub> alters community composition and response to nutrient enrichment of freshwater phytoplankton. *Oecologia* **177**:875-883.
- Low-Decarie, E., G. F. Fussmann, and G. Bell. 2011. The effect of elevated CO<sub>2</sub> on growth and competition in experimental phytoplankton communities. *Global Change Biology* **17**:2525-2535.
- Low-Décarie, E., G. F. Fussmann, and G. Bell. 2014. Aquatic primary production in a high-CO<sub>2</sub> world. *Trends in Ecology & Evolution* **29**:223-232.
- Low-Décarie, E., M. D. Jewell, G. F. Fussmann, and G. Bell. 2013. Long-term culture at elevated atmospheric CO<sub>2</sub> fails to evoke specific adaptation in seven freshwater phytoplankton species. *Proceedings of the Royal Society B: Biological Sciences* **280**.
- MacArthur, R., and R. Levins. 1967. The limiting similarity, convergence, and divergence of coexisting species. *The American Naturalist* **101**:377-385.
- Maloney, T. E., W. E. Miller, and T. Shiroyama. 1972. Algal responses to nutrient additions in natural waters. I. Laboratory assays.



- Martiny, A. C., C. T. A. Pham, F. W. Primeau, J. A. Vrugt, J. K. Moore, *et al.* 2013. Strong latitudinal patterns in the elemental ratios of marine plankton and organic matter. *Nature Geoscience* **6**:279-283.
- McGill, B. J., B. J. Enquist, E. Weiher, and M. Westoby. 2006. Rebuilding community ecology from functional traits. *Trends in Ecology & Evolution* **21**:178-185.
- Meinshausen, M., S. J. Smith, K. Calvin, J. S. Daniel, M. L. T. Kainuma, *et al.* 2011. The rcp greenhouse gas concentrations and their extensions from 1765 to 2300. *Climatic Change* **109**:213-241.
- Menden-Deuer, S., and T. Kiørboe. 2016. Small bugs with a big impact: Linking plankton ecology with ecosystem processes. *Journal of Plankton Research* **38**:1036-1043.
- Merilä, J., and A. P. Hendry. 2014. Climate change, adaptation, and phenotypic plasticity: The problem and the evidence. *Evolutionary applications* **7**:1-14.
- Miller, T. E., J. H. Burns, P. Munguia, E. L. Walters, J. M. Kneitel, *et al.* 2005. A critical review of twenty years' use of the resource-ratio theory. *The American Naturalist* **165**:439-448.
- Monod, J. 1949. The growth of bacterial cultures. *Annual Reviews in Microbiology* **3**:371-394.
- Naeem, S., L. J. Thompson, S. P. Lawler, J. H. Lawton, and R. M. Woodfin. 1994. Declining biodiversity can alter the performance of ecosystems. *Nature* **368**:734-737.
- Nakagawa, S., and H. Schielzeth. 2013. A general and simple method for obtaining  $r^2$  from generalized linear mixed-effects models. *Methods in Ecology and Evolution* **4**:133-142.
- Narwani, A., M. A. Alexandrou, J. Herrin, A. Vouaux, C. Zhou, *et al.* 2015. Common ancestry is a poor predictor of competitive traits in freshwater green algae. *Plos One* **10**.
- Narwani, A., and A. Mazumder. 2010. Community composition and consumer identity determine the effect of resource species diversity on rates of consumption. *Ecology* **91**:3441-3447.
- Narwani, A., and A. Mazumder. 2012. Bottom-up effects of species diversity on the functioning and stability of food webs. *Journal of Animal Ecology* **81**:701-713.
- O'Connor, M. I. 2009. Warming strengthens an herbivore-plant interaction. *Ecology* **90**:388-398.
- O'Connor, M. I., M. F. Piehler, D. M. Leech, A. Anton, and J. F. Bruno. 2009. Warming and resource availability shift food web structure and metabolism. *Plos Biology* **7**:6.

- Pawar, S., A. I. Dell, and M. S. Van. 2012. Dimensionality of consumer search space drives trophic interaction strengths. *Nature* **486**:485-489.
- Perkins, D. M., R. A. Bailey, M. Dossena, L. Gamfeldt, J. Reiss, *et al.* 2015. Higher biodiversity is required to sustain multiple ecosystem processes across temperature regimes. *Global Change Biology* **21**:396-406.
- Petchey, O. L., P. T. McPhearson, T. M. Casey, and P. J. Morin. 1999. Environmental warming alters food-web structure and ecosystem function. *Nature* **402**:69-72.
- Petchey, O. L., M. Pontarp, T. M. Massie, S. Kéfi, A. Ozgul, *et al.* 2015. The ecological forecast horizon, and examples of its uses and determinants. *Ecology Letters* **18**:597-611.
- R Development Core Team. 2014. R: A language and environment for statistical computing. R Foundation for Statistical Computing, Vienna, Austria.
- R Development Core Team. 2016. R: A language and environment for statistical computing. R Foundation for Statistical Computing, Vienna, Austria.
- Rall, B. C., O. Vucic-Pestic, R. B. Ehnes, M. Emmerson, and U. Brose. 2010. Temperature, predator-prey interaction strength and population stability. *Global Change Biology* **16**:2145-2157.
- Rasilo, T., Prairie, Y.T., Giorgia, P.A. 2015. Large-scale patterns in summer diffusive CH<sub>4</sub> fluxes across boreal lakes, and contribution to diffusive C emissions. *Global Change Biology* **21**:112401139.
- Raymond, P. A., J. Hartmann, R. Lauerwald, S. Sobek, C. McDonald, *et al.* 2013. Global carbon dioxide emissions from inland waters. *Nature* **503**:355-359.
- Reynolds, C. S., V. Huszar, C. Kruk, L. Naselli-Flores, and S. Melo. 2002. Towards a functional classification of the freshwater phytoplankton. *Journal of Plankton Research* **24**:417-428.
- Ricklefs, R. E. 2004. A comprehensive framework for global patterns in biodiversity. *Ecology Letters* **7**:1-15.
- Rosenzweig, M. L. 1971. Paradox of enrichment: Destabilization of exploitation ecosystems in ecological time. *Science* **171**:385-387.
- Sanders, I. A., C. M. Heppell, J. A. Cotton, G. Wharton, A. G. Hildrew, *et al.* 2007. Emission of methane from chalk streams has potential implications for agricultural practices. *Freshwater Biology* **52**:1176-1186.
- Savage, V. M., J. F. Gillooly, J. H. Brown, G. B. West, and E. L. Charnov. 2004. Effects of body size and temperature on population growth. *American Naturalist* **163**:429-441.

- Schabhüttl, S., P. Hingsamer, G. Weigelhofer, T. Hein, A. Weigert, *et al.* 2013. Temperature and species richness effects in phytoplankton communities. *Oecologia* **171**:527-536.
- Schaum, C.-E., S. Barton, E. Bestion, A. Buckling, B. Garcia-Carreras, *et al.* 2017. Adaptation of phytoplankton to a decade of experimental warming linked to increased photosynthesis. *Nature Ecology & Evolution* **1**:s41559-41017-40094.
- Schindler, D. W. 1998. Whole-ecosystem experiments: Replication versus realism: The need for ecosystem-scale experiments. *Ecosystems* **1**:323-334.
- Schleuss, P. M., F. Heitkamp, C. Leuschner, A. C. Fender, and H. F. Jungkunst. 2014. Higher subsoil carbon storage in species-rich than species-poor temperate forests. *Environmental Research Letters* **9**:10.
- Schloss, C. A., T. A. Nuñez, and J. J. Lawler. 2012. Dispersal will limit ability of mammals to track climate change in the western hemisphere. *Proceedings of the National Academy of Sciences* **109**:8606-8611.
- Schluter, D., and J. D. McPhail. 1992. Ecological character displacement and speciation in sticklebacks. *The American Naturalist* **140**:85-108.
- Schlüter, L., K. T. Lohbeck, M. A. Gutowska, J. P. Gröger, U. Riebesell, *et al.* 2014. Adaptation of a globally important coccolithophore to ocean warming and acidification. *Nature Climate Change* **4**:1024.
- Schwaderer, A. S., K. Yoshiyama, P. T. Pinto, N. G. Swenson, C. A. Klausmeier, *et al.* 2011. Eco-evolutionary differences in light utilization traits and distributions of freshwater phytoplankton. *Limnology and Oceanography* **56**:589-598.
- Sentis, A., A. Binzer, and D. S. Boukal. 2017. Temperature-size responses alter food chain persistence across environmental gradients. *Ecology Letters* **20**:852-862.
- Shatwell, T., J. Köhler, and A. Nicklisch. 2014. Temperature and photoperiod interactions with phosphorus-limited growth and competition of two diatoms. *Plos One* **9**:e102367.
- Shurin, J. B., J. L. Clasen, H. S. Greig, P. Kratina, and P. L. Thompson. 2012. Warming shifts top-down and bottom-up control of pond food web structure and function. *Philosophical Transactions of the Royal Society B-Biological Sciences* **367**:3008-3017.
- Simis, S. G., Y. Huot, M. Babin, J. Seppälä, and L. Metsamaa. 2012. Optimization of variable fluorescence measurements of phytoplankton communities with cyanobacteria. *Photosynthesis Research* **112**:13-30.
- Sommer, U. 1985. Comparison between steady state and non-steady state competition: Experiments with natural phytoplankton. *Limnology and Oceanography* **30**:335-346.

- Sterner, R. W., and J. J. Elser. 2002. Ecological stoichiometry: The biology of elements from molecules to the biosphere. Princeton University Press.
- Stinchcombe, J. R., and M. Kirkpatrick. 2012. Genetics and evolution of function-valued traits: Understanding environmentally responsive phenotypes. *Trends in Ecology & Evolution* **27**:637-647.
- Stoks, R., L. Govaert, K. Pauwels, B. Jansen, and L. De Meester. 2016. Resurrecting complexity: The interplay of plasticity and rapid evolution in the multiple trait response to strong changes in predation pressure in the water flea *daphnia magna*. *Ecology Letters* **19**:180-190.
- Sueoka, N. 1960. Mitotic replication of deoxyribonucleic acid in *chlamydomonas reinhardi*. *Proceedings of the National Academy of Sciences* **46**:83-91.
- Suggett, D. J., C. M. Moore, A. E. Hickman, and R. J. Geider. 2009. Interpretation of fast repetition rate (frr) fluorescence: Signatures of phytoplankton community structure versus physiological state. *Marine Ecology Progress Series* **376**:1-19.
- Thomas, M. K., M. Aranguren - Gassis, C. T. Kremer, M. R. Gould, K. Anderson, *et al.* 2017. Temperature–nutrient interactions exacerbate sensitivity to warming in phytoplankton. *Global Change Biology*.
- Thomas, M. K., C. T. Kremer, and E. Litchman. 2016. Environment and evolutionary history determine the global biogeography of phytoplankton temperature traits. *Global Ecology and Biogeography* **25**:75-86.
- Tilman, D. 1977. Resource competition between planktonic algae: An experimental and theoretical approach. *Ecology* **58**:338-348.
- Tilman, D. 1980. Resources: A graphical-mechanistic approach to competition and predation. *The American Naturalist* **116**:362-393.
- Tilman, D. 1981. Tests of resource competition theory using four species of lake michigan algae. *Ecology* **62**:802-815.
- Tilman, D. 1982. Resource competition and community structure. Princeton university press.
- Tilman, D. 2004. Niche tradeoffs, neutrality, and community structure: A stochastic theory of resource competition, invasion, and community assembly. *Proceedings of the National Academy of Sciences of the United States of America* **101**:10854-10861.
- Tilman, D., R. Kiesling, R. Sterner, S. S. Kilham, and F. A. Johnson. 1986. Green, bluegreen and diatom algae - taxonomic differences in competitive ability for phosphorus, silicon and nitrogen. *Archiv Fur Hydrobiologie* **106**:473-485.
- Tilman, D., M. Mattson, and S. Langer. 1981. Competition and nutrient kinetics along a temperature gradient - an experimental test of a mechanistic approach to niche theory. *Limnology and Oceanography* **26**:1020-1033.

- Toseland, A., S. J. Daines, J. R. Clark, A. Kirkham, J. Strauss, *et al.* 2013. The impact of temperature on marine phytoplankton resource allocation and metabolism. *Nature Climate Change* **3**:979-984.
- Trall, L. W., M. L. M. Lim, N. S. Sodhi, and C. J. A. Bradshaw. 2010. Mechanisms driving change: Altered species interactions and ecosystem function through global warming. *Journal of Animal Ecology* **79**:937-947.
- Tranvik, L. J., J. A. Downing, J. B. Cotner, S. A. Loiselle, R. G. Striegl, *et al.* 2009. Lakes and reservoirs as regulators of carbon cycling and climate. *Limnology and Oceanography* **54**:2298-2314.
- Trolle, D., P. A. Staehr, T. A. Davidson, R. Bjerring, T. L. Lauridsen, *et al.* 2012. Seasonal dynamics of CO<sub>2</sub> flux across the surface of shallow temperate lakes. *Ecosystems* **15**:336-347.
- U. E. P. A. 2009. National lakes assessment: A collaborative survey of the nation's lakes. Washington, D.C.
- Urban, M. C., G. Bocedi, A. P. Hendry, J.-B. Mihoub, G. Pe'er, *et al.* 2016. Improving the forecast for biodiversity under climate change. *Science* **353**:aad8466.
- van Donk, E., and S. S. Kilham. 1990. Temperature effects on silicon- and phosphorus-limited growth and competitive interactions among three diatoms. *Journal of Phycology* **26**:40-50.
- Vasseur, D. A., and J. W. Fox. 2011. Adaptive dynamics of competition for nutritionally complementary resources: Character convergence, displacement, and parallelism. *The American Naturalist* **178**:501-514.
- Velicer, G. J. 1999. Pleiotropic effects of adaptation to a single carbon source for growth on alternative substrates. *Applied and Environmental Microbiology* **65**:264-269.
- Via, S., and R. Lande. 1985. Genotype - environment interaction and the evolution of phenotypic plasticity. *Evolution* **39**:505-522.
- Violle, C., B. J. Enquist, B. J. McGill, L. Jiang, C. H. Albert, *et al.* 2012. The return of the variance: Intraspecific variability in community ecology. *Trends in Ecology & Evolution* **27**:244-252.
- Ward, B. A., E. Marañón, B. Sauterey, J. Rault, and D. Claessen. 2017. The size dependence of phytoplankton growth rates: A trade-off between nutrient uptake and metabolism. *The American Naturalist* **189**:170-177.
- Watson, R. T., L. G. M. Filho, E. Sanheuzza, L. G. M. Filho, and E. Sanheuzza. 1992. Greenhouse gases: Sources and sinks. *Climate Change 1992: the supplementary report to the IPCC scientific assessment edition*. Cambridge University Press, Cambridge, UK.

- Weiss, R. F. 1974. Carbon dioxide in water and seawater: The solubility of a non-ideal gas. *Marine Chemistry* **2**:203-215.
- Wiebe, R., and V. L. Gaddy. 1940. The solubility of carbon dioxide in water at various temperatures from 12 to 40° and at pressures to 500 atmospheres. Critical phenomena. *Journal of the American Chemical Society* **62**:815-817.
- Wilson, J. B., E. Spijkerman, and J. Huisman. 2007. Is there really insufficient support for tilman's r concept? A comment on miller et al. *American Naturalist* **169**:700-706.
- Woodward, G., L. E. Brown, F. K. Edwards, L. N. Hudson, A. M. Milner, *et al.* 2012. Climate change impacts in multispecies systems: Drought alters food web size structure in a field experiment. *Philosophical Transactions of the Royal Society B-Biological Sciences* **367**:2990-2997.
- Yamamoto, S., J. B. Alcauskas, and T. E. Crozier. 1976. Solubility of methane in distilled water and seawater. *Journal of Chemical & Engineering Data* **21**:78-80.
- Yang, L. H., J. L. Bastow, K. O. Spence, and A. N. Wright. 2008. What can we learn from resource pulses. *Ecology* **89**:621-634.
- Yoshida, T., L. E. Jones, S. P. Ellner, G. F. Fussmann, and N. G. Hairston. 2003. Rapid evolution drives ecological dynamics in a predator-prey system. *Nature* **424**:303-306.
- Yuan, Z. Y., and H. Y. H. Chen. 2015. Decoupling of nitrogen and phosphorus in terrestrial plants associated with global changes. *Nature Climate Change* **5**:465-469.
- Yvon-Durocher, G., A. P. Allen, M. Cellamare, M. Dossena, K. J. Gaston, *et al.* 2015a. Five years of experimental warming increases the biodiversity and productivity of phytoplankton. *PLoS Biol* **13**:e1002324.
- Yvon-Durocher, G., M. Dossena, M. Trimmer, G. Woodward, and A. P. Allen. 2015b. Temperature and the biogeography of algal stoichiometry. *Global Ecology and Biogeography* **24**:562-570.
- Yvon-Durocher, G., J. I. Jones, M. Trimmer, G. Woodward, and J. M. Montoya. 2010. Warming alters the metabolic balance of ecosystems. *Philosophical Transactions of the Royal Society of London B: Biological Sciences* **365**:2117-2126.
- Yvon-Durocher, G., C. E. Schaum, and M. Trimmer. 2017. The temperature dependence of phytoplankton stoichiometry: Investigating the roles of species sorting and local adaptation. *Frontiers in Microbiology* **8**.
- Zuur, A., E. N. Ieno, N. Walker, A. A. Saveliev, and G. M. Smith. 2009. Mixed effects models and extensions in ecology with r. Springer New York.

